NAVAL POSTGRADUATE SCHOOL

MONTEREY, CALIFORNIA

THESIS

PREDICTION OF TROPICAL CYCLONE FORMATION IN THE WESTERN NORTH PACIFIC USING THE NAVY GLOBAL MODEL

by

Caroline A. Bower

March 2004

Thesis Co-Advisors:
Patrick A. Harr
Russell L. Elsberry

Approved for public release; distribution is unlimited.

THIS PAGE INTENTIONALLY LEFT BLANK

REPORT DOCUMENTATION PAGE	*Form Approved OMB No. 0704-0188*

Public reporting burden for this collection of information is estimated to average 1 hour per response, including the time for reviewing instruction, searching existing data sources, gathering and maintaining the data needed, and completing and reviewing the collection of information. Send comments regarding this burden estimate or any other aspect of this collection of information, including suggestions for reducing this burden, to Washington headquarters Services, Directorate for Information Operations and Reports, 1215 Jefferson Davis Highway, Suite 1204, Arlington, VA 22202-4302, and to the Office of Management and Budget, Paperwork Reduction Project (0704-0188) Washington DC 20503.

1. AGENCY USE ONLY *(Leave blank)*	2. REPORT DATE March 2004	3. REPORT TYPE AND DATES COVERED Master's Thesis	
4. TITLE AND SUBTITLE: Prediction of Tropical Cyclone Formation in the Western North Pacific Using the Navy Global Model		**5. FUNDING NUMBERS**	
6. AUTHOR(S) : Bower, Caroline A.			
7. PERFORMING ORGANIZATION NAME(S) AND ADDRESS(ES) Naval Postgraduate School Monterey, CA 93943-5000		**8. PERFORMING ORGANIZATION REPORT NUMBER**	
9. SPONSORING /MONITORING AGENCY NAME(S) AND ADDRESS(ES) N/A		**10. SPONSORING/MONITORING AGENCY REPORT NUMBER**	
11. SUPPLEMENTARY NOTES The views expressed in this thesis are those of the author and do not reflect the official policy or position of the Department of Defense or the U.S. Government.			
12a. DISTRIBUTION / AVAILABILITY STATEMENT Approved for public release; distribution is unlimited.		**12b. DISTRIBUTION CODE**	

13. ABSTRACT (maximum 200 words)

The Tropical Cyclone Vorticity Tracking Program is used to identify vortices in the western North Pacific from the Navy Operational Global Atmospheric Prediction System (NOGAPS) analyses and forecasts during May – October 2002 and 2003. Based on the NOGAPS analyses, several parameters are different between the 23 vortices that developed into storms during 2002 according to the Joint Typhoon Warning Center (JTWC) and the 231 vortices that did not develop. After eliminating 127 vortices that did not persist at least 24 h, this left 104 non-developing cases. For the developing circulations, the average 850-mb relative vorticity value at the first JTWC-warning time was 5.0×10^{-5} s^{-1}, with an easterly deep layer wind shear of -1.8 m s^{-1}. The average 850-mb relative vorticity maximum for the non-developing cases was 3.3×10^{-5} s^{-1}, with a westerly vertical shear of 4.1 m s^{-1}. The NOGAPS model tends to over-forecast relative vorticity prior to formation time for both developers and non-developers. Especially for the 72-h and 96-h forecasts, the over-forecasting tendency leads to non-developing vortices meeting the threshold vorticity value of the developing vortices. The tendency for NOGAPS to forecast the non-developing deep layer wind shear to become increasingly easterly with time is considered to be a major factor in these over-forecasts of formation. Some adjustments in the cumulus parameterization heating and moistening plus convective momentum transport may improve these forecasts of tropical cyclone formation.

14. SUBJECT TERMS: Tropical Meteorology, Tropical Cyclone Genesis, Tropical Cyclone Formation Forecasts			**15. NUMBER OF PAGES** 139
			16. PRICE CODE
17. SECURITY CLASSIFICATION OF REPORT Unclassified	**18. SECURITY CLASSIFICATION OF THIS PAGE** Unclassified	**19. SECURITY CLASSIFICATION OF ABSTRACT** Unclassified	**20. LIMITATION OF ABSTRACT** UL

THIS PAGE INTENTIONALLY LEFT BLANK

PREDICTION OF TROPICAL CYCLONE FORMATION IN THE WESTERN NORTH PACIFIC USING THE NAVY GLOBAL MODEL

Caroline A. Bower
Captain, United States Air Force
B.S., Cornell University, 1999

Submitted in partial fulfillment of the

requirements for the degree of

MASTER OF SCIENCE IN METEROLOGY

from the

NAVAL POSTGRADUATE SCHOOL

March 2004

Author: Caroline A. Bower

Approved by: Patrick A. Harr
                        Thesis Co-Advisor

                        Russell L. Elsberry
                        Thesis Co-Advisor

                        Carlyle H. Wash
                        Chairman, Department of Meteorology

THIS PAGE INTENTIONALLY LEFT BLANK

ABSTRACT

The Tropical Cyclone Vortex Tracking Program is used to identify vortices in the western North Pacific from the Navy Operational Global Atmospheric Prediction System (NOGAPS) analyses and forecasts during May – October 2002 and 2003. Based on the NOGAPS analyses, several parameters are different between the 23 vortices that developed into storms during 2002 according to the Joint Typhoon Warning Center (JTWC) and the 231 vortices that did not develop. After eliminating 127 vortices that did not persist at least 24 h, this left 104 non-developing cases. For the developing circulations, the average 850-mb relative vorticity value at the first JTWC-warning time was $5.0 \times 10^{-5} \, s^{-1}$, with an easterly deep layer wind shear of $-1.8 \, m \, s^{-1}$. The average 850-mb relative vorticity maximum for the non-developing cases was $3.3 \times 10^{-5} \, s^{-1}$, with a westerly vertical shear of $4.1 \, m \, s^{-1}$. The NOGAPS model tends to over-forecast relative vorticity prior to formation time for both developers and non-developers. Especially for the 72-h and 96-h forecasts, the over-forecasting tendency leads to non-developing vortices meeting the threshold vorticity value of the developing vortices. The tendency for NOGAPS to forecast the non-developing deep layer wind shear to become increasingly easterly with time is considered to be a major factor in these over-forecasts of formation. Some adjustments in the cumulus parameterization heating and moistening plus convective momentum transport may improve these forecasts of tropical cyclone formation.

THIS PAGE INTENTIONALLY LEFT BLANK

TABLE OF CONTENTS

LIST OF FIGURES

THIS PAGE INTENTIONALLY LEFT BLANK

LIST OF TABLES

I. INTRODUCTION

Recent improvements in operational global models have lead to improvements in tropical cyclone track forecasting. Accurate 72-h track forecasts are now common, and 120-h forecasts have been issued beginning in 2003 because of their utility in military and civilian operations. The requirement to accurately forecast to 120 h makes it necessary that the models be able to forecast the entire lifecycle of a tropical storm within a single numerical model run. These global models must be able to forecast tropical cyclone formation, because a cyclone may form and intensify to a damaging storm within the 120-h forecast period. Accurate tropical cyclone formation forecasts would greatly enhance the ability of the U.S. Armed Forces to evaluate, plan, and execute any actions necessary to minimize damage or loss of assets or personnel.

An assessment of the current capabilities of operational global (dynamical) models is thus necessary to determine the potential for an accurate tropical cyclone formation forecast product. Such a product would provide a useful tool for determining which tropical cyclone precursors have the most predictive value in discriminating between developing and non-developing circulations. The first step towards developing a tropical cyclone formation product is to analyze the atmospheric variables at the time of formation.

A. FORMATION DEFINITION

The lack of a single unambiguous definition of tropical cyclone formation provides a significant challenge to both operational forecasters and researchers. Researchers may cite formation as occurring when an organized rotary circulation develops a warm core thermal structure and tangential winds decreasing with height (i.e., Enagonio and Montgomery 2001), or after the development of "a mesoscale, warm core vortex capable of self-amplification through air-sea interaction" (Davis and Bosart 2003). Both of these definitions lack the necessary objectivity required for use in operations, and require significant subjective interpretation by the forecaster or analyst.

Operationally, the Joint Typhoon Warning Center (JTWC) designated a circulation as a tropical cyclone when a specific tangential wind speed threshold is reached ($\geq$ 25 knots (kt) in the western North Pacific). Elsberry (2003) adds more

1

stringent requirements, requiring "a non-frontal, cyclonic circulation in the tropics that is closed (ground relative westerly on the equatorward side) with maximum 10-minute averaged surface sustained winds of at least 25 kt (12 m s^{-1}) that is accompanied by deep (throughout most of the troposphere) convection and a radius of maximum winds such that the Rossby number is at least one." The formation definition used here follows Elsberry (2003), with the additional requirements of a closed outer contour of 850-mb relative vorticity, and a minimum duration or persistence in the model analysis of at least 24 hours. Due to the ambiguity of determining the actual formation time for each developing cyclone, the specific formation time for a numbered circulation is assumed to be the time of the first warning issued by JTWC.

B.   TROPICAL CYCLONE FORMATION MECHANISMS

Tropical cyclone formation has long been associated with a set of necessary large-scale environmental conditions (e.g., Gray 1968). These conditions can be summed up as "high sea-surface temperature with a relatively deep ocean mixed layer, large values of absolute vorticity in the lower troposphere, weak vertical wind shear over a pre-existing disturbance, and mean upward motion" (Harr et al. 1996). In the presence of such environmental conditions, a disturbance often experiences tropical cyclone formation. Scientists understand that maintenance and enhancement of the necessary conditions in the large-scale tropical atmosphere is necessary, yet the actual mechanisms that cause or lead to the development of a warm core remain uncertain.

Davis and Bosart (2001) cite the importance of a pre-existing large-scale disturbance capable of organizing convection in the tropical cyclone formation process. This large-scale disturbance can be a synoptic baroclinic zone, the monsoon trough, or a monsoon depression. By concentrating potential vorticity, this large-scale disturbance allows the growth of the incipient tropical seed disturbance.

The process by which the seed disturbance becomes a coherent mesoscale circulation may not be a single mechanism, but a series of processes or events (Davis and Bosart 2001) that concentrate mesoscale vorticity. Possible processes capable of this undertaking that have been explored are the vortex interaction theories of Simpson et al.

(1997) and Harr et al. (1996), and formation from a wave in the tropical easterlies (Molinari et al. 2000).

The two prevailing formal theories of tropical cyclogenesis are conditional instability of the second kind (CISK) and wind-induced surface heat exchange (WISHE) (Molinari et al. 2000). Both of these theories can explain processes during the mature stage of a tropical cyclone, but do not sufficiently explain the interaction between the background synoptic environment and a mesoscale seedling disturbance.

Hypotheses for development of a tropical circulation generally include some sort of interaction between mesoscale and synoptic-scale systems. While synoptic- and planetary-scale features can be diagnosed using relatively coarse satellite imagery, and global model analyzes, the inability to verify these hypotheses provides a significant challenge to scientists due to the lack of mesoscale observations. Improved spatial and temporal resolution of satellite imagery over the tropical oceans adds value to the forecast process. However, the paucity of regular *in situ* observations continues to hinder verification of a single plausible mechanism for tropical cyclone formation. Given the challenge of actually verifying formation mechanism hypotheses, past research has often focused on tropical cyclone formation after a symmetric low-level circulation has already been established (Davis and Bosart 2001).

The ability of global models to accurately represent the thermodynamic conditions necessary for tropical cyclone formation, i.e., high sea-surface temperature and conditional instability with a moist mid-troposphere, is simplified by the lack of substantial daily variation of these variables. The global numerical models, even with relatively coarse spatial resolution, are capable of accurately resolving these slowly changing features. By contrast, the dynamic variables associated with tropical cyclone formation, i.e., low-level cyclonic vorticity and upper-level anticyclonic vorticity plus minimum vertical wind shear, vary on much shorter temporal and spatial scales and are thus more challenging to accurately resolve in the global numerical models.

The current predictability limit for mid-latitude synoptic-scale circulations is about five days. In the more slowly varying tropics, predictability of thermodynamic features may exceed the five-day mid-latitude threshold. However, given that a tropical

3

disturbance can develop, intensify, and dissipate in less than five days, the ability of the global model to accurately forecast this process is questioned.

C. TROPICAL CYCLONE FORMATION IN THE WESTERN NORTH PACIFIC

Adding another significant challenge to both tropical cyclone forecasters and modelers in the western North Pacific is the large number of potential seed disturbances that form year-round in the region. Prior to extensive analysis, over 300 potential seed disturbances were identified in the Navy Operational Global Atmospheric Prediction System (NOGAPS) model in the western North Pacific during 2002. Only 31 of these potential seedlings developing into tropical circulations that were later warned on by JTWC.

In the western North Pacific, monsoon conditions dominate the favored tropical cyclone formation regions. These include formation within and along the periphery of the monsoon trough, and from monsoon depressions and gyres. Non-monsoonal formations do occur north of the monsoon trough, but with far less frequency than monsoon-type formations.

1. Monsoon Trough

A significant number of tropical cyclone formations occur in the western North Pacific Ocean basin within the monsoon trough (Elsberry 2003) during the Northern Hemisphere summer. The monsoon trough is manifest as a cyclonic shear zone between the equatorial westerlies and trade-wind easterlies (Harr et al. 1996), and is characterized by high sea-surface temperatures, a conditionally unstable atmosphere with a moist mid-troposphere, and a region of weak vertical wind shear between strong westerly shear to the north and easterly shear to the south. Within the favorable background cyclonic vorticity of the synoptic-scale monsoon trough, cloud clusters easily develop. These cloud clusters are a known precursor to tropical cyclone formation (Simpson et al. 1997), and may potentially trigger tropical cyclone formation on the mesoscale.

Low-level convergence in the monsoon trough produces clusters of deep convection. Latent heat release within the deep convection helps to enhance the strength of these cloud clusters, and may allow for the formation of embedded mesoscale

4

convective systems (MCSs). As outlined by Elsberry (2003), mid-level mesoscale cyclonic vortices (MCVs) tend to spin up in the stratiform rain region behind the deep convection of a long-lived MCS as a result of vertical stretching of the atmospheric column between ascent in the upper-level cloud and subsidence below the cloud resulting from evaporation of the stratiform precipitation. The maximum amplitude of the MCV occurs in the middle troposphere between the 700 and 300 millibar (mb) levels where vertical stretching is maximized between low-level subsidence, divergence aloft, and the resulting horizontal convergence. The MCV is warm core above the level of maximum intensity, and cold core below it. Key requirements for the downward translation of the mid-level warm core vortex include a localized potential vorticity maximum and strong convergence in the low levels below the vortex, and an associated atmospheric warm anomaly. The actual mechanism for translating the warm core vortex from the mid-troposphere down to the surface remains uncertain (Davis and Bosart 2001), but once the warm core vortex is translated down to the surface, it can tap into the latent heat energy of the ocean (Nielsen-Gammon 1996), and CISK and WISHE may then processes begin to intensify the developing circulation. Harr et al. (1996) and Simpson et al. (1997) propose that MCS interactions within the monsoon trough can lead to merger of MCVs, downward extension of the merged circulation, and eventual development of the eye and inner rain band from these MCVs.

2. **Eastern Monsoon Trough**

The eastern end of the monsoon trough is also highly favored for tropical cyclone formation (Elsberry 2003). In this region, the confluence of tradewind easterlies and equatorial westerlies produces favorable low-level convergence and cyclonic vorticity, and deep convection is favored. Ritchie (1995) and Holland (1995) associate the preferential formation in this region as a result of a wave-energy accumulation from westward-propagating waves in the easterly flow. The actual presence of low-level easterly waves in the western North Pacific remains uncertain though the regression analysis and band-pass filtering studies of Sobel and Bretherton (1999) indicate the presence of such waves in the easterly flow. With no other obvious synoptic-scale features present at the time of tropical cyclone formation, mesoscale features likely play a substantial, though as yet unobserved, role in formation.

5

D. PLAN FOR THESIS

The 2002 NOGAPS model analysis and forecast fields will be analyzed for developing and non-developing circulations to determine threshold values for specific forecast variables that distinguish the developing from non-developing vortices. These thresholds will then be applied to define false alarms during 2002. The false alarm is defined when the NOGAPS model forecast development to surpass the threshold for circulations that were not eventually numbered or warned on by JTWC. The threshold values will also be applied to storms that developed in 2003, and the NOGAPS forecasts of non-developing circulations during the same year.

The NOGAPS model data and the analysis procedures will be described in Chapter II. Developing and non-developing circulations identified in Chapter II will be presented in Chapter III. Developing circulations, identified as those numbered by the Joint Typhoon Warning Center (JTWC) from 1 May – 31 October 2002, are examined as a whole, and also broken into several subsets to highlight potential formation indicators and proxies for formation among several selected atmospheric variables. These subsets include formation subregion and formation time relative to a formation time window determined for each storm by the JTWC. Non-developing vortices are examined in a similar fashion to the developing circulations. Additionally, several subsets of the non-developing circulations dataset are examined: model false alarms and model over-forecasts. Developing and non-developing circulations from 2003 are also presented, as well as two case studies from 2002.

II.   METHODOLOGY

A large number of analyzed and forecast fields must be examined to assess the potential for tropical cyclone formation. The technique summarized here uses the Tropical Cyclone Vortex Tracking Program (TCVTP) developed by Professor Patrick Harr. This program, which is summarized in Figure 2.1, searches model-analyzed and forecast vorticity fields to define circulation centers that may or may not develop into tropical cyclones. It provides an objective method to detect vorticity centers at the 850-mb level and matches forecast circulation centers with analyzed circulation centers at the verification time. For each circulation, a series of formation-related environmental parameters relative to each circulation center is extracted throughout its life cycle.

A.   MODEL DATA

The model fields used in the analysis (Table 2.1) are Navy Operational Global Atmospheric Prediction System (NOGAPS) version 4.0 (Hogan and McClune 2002) analyses and forecasts at 12, 24, 36, 48, 60, 72, 84, 96, and 120 hours. Since the area of interest is the western North Pacific Ocean, the spatial domain covers 105°E – 180°E, and from the Equator to 30°N. Model resolution is one degree latitude and longitude and the time resolution is 12 hours (00 UTC and 12 UTC) for the analysis fields and six hours for the forecast fields. The period of study is from 1 May – 31 October 2002.

Table 2.1. NOGAPS fields used in TCVTP analysis.

850 mb relative vorticity (10^{-5} s^{-1})
Shallow layer vertical wind shear (500 – 850 mb) (m s^{-1})
Deep layer vertical wind shear (200 – 850 mb) (m s^{-1})
Geopotential height thickness (200 – 1000 mb) (gpm)
Shallow (1000 – 500 mb) warm anomaly (K)
Surface latent heat flux (W m^{-2})
Total (convective plus grid scale) precipitation (kg m^{-2})
Vertical motion (Pa s^{-1})
Vapor pressure (500 – 700 mb average) (Pa)
Sea-level pressure (SLP) (mb)
925-mb wind speed (m s^{-1})
700-mb wind speed (m s^{-1})
500-mb wind speed (m s^{-1})

B. ANALYSIS PROCEDURES

Figure 2.1 is a summary of the steps in the TCVTP algorithm. The TCVTP total system is designed to identify, track, catalog, and summarize tropical circulations within numerical model analyzed and forecast fields. Figure 2.1a is a summary of the databases and catalogs generated by the TCVTP process, and Figure 2.1b is an extension of the TCVTP algorithm that extracts, identifies and catalogs tropical circulations within the model analysis and forecast fields. Individual steps within the TCVTP algorithm are indicated by the number on the left side of Figure 2.1b.
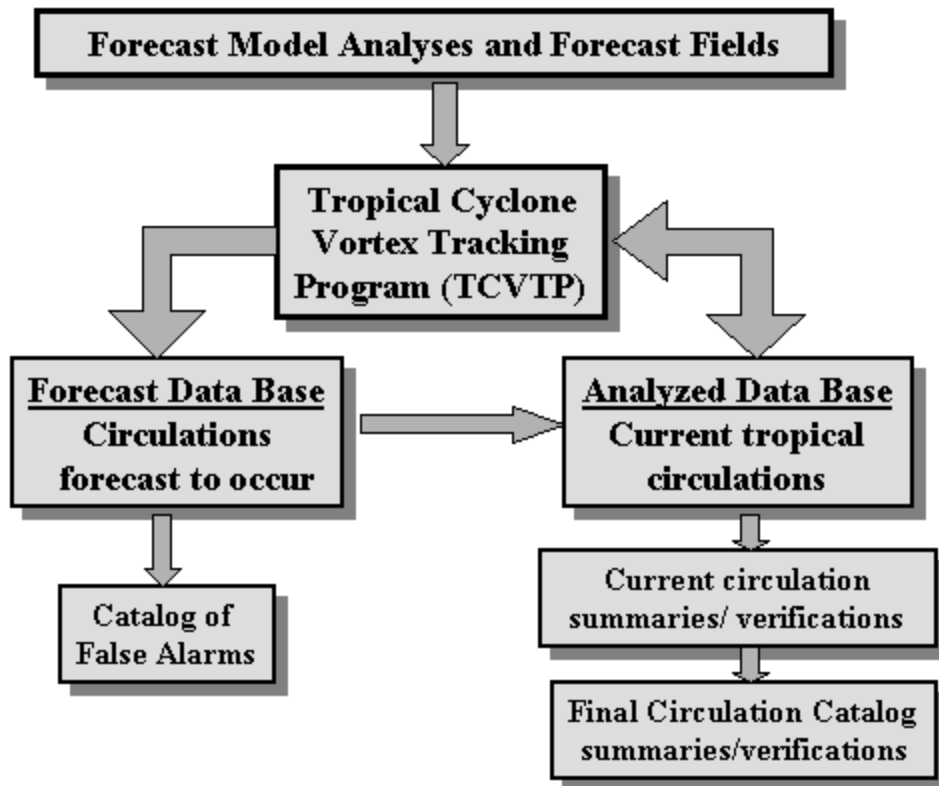
Figure 2.1a. Summary of steps used in the TCVTP algorithm.

1. Analyzed Circulation Identification

As part of the first step in Figure 2.1b, 850-mb relative vorticity from each NOGAPS initial analysis is computed to identify each circulation. All relative vorticity maxima greater than 1.5×10^{-5} s^{-1} are identified as trackable circulations. In previous research by Dorics (2002) for the North Atlantic, the minimum vorticity threshold was set to 1.0×10^{-5} s^{-1}. The threshold of 1.5×10^{-5} s^{-1} is used for western North Pacific vortices

Tropical Cyclone Vortex Tracking Program (TCVTP)

1 — Circulations identified in current analysis

2 — Does this match a pre-existing circulation?

YES
Link with current circulation file in Analyzed Database

NO
Create new circulation file in Analyzed Database

3 — Loop through current forecast sequence Tau = 06, 12, ..., 120

Identify forecast circulations

4 — Do forecast circulations match analyzed circulations?

YES
Add forecast circulation to Analyzed Database

NO
Store circulation as unclaimed forecast in Forecast Database

Figure 2.1b. Expansion of steps contained in TCVTP block of Figure 2.1a.

due to the more cyclonic monsoon trough environment. The 850-mb relative vorticity field for the current model analysis is examined first. An ellipse is fit to each trackable circulation with an outer closed vorticity contour of at least 1.5×10^{-5} s^{-1} (Figure 2.2). The center of the ellipse is defined at the position of the relative vorticity maximum. The ellipse-fitting routine is based on a bivariate normal probability distribution and spans the

9
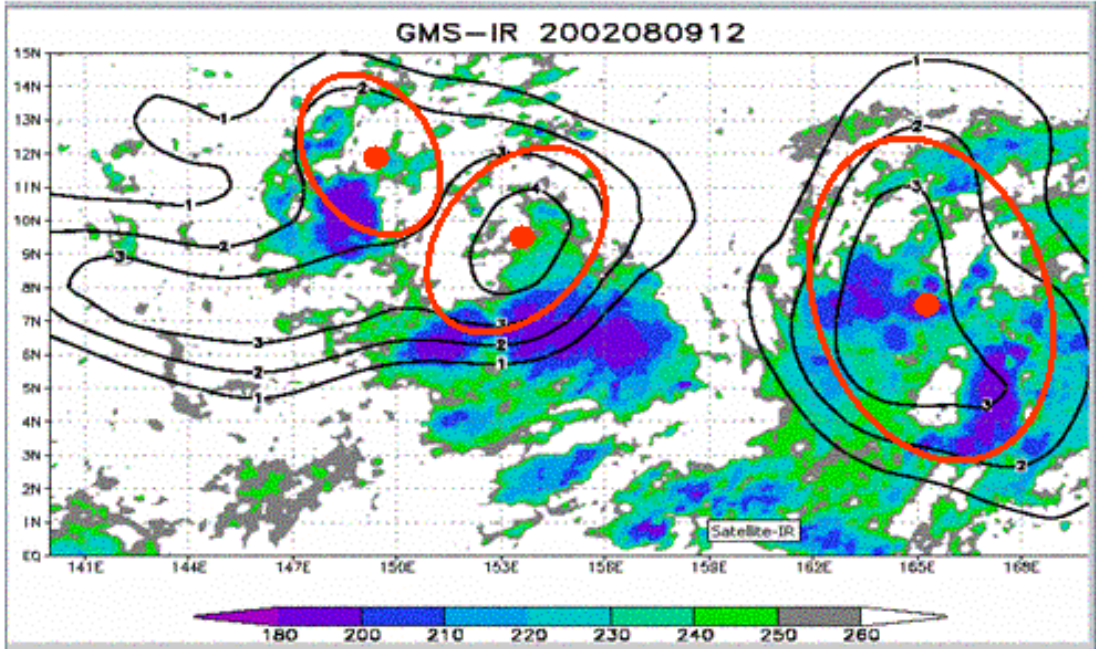
Figure 2.2. Example of ellipses (red lines) fit to an analyzed vorticity field (x 10^{-5} s^{-1}; solid lines) by the TCVTP. The large dots indicate the TCVTP-identified circulation centers. Shading defines cloud-top temperatures derived from infrared satellite imagery.

0.95 probability levels of the distributions. Thus, the size of the circulation is characterized by the area enclosed by the ellipse. Each circulation is given a unique designator related to the time and location and is then saved into the Analyzed Database (right box in Figure 2.1a). This vorticity analysis process is repeated for each model forecast time.

2. Identifying Tracks of Analyzed Circulations

To generate a vortex track, circulations identified in the current model analysis using the process outlined in the Step 1 are compared to circulations identified in the previous 12-hour analysis. This comparison forms the basis of step 2 of Figure 2.1b, and determines if a recently identified circulation can be matched to a previously identified circulation stored in the Analyzed Database of the TCVTP (right box in Figure 2.1a). This directory contains all previously analyzed circulations that are currently active. The distance and direction of the new circulation relative to each previous circulation are used to match circulations in the current analysis with previously analyzed circulations.

The distance and direction criteria vary based on the translation speed of the analyzed circulation (Table 2.2). If the prior translation speed is small (less than 5 kt),

the allowable direction orientation to the new circulation is relaxed to a circle to allow for a stalled situation. When a circulation from the current analysis is matched to a pre-existing circulation, it becomes the next point of the circulation track. If the circulation cannot be matched to a pre-existing circulation, it is stored as a new vortex to be potentially matched in the next analysis.

Table 2.2. Summary of speed and distance criteria used by the TCVTP algorithm to potentially match forecast circulations to analyzed circulations.

Speed	Distance change in 6 h	Direction change
Slow ($\leq$ 5 kt)	$\leq$ 50 km	360°
Medium (6-15 kt)	51-150 km	+/- 90°
Fast (> 15 kt)	> 150 km	+/- 45°

Information used to identify and characterize each circulation via the ellipse parameters is given in Table 2.3. Analyzed circulations are assigned a unique identifier (wpcyyyymmddhh_ll_nnn), where wpc designates a western North Pacific circulation, yyyy is the year, mm the month, dd the day, hh the time in UTC, ll the initial latitude, and nnn the initial longitude corresponding to the time and location of the first appearance of the circulation in the NOGAPS analysis (+00). Tracks are thus identified by the designation given to the first analyzed circulation position in the series. Each circulation is also described by the circulation size (number of grid points within the ellipse fit to the outer closed vorticity contour), shape (lengths of major and minor axes, angle of major axis with respect to north), and orientation of the ellipse with respect to the bivariate distribution (Table 2.3). These data are used to regenerate the ellipse during post-analysis. The data in Table 2.3 are then used to generate a history file unique to each analyzed circulation.

Table 2.3. Information used to identify each circulation and characterize the ellipse fitted to each analyzed circulation (after Dorics 2002 Table 2.2).

Vortex identification & model prognosis		Vortex (ellipse) specification
Name	wpcyyyymmddhh_ll_nnn	Size (number of enclosed grid points)
Model DTG	yyyymmddhh	Shape (ratio of major/minor axes)
Forecast time (tau)	ttt	Ellipse major axis (km)
Latitude (°N)	ll	Ellipse minor axis (km)
Longitude (°E)	nnn	Ellipse angle (relative to North)
		Bivariate distribution correlation

In addition to the identification and ellipse characteristics, the NOGAPS fields listed in Table 2.1 are used to calculate average values over the ellipse of other atmospheric variables that characterize each circulation. As listed in Table 2.4, maximum or minimum and the average value for each variable are calculated for the entire ellipse, or for each quadrant. These values then characterize the vortex environment for each model analysis and forecast time in terms of variables that are commonly associated with tropical cyclone formation. As a circulation is tracked in the analyses or forecasts, a history file of the variables in Table 2.4 is created, with one line per analysis or forecast time. Comparisons of the analyzed and forecast history files will form the basis of the analysis of the model forecast accuracy.

3.   Forecast Circulation Identification

The same ellipse-fitting process described in section II.A.1 is applied to all 850-mb relative vorticity forecast fields from the current model integration (step 3 of Figure 2.1b). An ellipse is fit to each forecast relative vorticity maximum that meets the threshold criterion to define circulations from each forecast time in the current model integration. All variables listed in Tables 2.2 and 2.4 are assigned to forecast circulations as well.

After the circulations in the 6-hour forecast fields are identified, they are matched, if possible, to circulations that were identified in the current (+00) analysis. Similarly, circulations tracked in the 12-hour forecast field are matched, if possible, to circulations in the 6-hour forecast field. This process continues to the 120-hour forecast and defines the track of each forecast vortex. The track is continued until a vortex can no longer be identified in the forecast vorticity fields. In the vortex history file, a line is added for each forecast field (i.e., +06, +12, …+120) to summarize the location, ellipse parameters, and model forecast environmental parameters.

If a vortex is identified in a forecast field, but was not matched with a previously analyzed vortex, it is classified as a "forecast vortex." Forecast vortices are named based on the DTG of the model integration, location, and forecast time in which they first appear. Although the history files for these cases are written as defined with analyzed vortices, the files are stored as "unclaimed forecasts" in the Forecast Database in Figure 2.1a.

Table 2.4. Values tracked by the TCVTP for each atmospheric variable.

	Quadrant	Ellipse		
Variable	Average	Average	Maximum	Minimum
Relative vorticity (10^{-5} s^{-1})		X		
Shallow layer vertical wind shear (500 – 850 mb) (m s^{-1})		X		
Deep layer vertical wind shear (200 – 850 mb) (m s^{-1})		X		
Geopotential height thickness (200 – 850 mb) (gpm)	X	X	X	
Warm anomaly (1000 – 500 mb) (K)	X	X	X	
Surface latent heat flux (W m^{-2})	X	X	X	
Total precipitation (kg m^{-2})	X	X	X	
Vertical motion (Pa s^{-1})	X	X	X	
Vapor pressure (500 – 700 mb average) (Pa)	X	X	X	
Sea-level pressure (SLP) (mb)	X	X		X
925 mb wind speed (m s^{-1})	X	X		
700 mb wind speed (m s^{-1})	X	X		
500 mb wind speed (m s^{-1})	X	X		

4.   Linking Forecast Circulations from Previous Model Integrations with Analyzed Circulations from the Current Model Integration

The unclaimed forecasts catalog in the Forecast Database (left box of Figure 2.1a) contains all forecasts not yet matched to an analyzed circulation. In step 4 of Figure 2.1b, all unmatched forecast circulations from previous model integrations are next compared to the analyzed circulations from the current model integration. When the matching criteria are first met, that unclaimed forecast circulation is attached to the analyzed circulation and becomes the formation forecast for the analyzed circulation.

5.   Finalization of Tracks and Forecasts

At the completion of the TCVTP process shown in Figure 2.1b, only two outcomes are possible: finalization of a tracked circulation, or failure to successfully match a forecast circulation with an analyzed circulation. A tracked circulation is finalized when no subsequent model analyses contain a circulation that can be matched with an existing track. When this occurs, the track is finalized and stored in the Final Circulation Catalog (bottom right box of Figure 2.1a). The circulations stored in the final circulation directory represent the data available for further analysis. When a forecast

circulation cannot be successfully matched to an analyzed circulation, the forecast circulation is stored as a potential false alarm (bottom left box of Figure 2.1a).

C. QUALITY CONTROL AND POST-PROCESSING

As with any automated process, quality control measures are necessary when analyzing model fields with the TCVTP. The program identifies only circulations that meet the specified threshold criteria (e.g., outer closed relative vorticity contour). Additionally, individual circulations are matched to form tracks only when the translation speed and track orientation threshold criteria are met. Data gaps due to non-availability of NOGAPS data fields also may result in tracking errors. Since the TCVTP program is presently not coded to detect such data gaps, a review of the objectively analyzed tracks is required to correct for such errors. Additionally, human interaction is required to associate TCVTP vortices with specific named storms if comparisons of model forecasts and observed storm tracks are required.

III. ANALYSIS AND RESULTS

A. TRACKED VORTICITY CIRCULATIONS

The TCVTP was used to track all circulations meeting the threshold 850-mb relative vorticity criterion in the tropical western North Pacific from 1 May – 31 October 2002. The resulting 254 tracked circulations were further sampled to remove all circulations that did not survive at least one diurnal cycle, which requires existence of the circulation center in three consecutive model analyses separated by 12 h. Hennon and Hobgood (2003) used a similar duration criterion, which eliminates short-term convectively-driven circulations and one-time spurious circulations spun up by anomalous wind observations. By using this minimum duration criterion, the number of potential vortices was decreased to 127 (columns one and two in Table 3.1). The average duration of these 127 vortices was 4.2 days. Vortices that did not meet the minimum duration criterion, but did satisfy the over-forecast criteria (ND2) (discussed later in this section), are included in column 3 of Table 3.1. Additionally, each circulation identified by the TCVTP was assigned to one of three formation regions based on the initial latitude less than 30ºN and longitude (see subregion definitions in Table 3.1).

The vortices that met the minimum duration criterion were further separated into developing, non-developing, and false alarm categories. Storms were considered "developers" if at least Tropical Depression (TD) strength (Table 3.2) was reached, and

Table 3.1. Circulations tracked in NOGAPS analyses from 1 May – 31 Oct 2002 numbered by the JTWC (column 1), non-developing circulations meeting the minimum duration criterion of at least 24 h (column 2), those non-developing circulations not meeting the minimum duration criterion but meeting the over-forecast criteria (column 3), and those that did not meet the minimum duration criterion, but had 850-mb relative vorticity forecasts exceeding 5.0×10^{-5} s^{-1} (column 4), or judged to be model false alarms (column 5) in each of the tropical subregions.

Formation Subregion	Numbered TCs	ND $\geq$ 24 h (ND1)	ND < 24 h (NDOF)	ND $\geq$ 24 h (NDG2)	Model False Alarms
South China Sea (105E-124E)	5	34	16	19	4
Philippine Sea (125E-159E)	10	49	28	21	10
East Monsoon Trough (160E-180E)	8	21	16	10	1
Total	**23**	**104**	**60**	**50**	**15**

the circulation was thus given a number by the Joint Typhoon Warning Center (JTWC). During the period of study, only 23 circulations reached at least TD strength, with six each reaching STY and TY, eight reaching TS status, and three reaching only TD (Tables 3.3 – 3.5). Twenty-two of these developing cyclones were present in the NOGAPS analyses prior to the first JTWC warning time (intensity $\geq$ 25 kt). One "surprise" cyclone was not present in the NOGAPS analysis prior to the first warning time. That is, the NOGAPS analysis did not include the storm (TD 27) until a synthetic vortex was inserted upon receipt of the JTWC warning message. Vortices were considered "non-developers" if they did not reach at least TD strength as defined by JTWC.

All circulations were sorted into two categories: circulations that met the minimum duration criterion (ND1) and circulations that did not (ND2). Circulations that did not meet the minimum duration criterion are the subset of NOGAPS-forecast vortices that could be matched with a vortex in the NOGAPS analysis for less than the required 24 h, but were forecast to live much longer. If the NOGAPS model forecast the vortex to exist longer than 24 hours, but the analyzed circulation did not persist for 24 hours, then the forecast vortex is categorized as an over-forecast (NDOF).

Model false alarms (column 5 of Table 3.1) were identified as forecast vortices that could not be matched to a circulation in the verifying analysis. In the TCVTP system, these are tracked forecast circulations in the forecast database (Figure 2.1a) that never get moved to the analyzed circulation database. The number of false alarms in each subregion is listed in column five of Table 3.1. Cheung and Elsberry (2002) also found that NOGAPS was more skillful (fewer false alarms) in the South China Sea (SCS) and Eastern Monsoon Trough (EMT) than in the Philippine Sea (PS).

Table 3.2. Tropical cyclone designations used by the JTWC, where 10-minute average wind speeds are used.

Description	Maximum Sustained Wind Speed
Tropical Depression (TD)	12-17 m s^{-1} (25-34 kt)
Tropical Storm (TS)	18-32 m s^{-1} (35-63 kt)
Typhoon (TY)	33-66 m s^{-1} (64-129 kt)
Super Typhoon (STY)	> 67 m s^{-1} (130 kt)

1.   South China Sea Formation

The presence of the monsoon trough in this subregion (McBride 1981) makes it a favored region for potential tropical cyclone seedling development (Figure 3.1), with 30.7% (39 of 127) of the analyzed vortices during the study period present in the SCS subregion. The frequent occurrence of a broad area of background cyclonic vorticity between cross-equatorial westerlies and easterlies to the north contributed to the relatively large number of non-developing circulations in the NOGAPS analyses. However, the number of vortices that developed to TD strength or greater was only five of 23 (21.7%) (Table 3.3). Consequently, only five of the 39 (12.8%) potential tropical cyclone seedlings in the NOGAPS analyses developed to warning status. Conversely, many more (87.2%) of the potential seedlings in the SCS in the NOGAPS analyses never achieve TD status. These may be weak monsoon depressions (perhaps with considerable precipitation and winds in rain bands at large radii), or may be spurious vortices that persisted in the analyses for 24 h. The average duration of both developing and non-developing vortices in this basin was 3.7 days, which is less than in the other basins due to the small size and limited fetch of this subregion.
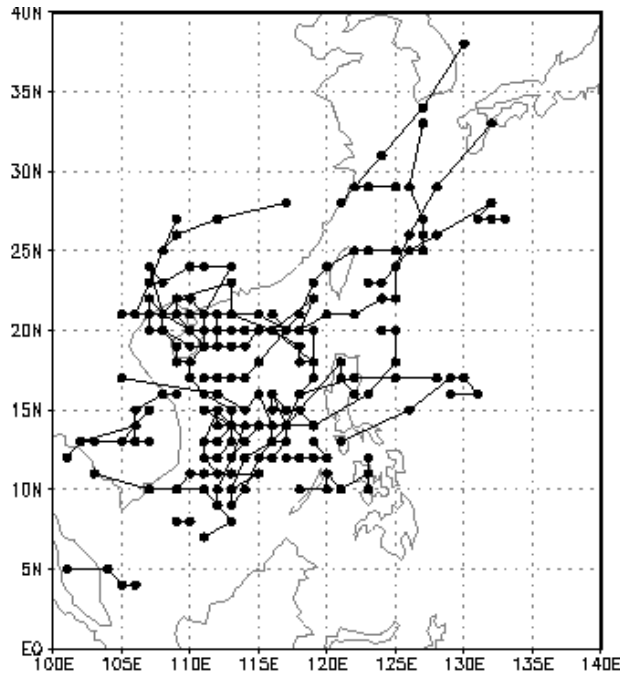
Figure 3.1.   Tracks of 39 vortices in the NOGAPS analyses that formed in the SCS (105°E - 125°E) subregion from 1 May – 31 October 2002.

Table 3.3. Maximum intensity (see definitions in Table 3.2) during the life cycle and formation month of numbered tropical cyclones in the SCS subregion.

	May	Jun	Jul	Aug	Sep	Oct	Total
TD	1	0	0	0	0	0	**1**
TS	0	0	1	0	2	0	**3**
TY	0	1	0	0	0	0	**1**
STY	0	0	0	0	0	0	**0**
Total	**1**	**1**	**1**	**0**	**2**	**0**	**5**

2.   Philippine Sea Formation

The Philippine Sea (PS) subregion, which is also characterized by a broad area of cyclonic relative vorticity (McBride 1981) associated with the monsoon trough, was the most active of the three subregions studied, with 59 of 127 (46.5%) circulations (Figure 3.2).   During the study period, 10 of the 23 vortices (43.5%) that developed to TD strength or greater formed in the PS region (Table 3.4). However, these 10 named vortices represent only a 16.9% formation rate in terms of the circulations in the NOGAPS analyses. As in the SCS, many of the non-developing vortices in the NOGAPS analyses are probably monsoon depressions that never achieve TD status with central convection and high winds. The average duration of vortices in this region was 4.1 days.
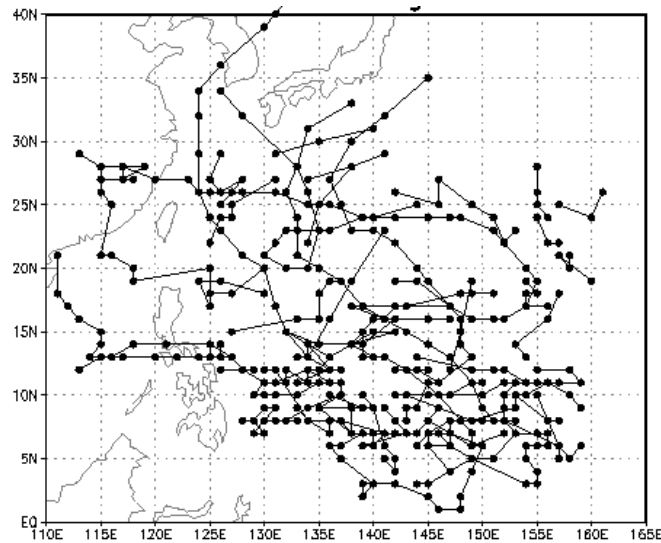
Figure 3.2. Tracks of 59 vortices in the NOGAPS analyses that formed in the PS (125°E - 160°E) subregion from 1 May – 31 October 2002.

18

Table 3.4. Maximum intensity by formation month as in Table 3.3, except for numbered tropical cyclones in the PS subregion.

	May	Jun	Jul	Aug	Sep	Oct	Total
TD	0	0	0	0	0	0	**0**
TS	0	0	1	2	0	1	**4**
TY	0	1	1	1	0	1	**4**
STY	1	1	0	0	0	0	**2**
Total	**1**	**2**	**2**	**3**	**0**	**2**	**10**

3.   East Monsoon Trough Formation

The east monsoon trough (EMT) subregion, which extends from 160°E to 180°E, had 29 of the 127 (22.8%) circulations tracked by the TCVTP in the NOGAPS analyses during the study period (Figure 3.3). During the study period, only eight of the 23 (34.8%) vortices that developed to TD strength or greater formed in the EMT subregion (Table 3.5). These eight JTWC-numbered circulations represent 27.6% of the 29 tracked vortices verifying in the NOGAPS analyses. The average duration of vortices within general area of the east end of the monsoon trough was 5.0 days, which is the longest of the three subregions studied. Although this subregion is also relatively small, vortex duration is greater than in the other two regions due to the large distance from land. Perhaps for the
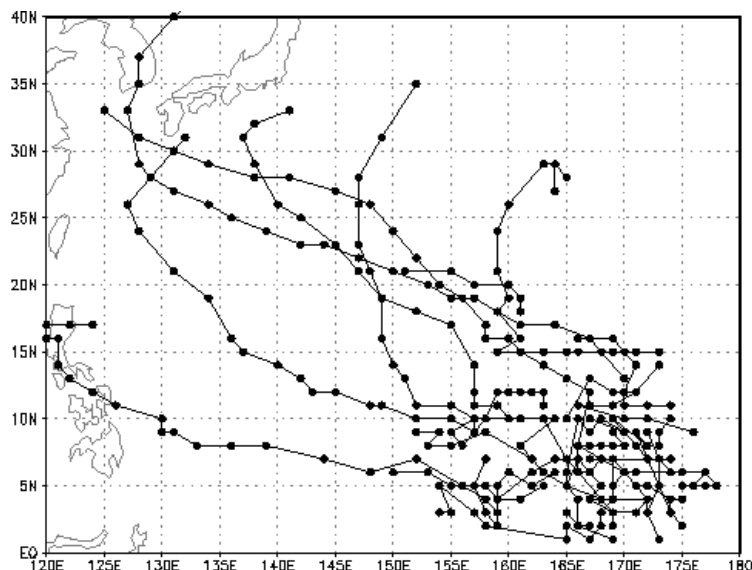
Figure 3.3. Tracks of 29 vortices in the NOGAPS analyses that formed in the EMT (160°E - 180°E) subregion from 1 May – 31 October 2002.

19

same reason, the cyclones that developed within the EMT subregion also achieved, on average, a greater maximum intensity than cyclones that developed in the other two regions. One factor favoring formation and intensification within this region is the extensive area of cyclonic vorticity associated with the oceanic monsoon trough when tropical cyclones form at the eastern end.

Table 3.5. Maximum intensity and formation month as in Table 3.3, except for numbered tropical cyclones in the EMT subregion.

	May	Jun	Jul	Aug	Sep	Oct	Total
TD	0	0	1	0	0	1	**2**
TS	0	0	1	0	0	0	**1**
TY	0	0	0	1	0	0	**1**
STY	0	0	2	1	1	0	**4**
Total	**0**	**0**	**4**	**2**	**1**	**1**	**8**

B.   TROPICAL CYCLONE FORMATION ALERT MESSAGES

In this section, an overall summary of tropical cyclone formation is given with respect to official forecasts and tropical cyclone formation alert (TCFA) messages issued by the JTWC. This summary is provided as a baseline by which the model forecast performance of tropical cyclone formation, which is discussed in the next section, may be compared.

The JTWC issues a TCFA based on wind and pressure analyses at the surface/gradient level, 500 mb, and 200 mb, and a subjective Dvorak analysis of satellite imagery (see Appendix A). Such formation alerts are valid for 24 hours, and they may be either extended or cancelled at the end of the valid period depending on the current status of the circulation center. If the circulation develops to tropical depression strength (Table 3.2), the first warning issued for the system replaces the TCFA. All TCFA messages were gathered from the Automated Tropical Cyclone Forecast (ATCF) database maintained at the Naval Research Laboratory – Monterey.

The TCFA applies within a formation box specified as an area on either side of a line defined by two grid points. Alternately, a formation circle may be specified by a single grid point and radial distance. The size of the formation box or circle is subjectively determined by the forecaster's confidence in the objective aids. The

temporal window during which tropical cyclone formation is expected to occur is provided in each TCFA. Additionally, an estimate of the wind speed, translation speed, and heading of the developing circulation is provided, along with the location of the center of the circulation determined from satellite imagery. Latitude and longitude positions contain a "checksum" at the end of each string. The checksum is calculated by summing the numbers in the latitude or longitude value, and then the last digit of the value is listed at the end of the string, e.g., latitude 147.7E9 sums to 19, and 9 is encoded as the checksum. A sample of the text portion of the TCFA (for STY05 - Hagibis) follows:

```
FORMATION   OF   A   SIGNIFICANT   TROPICAL   CYCLONE   IS
POSSIBLE  WITHIN  160  NM  EITHER  SIDE  OF  A  LINE  FROM
3.5N7 147.7E9 TO 9.4N3 145.6E6 WITHIN THE NEXT 06 TO
24  HOURS.    AVAILABLE  DATA  DOES  NOT  JUSTIFY  THE
ISSUANCE OF NUMBERED TROPICAL CYCLONE WARNINGS AT THIS
TIME.   WINDS  IN  THE  AREA  ARE  ESTIMATED  TO  BE  15  TO  22
KNOTS.    METSAT   IMAGERY   AT   131430Z2   INDICATES   THAT   A
CIRCULATION CENTER IS LOCATED NEAR 4.7N1 148.9E2.  THE
SYSTEM IS MOVING NORTHWESTWARD AT 10 KNOTS.
```

During 1 May – 31 Oct 2002, the JTWC issued 32 TCFAs (excluding the TCFAs for TD17 and TD27). For six storms (STY05, TY07, TY09, TD15, TS24, and TY26), two TCFAs were issued with nominal changes between the first and the second. In general, changes were made to extend the formation forecast window if the formation had not occurred within the specified time, but was still expected to occur. The formation box or circle was also slightly modified to account for motion of the developing circulation. Six of these 32 TCFAs were false alarms (two in August, and four during one week September). For these six TCFAs, the circulation center dissipated or weakened significantly, and therefore a warning was never issued. In two cases (STY10 and TS16), no prior TCFA had been issued before the first warnings were issued.

1. Lead Time

Lead time (? t) was defined as the time between the issuance of a TCFA and the first warning time. The average ?t for successful TCFAs was 12.1 hours. Maximum and minimum ?t values ranged from zero hours for STY05 to 42 hours for TY09 and TD15 (Figure 3.4). TCFAs were reissued for all TCFAs that did not verify within 24 h to extend the formation spatial and temporal windows (R. Leejoice, JTWC, personal
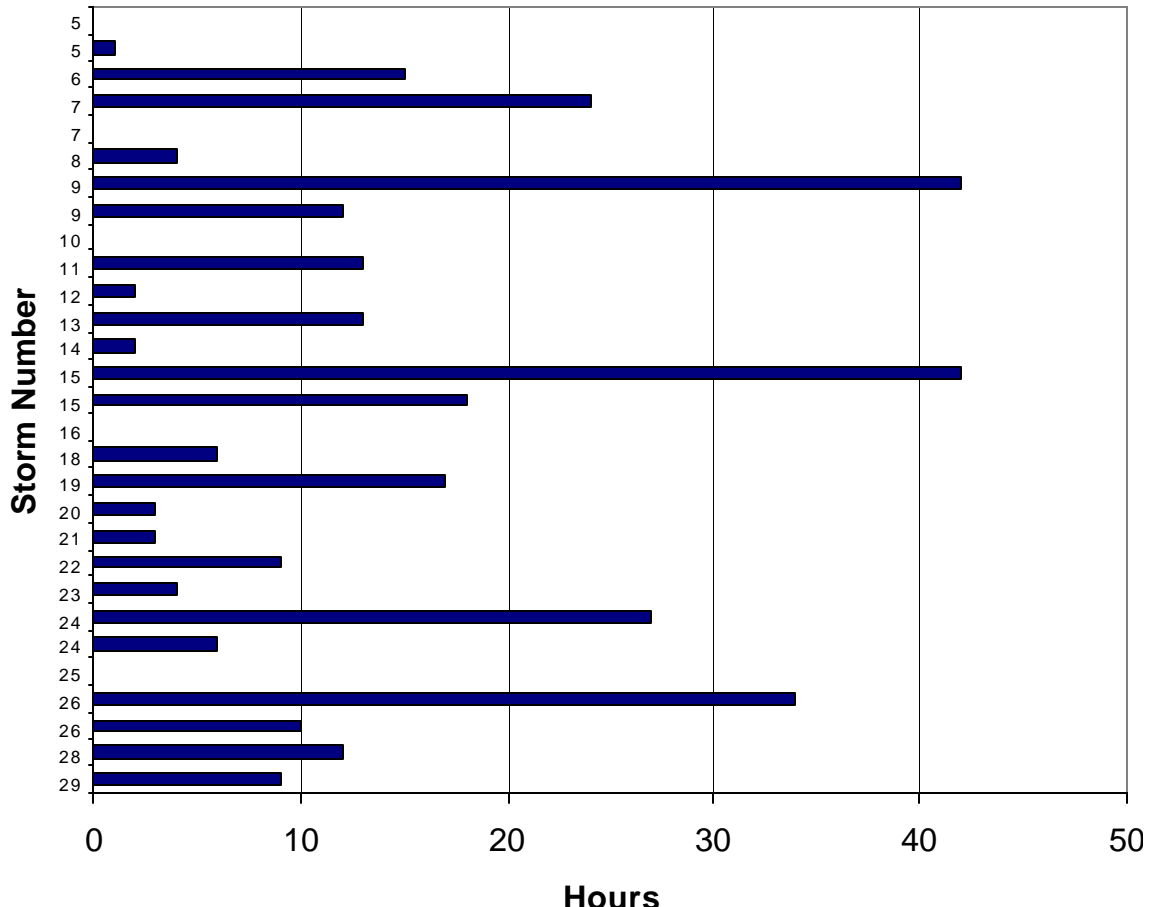
Figure 3.4. Lead time (?t) of the TCFAs for developing storms. Bars indicate the number of hours between the TFCA issue time and the first JTWC warning time. The ?t for the first TCFA for STY05 and STY25 and second TCFA for TY 07 was less than 1 hour. TCFA messages were not issued for STY10 and TS16. Repeated numbers indicate multiple TCFAs issued for a single storm.

communication). No ?t was calculated for STY10 or TS16 since no TCFA was issued prior to the first warning for either the storm.

2. Formation Window

A formation window, which indicates when a circulation is expected to reach tropical depression strength, is specified in each TCFA. This window is generally 6-24 hours but can range from 8-24, or 12-24 hours. The onset of the formation window is more a function of the individual forecaster than of model certainty (S. Vilpors, JTWC, personal communication). Verification of the formation window (Table 3.6), which is scored as a success if the issuance of the first JTWC warning occurred within that window, which only occurred in 11 (41%) of the 27 available TCFAs. Of the 16 (59%) TCFAs that failed to result in a formation within the specified time window, 11 (61%)

22

first warnings were issued prior to the onset of the formation window (i.e., formed too early), and five (19%) first warnings occurred more than 24 hours after the TCFA was issued (i.e., formed too late). All five of these late forecasts were reissued to extend the formation window. Of the 11 TCFAs that verified prior to the onset of the formation window, nine (82%) of the first warnings were less than 4 hours from the time of TCFA issue.

Table 3.6. Summary of formation times (first JTWC-issued warning) relative to TCFA-specified formation window.

Formation Time	Number of Occurrences
Outside of specified window	**16**
Early	11
Late	5
During specified window	**8**
Total	**24**

C.   VERIFICATION OF FORECAST VARIABLES

Thirteen variables listed in Table 2.1 were recorded based on the vortex representation defined by the TCVTP. Of those 13 variables, five were selected as having some measure of utility for forecasting the formation of the developing vortices. Those six variables were: 850-mb relative vorticity (VOR), 200-850 mb or deep wind shear (DSH), sea-level pressure (SLP), 925-mb wind speed (925), and 500 – 700 mb average vapor pressure (VPR). Whereas the database contained three wind speed variables (at 925, 700, and 500 mb) that were potentially useful in forecasting tropical cyclone formation, the 700- and 500-mb wind speed variables did not show a distinct signal for identification of developing vortices, and so were not added to the list of selected variables. Several other variables were not selected since they represent derived quantities that are based on model formulations rather than analyzed variables. These model-diagnostic variables did not appear to contain as much information regarding the formation condition as those variables based on analyzed quantities. Other measured variables, i.e., 200-850 mb thickness, and 500-850 mb wind shear, showed little or no signal for distinguishing developing from non-developing vortices, and so were not included in the list of selected variables.

The five selected variables were then analyzed to determine their utility at forecasting the potential development or non-development of the circulation dataset. The impact of the selected variables on the developing vortices, i.e., those numbered by JTWC during 1 May – 31 Oct 2002, were analyzed first. Each selected variable was examined at 12-h intervals extending from 120 h prior to and 120 h after the first JTWC warning and first Best-Track times. For each time step, the range, mean, and standard deviation of each variable were calculated. Threshold values for each variable at the first JTWC warning time and first Best-Track time were determined, and will be used as a benchmark for the comparison of non-developing vortices.

These statistics will be displayed based on the NOGAPS forecast verification time relative to the first JTWC warning (e.g., Figure 3.5) or the first Best-Track time (e.g., Figure 3.6). Since these are the first of many such displays, some extended comments on Figure 3.5 will be made to introduce the figures. A representative sampling of forecast times (i.e., 24 h, 48 h, 72 h, and 96 h) are presented in the four panels. For each forecast interval, the average analyzed (at +00) value is plotted against the average forecast value for the indicated forecast verification time, with the range, mean, and standard deviation at each time interval relative to the first JTWC warning time in Figure 3.5. The average forecast value (red line) is only displayed if five or more cases were available at each time interval. This minimum sample size criterion will be relaxed for a handful of variables in which fewer than five cases were available for analysis. Statistical significance was calculated for the differences in the means of the forecast and analyzed variable using a two-tailed t-test, and significant differences are indicated in the following figures by a dark-shaded box plot.

Consider first the 24-h forecast verifications in the upper left panel of Figure 3.5. A difference between the mean forecast (heavy red line) and analyzed (heavy black line) 850-mb vorticity of the circulations is first noted at 36 h prior to the first JTWC warning time. These mean values then are the averages of all 24-h forecasts verifying at 36 h prior to the first warning time, which means that these 24-h forecasts were initiated at 60 h prior to the first warning time. Looking at the sample size at –36 h, only 18 such 24-h forecasts are available from the 23 developing storms, which means that in five cases, even a 24-h forecast initiated 60 h prior to the first warning time did not exist for
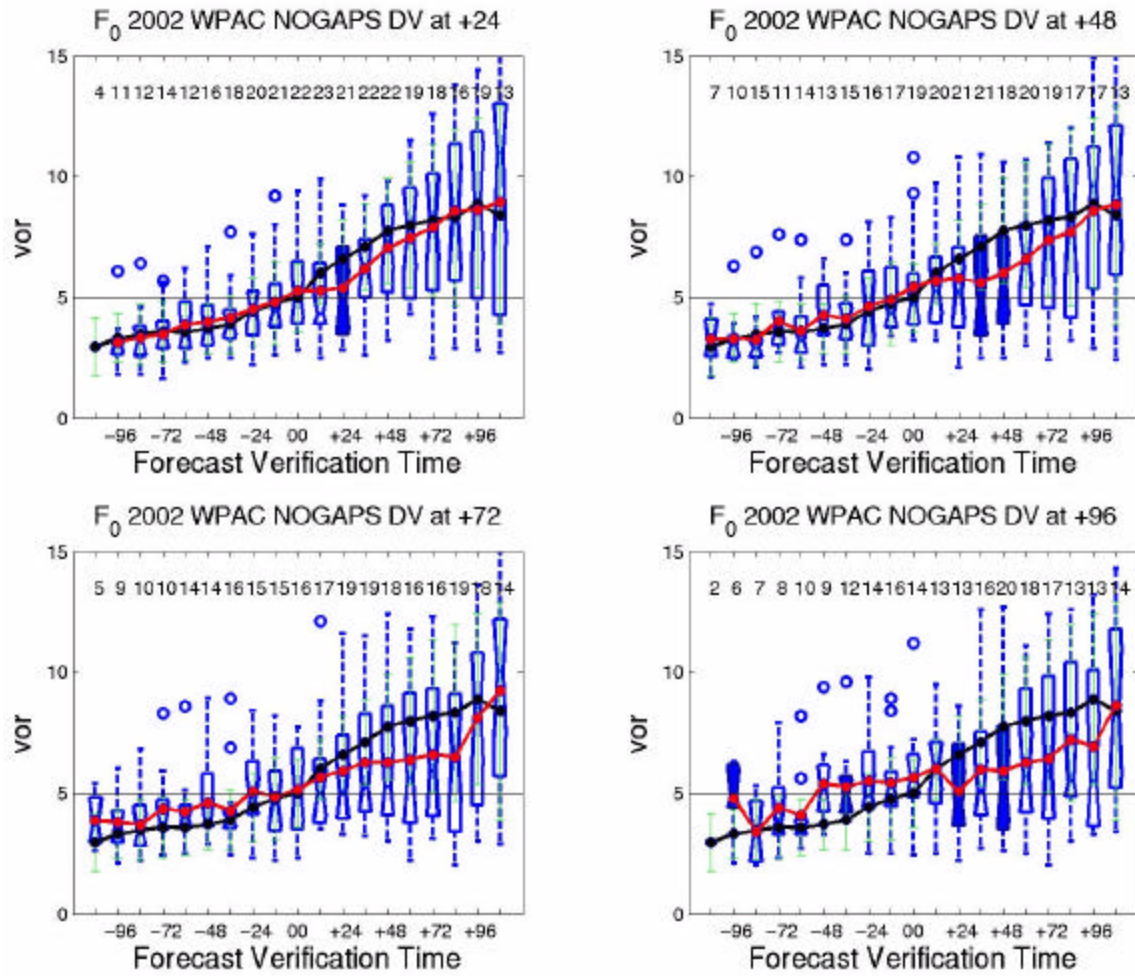
Figure 3.5. Average analyzed and forecast 850-mb relative vorticity for developing vortices relative to the first JTWC warning time (F_0). Heavy black line represents analyzed average 850-mb relative vorticity (at +00), and red line represents average forecast 850-mb relative vorticity for the indicated forecast time. Average 850-mb relative vorticity at F_0 (light solid black line) was 5.0×10^{-5} s^{-1}, which is then a reference for the vorticity magnitudes before (to the left) and after (to the right) the first warning time. The sample sizes available for comparison of the analyzed and forecast values at each forecast verification time are listed near the top of each panel for 24-h (upper-left), 48-h (upper-right), 72-h (lower-left), and 96-h (lower-right) forecasts of these developing storms.

verification 36 h prior to that first warning time. Even larger fall-offs in sample size are noted for the 24-h forecasts that are available for comparison with the analyzed values at the earlier forecast verification times. For the sample of 24-h forecast in the upper-left panel, only four cases were available for verification 120 h prior to the first warning time, because these forecasts would have been initiated 144 h prior to the first warning time

when either that pre-tropical cyclone circulation could not be tracked in the forecast or in the analysis so early in the life cycle.

Although the 24-h forecast vorticity value is larger than the analyzed vorticity value at 36 h prior to the first warning time, the overlapping box plots at this time suggest that the difference is not significant. Notice also that the range of forecast values is relatively large compared to the difference between the means of the 24-h forecast vortices and the corresponding analyzed vortices at 36 h prior to the first warning time. An outlier forecast vorticity of about 8×10^{-5} s^{-1} is indicated by the open circle at the -36 h verification time in the upper-left panel of Figure 3.5, which means that one of the 24-h forecasts initiated 60 h prior to the first warning time grossly over-forecast the 850-mb vorticity compared to the average threshold value of 5.0×10^{-5} s^{-1} for all 23 developing vortices at the first warning time.

Consider next the 24-h forecast verifications at 00 h in the upper left panel of Figure 3.5. Here, the 24-h analyzed and forecast vorticity values are almost identical, which means that the NOGAPS forecasts initiated only 24 h prior to the first warning time are quite accurate. A more accurate 24-h forecast verifying at the first warning time compared to verifying 36 h prior to the first warning time (as discussed above) might be expected if the initial conditions at 24 h prior to warning time are more accurate than the initial conditions at 60 h prior to the first warning time. However, the size of the box plots and range of 24-h forecast vortices verifying at 00 h are relatively large, which means considerable variability exists among the 22 cases at this verification time.

The only statistically significant difference between the mean 24-h analyzed and forecast vorticity in the upper-left panel in Figure 3.5 occurs for forecasts verifying 24 h after the first warning time. At this time, the mean 24-h forecast vorticity is much smaller than the verifying vorticity, and for the 21 forecasts verifying at this time the difference in the means is statistically significant according to the two-tailed t test.

The above discussion indicates the amount of information that can be extracted from the 24-h forecasts in the upper-left panel of Figure 3.5. Similar interpretations can be made for the 48-h (upper-right panel), 72-h (lower-left panel), or 96-h (lower-right panel) forecast verifying at the various times relative to the first JTWC warning time. These other panels illustrate the capability of the NOGAPS model to forecast these

developing vortices at longer and longer forecast intervals, and thus how useful the NOGAPS model will be in forecasting the formation defined as occurring at the first JTWC warning time. Similar interpretations can be made in Figure 3.6 for an earlier definition of forecast time as being the first Best-Track time. In these two examples, the interpretations are with respect to the 850-mb relative vorticity for just the developing vortices, but other variables that might characterize the differences between developing and non-developing vortices will also be presented in similar plots in the following sections.

Appendix B contains a more detailed explanation of the data contained in each of the different types of plots presented in the following sections. Readers who are not familiar with such forecast verification procedures are advised to read Appendix B before continuing.

1. Developing Vortices

The time of the first warning issued for each numbered storm (designated F_0) is one possible definition of formation time and was determined from the 2002 Annual Tropical Cyclone Report (ATCR). An alternate formation time is the time of the initial Best-Track position for each numbered storm (designated F^*_0) and was also determined from the 2002 ATCR. The initial Best-Track position, intensity, and time are determined during post-storm analysis by the JTWC, and correspond to the first model analysis, subjective analysis or satellite image in which the developing circulation is apparent. It should be noted that both F_0 and F^*_0 occur prior to the first insertion of any synthetic tropical cyclone observations into the NOGAPS model, which occurs when the maximum analyzed wind speed first reaches 25 kt. Threshold values for these two potential definitions of formation time were determined to be the mean values of each variable in the NOGAPS analyses at the times of F_0 and F^*_0. For a developing storm, F^*_0 must either precede or equal F_0.

a. *850-mb Relative Vorticity*

(1) Entire Basin Assessment. Low-level (850-mb) relative vorticity (?) provided the strongest signal for identification of developing versus non-developing vortices. A positive value indicates a low-level cyclonic circulation, and as expected, higher 850-mb relative vorticity is analyzed at F_0 and F^*_0 for those vortices that

developed into numbered circulations than for those that did not develop, which will be shown in a later section.

Prior to F_0, the NOGAPS forecasts of 850-mb relative vorticity at the various forecast intervals shown by the panels in Figure 3.5 were consistently larger than analyzed, whereas after F_0 the vorticity forecasts were less than analyzed. This transition between over- and under-forecasts, which occurred within the first 12 hours after F_0, is likely due to the insertion of the synthetic tropical cyclone observations into the NOGAPS analysis. When the first warning for a developing storm is issued by the JTWC, an automated message is received at the Fleet Numerical Meteorology and Oceanography Center (FNMOC). The Navy data assimilation system (NAVDAS) searches hourly for these automated messages. If one is received, and it meets certain quality control criteria, then a pre-set synthetic tropical cyclone wind and sea-level pressure observations at 13 points centered on the reported storm position is inserted into the file for use in the next NOGAPS update cycle. The location, size, and magnitude of the synthetic wind observations are based on the data contained in the original warning from the JTWC. Although the NOGAPS update cycle is run hourly, and changes are frequently made to the model analysis, the first time the analysis will include the effect of the synthetic observations is in the next analysis after the first warning is issued. For example, if JTWC issues the first warning on a developing storm at 0200 UTC, the synthetic observation is ingested into the 0300 UTC update cycle, and will first be apparent in the 0600 UTC model analysis (B. Strahl, FNMOC, personal communication).

The mean analyzed 850-mb relative vorticity at F_0 ($?_0$) was 5.0 x 10^{-5} s^{-1}, which is indicated by the thin, solid horizontal line in Figure 3.5. Although the slope of the analyzed $?_0$ curve changed after F_0 due to the insertion of the synthetic tropical cyclone observations, the slope of the forecast $?$ ($?_{12}$, $?_{24}$,...) curves generally do not have a marked change in slope relative to F_0. However, a tendency is noted for the slope of the curves to flatten for forecasts initiated prior to the insertion of the synthetic tropical cyclone observations.

The impact of the synthetic tropical cyclone observations starts from the first analysis after F_0 when JTWC has numbered the storm and issued its first warning. The insertion of the synthetic tropical cyclone observations is obvious in the forecast relative

vorticity curves in Figure 3.5. The slope of the forecast ? curve in the upper-left panel of Figure 3.5, which represents the average forecast vorticity value of +24 h forecasts, is almost flat from F_0 to F_0+24 h, and then begins to increase after 24 h. The dramatic increase in slope about 12 h after the specified forecast time interval represents the response in the NOGAPS forecasts to the synthetic tropical cyclone observations. Forecasts made after the synthetic tropical cyclone observations were inserted are more accurate when compared to the analyzed relative vorticity values. Notice that the amount by which the forecast ? curves fall below the analyzed curve after F_0 generally increases with larger forecast range. Statistically significant differences between the analyzed means and forecast means are indicated in Figure 3.5 by darkened box plots.

This model response hypothesis is apparent for shorter-range forecasts, and is easily seen in the upper- and lower-left panels of Figure 3.5. At longer time ranges, the model response time is delayed by about 12 hours. The slight decrease in the +48-h forecast ? in the upper-right panel of Figure 3.5 prior to the insertion of the synthetic tropical cyclone observations is attributed to the NOGAPS model already beginning to intensify the developing tropical circulation prior to the insertion of the synthetic tropical cyclone observations. The relative failure of the response hypothesis at extended forecast times could be due to decreased dynamic predictability of the tropical atmosphere at longer forecast ranges, or the sample size is too small.

Because the NOGAPS vorticity forecasts about 12 hours after F_0 are consistently less than the average analyzed vorticity, this indicates a tendency for the NOGAPS model to under-forecast developing vortices after synthetic tropical cyclone observations are included in the analysis. This decrease in the magnitude of vorticity may be due to the structure of the synthetic tropical cyclone observations. Prior to insertion of the synthetic observations, the vorticity ellipse may be too large, and in addition may be too strong. The synthetic tropical cyclone observations force the circulation in the model to decrease in size and magnitude by concentrating the relative vorticity in the NOGAPS forecast.

The average time difference between F_0 and the first Best-Track position F^*_0 was 28.4 hours, and ranged from 6 hours to 84 hours, with a median value of 24 hours. This time difference between when the analyzed curve (heavy black solid) (Figure 3.6) crosses the F^*_0 (light dashed) vorticity threshold and when it crosses the F_0 (light solid) vorticity
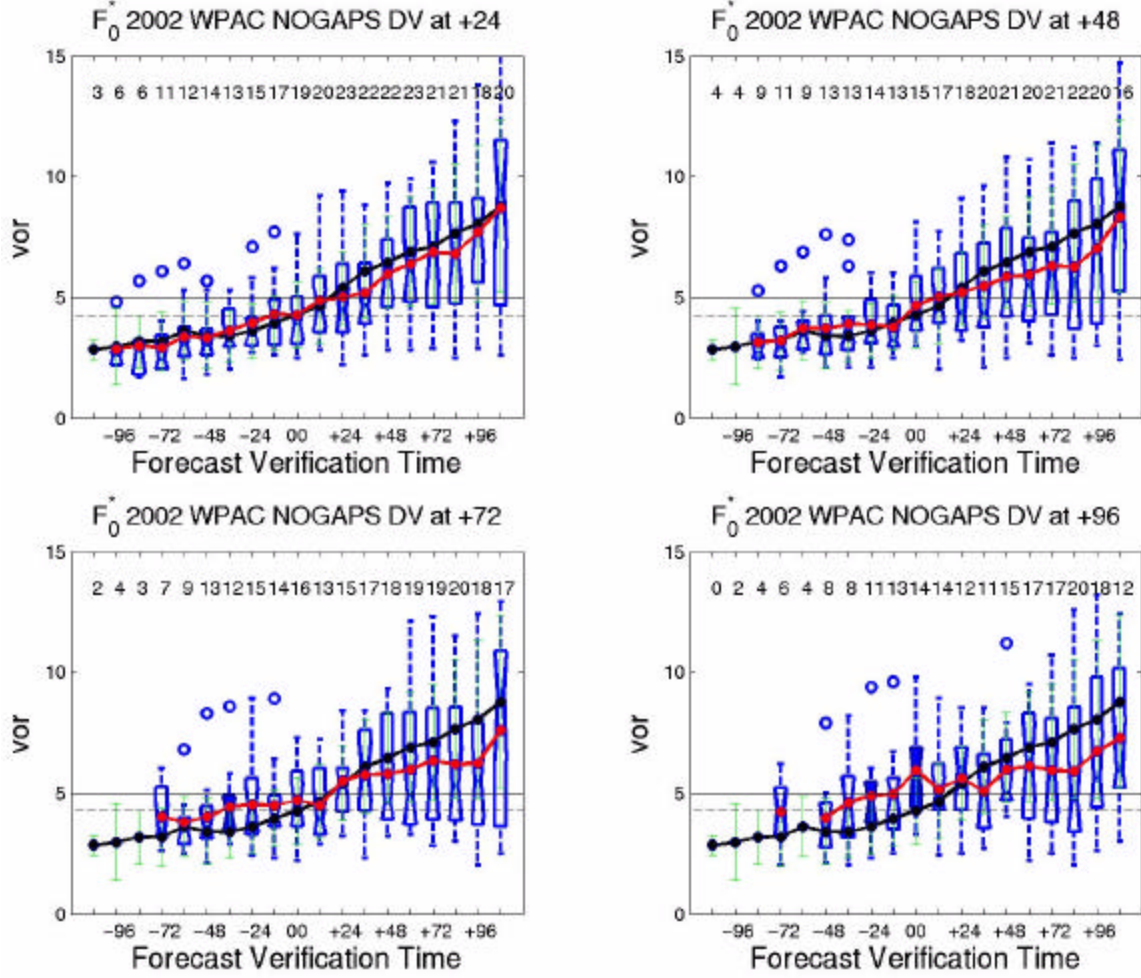
Figure 3.6. Average analyzed and forecast 850-mb relative vorticity for developing vortices as in Figure 3.5, except relative to the first Best-Track time (F^*_0). Heavy black line represents analyzed average 850-mb relative vorticity (at +00), and red line represents average forecast 850-mb relative vorticity for the indicated forecast time. Average 850-mb relative vorticity at F_0 (light solid black line) was 5.0 x 10^{-5} s^{-1}, and 4.3 x 10^{-5} s^{-1} (light dashed black line) at F^*_0.

threshold appears to be about 18 hours for the short-range forecasts. The 10 h difference between the graphical determination and calculation of timing difference is attributed to the varying F^*_0 times for each developing circulation. Some circulations were evident in the NOGAPS model analyses for 42 h or more before the JTWC issued the first warning. Removing the two greatest F^*_0 times (54 and 84 h) reduces the mean to 24.6 h and the median to 18 h, which is roughly what was estimated from Figure 3.6. The point at which the short-range forecast ? (heavy red solid) curves transition from over- to under-forecasts is approximately 12 to 24 hours after F^*_0. Given that in Figure 3.5 forecasts of

relative vorticity transitioned from over- to under-forecast at F_0, this interval is close to the expected value given the roughly 24 hours separating F_0 and F^*_0.

As in Figure 3.5, the 850-mb relative vorticity ($?^*$) forecasts in Figure 3.6 made prior to insertion of the synthetic tropical cyclone observations (at F_0) are consistently too large, whereas after F_0 the forecast vorticities are less than the analyzed vorticity. The mean analyzed 850-mb relative vorticity at F^*_0 ($?^*_0$) was 4.3×10^{-5} s^{-1}, which is indicated by the thin dashed horizontal line in Figure 3.6. As expected, $?^*_0$ is less than $?_0$, which reflects the increase in vorticity with time due to the development of the circulation that occurs during the roughly 24 hours separating F_0 and F^*_0. As in Figure 3.5, the insertion of the synthetic tropical cyclone observations is evidenced by the flattening and then sudden increase in the slope of the forecast $?^*$ curves (Figure 3.6). The time separation between F_0 and F^*_0 accounts for the temporal lag in the increase of the forecast $?^*$ curve. Since the forecast $?^*$ slope is not as dramatic at longer forecast ranges, it is possible that the NOGAPS model is less adept at correctly developing tropical circulations 96 h prior to the eventual first Best-Track time.

To examine whether the model forecast trends in vorticity might be due to a systematic error in the forecast vortex size due to the relatively coarse resolution in NOGAPS, forecast size, which is measured by the number of grid cells within the TCVTP ellipse, was examined (Figure 3.7). Based on the analyzed (at +00) values of vortex size (heavy black line in Figure 3.7) while the vortex is intensifying prior to F_0, it is also growing in size. In the 6 hours prior to F_0, the size decreases before beginning to increase again about 36 hours after F_0. This size decrease prior to F_0 may be due to a concentration of vorticity as the circulation becomes more organized, or may be due to a refocusing of the TCVTP ellipse on the most intense portion within a broader area of relative vorticity. In the 12 hours immediately following F_0 (Figure 3.7), the slight decrease in analyzed vortex size is attributed to the insertion of the synthetic vortex. Thirty-six hours after F_0, the vortex size increases as the vortex intensifies as a numbered system.

Since some of the NOGAPS forecasts of vortex size are larger and some smaller than analyzed (Figure 3.7), no significant trends toward over- or under-forecast of size relative to F_0 are evident, although the effect of the synthetic tropical cyclone
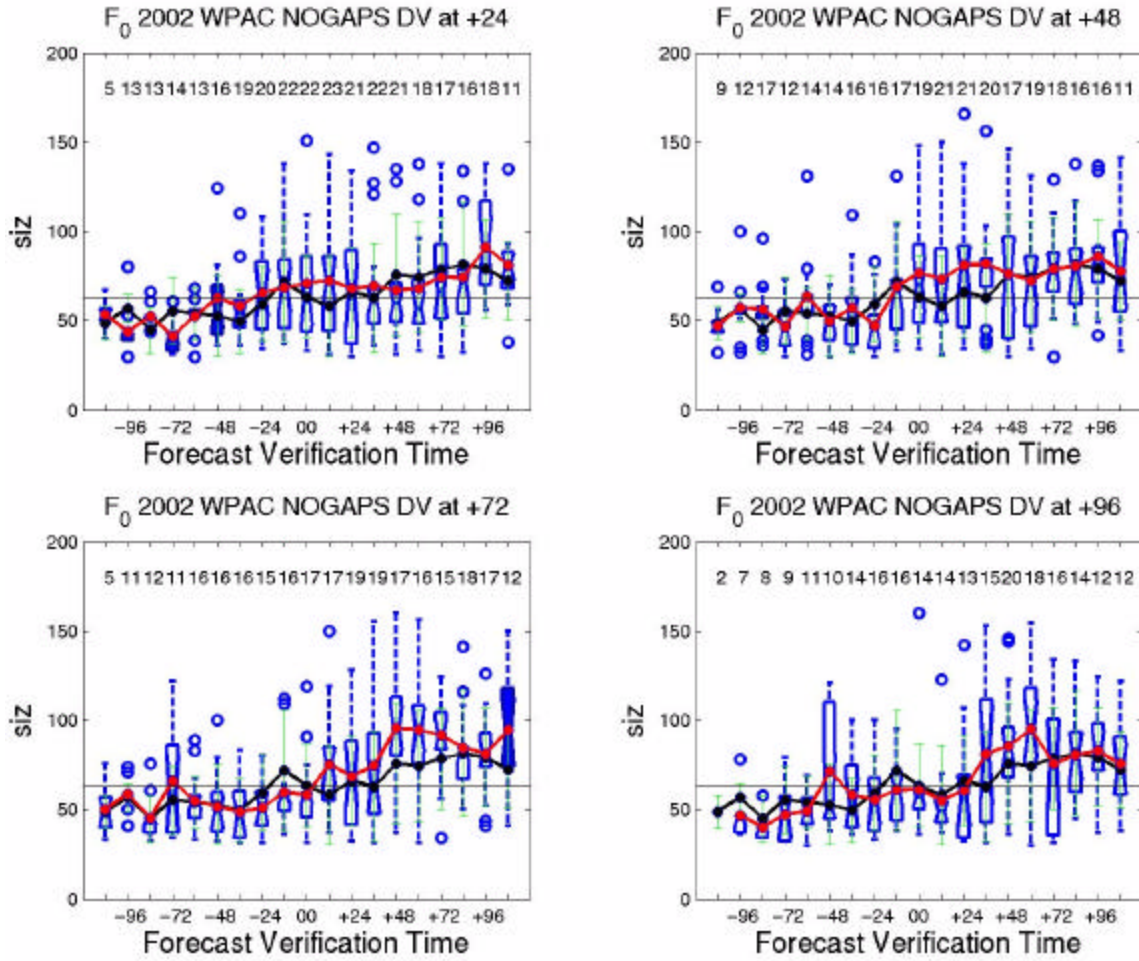
Figure 3.7. Average vortex size for all developing vortices relative to F_0. Average size at F_0 (light solid black line) was 60. Heavy black line represents average analyzed size (at +00); heavy red line represents average size at forecast time indicated. The display of boxes, ranges and outlier values are similar to Figure 3.5, and the same forecast intervals are shown in the various panels.

observations is again apparent. However, the short-range (less than 60 h) NOGAPS forecasts of vortex size tend to be larger than analyzed until about 36 hours after F_0, which may be attributed to the NOGAPS model tendency to inaccurately represent the size of the circulation because of the coarse model resolution (Goerss and Jeffries 1994). The short-term forecasts of vortex size dip to the analyzed vortex size threshold (60 grid cells) between 24 and 36 hours after F_0, which may indicate a delay in the model response to the inserted synthetic tropical cyclone observations.

Timing error ($?t_1$) was calculated as the amount of time that lapsed between F_0 and when the forecast 850-mb vorticity curve crossed the F_0 vorticity threshold in Figure 3.5 (Table 3.7). Since average values from Figure 3.5 are used to generate the timing error in the second column of Table 3.7, $?t_1$ is an average accurate to within ± 6 hours. As discussed above, the forecast 850-mb relative vorticity exceeded the F_0 threshold prior to F_0, which indicates that the model over-forecast the relative vorticity by forecasting the circulation to reach the relative vorticity threshold determined for developing vortices (5.0×10^{-5} s^{-1}) prior to when it actually reached that value. Although the timing error for all forecast times was –16.7 hours, the average timing error for the short-term forecasts ($\leq$ 60 hours) was just over –6 hours, which is approximately the resolution of the data. As expected, timing error increases for increasing forecast range, although due to the small sample size the decrease at +120 h may not be representative.

Table 3.7. Timing error ($?t_1$) between the time when a forecast 850-mb relative vorticity line crosses the F_0 vorticity threshold from Figure 3.5 and F_0. If the forecast curve crossed the F_0 threshold between x-axis values, the mean time between those two x-axis values was assigned. Average timing error is –16.7 hours. A negative number indicates that the forecast vorticity curve crossed the F_0 vorticity threshold prior to F_0 (+00 on x-axis of Figure 3.5). No value is calculated for the +00 forecast time because, by definition, the threshold value is determined by the value of the analyzed curve (+00) at F_0.

Forecast Time	$?t_1$
+00	--
+12	-6
+24	-6
+36	-6
+48	-12
+60	-6
+72	-6
+84	-18
+96	-54
+120	-36

A second timing error ($?t_2$) was calculated as the difference between when the forecast vorticity curve crossed the F_0 vorticity threshold and when it crossed the F^*_0 vorticity threshold in Figure 3.6 (Table 3.8). The average $?t_2$ was 29.4 hours, which indicates that the F^*_0 threshold was crossed prior to the F_0 threshold (Figure 3.6), as

expected based on the definitions of F_0 and F^*_0. The average time difference between the forecast curves crossing the F_0 threshold and F^*_0 was 12 hours, and the average time difference between the forecast vorticity curves crossing the F^*_0 vorticity threshold and F^*_0 was –16.2 hours. These values indicate that while the forecast vorticity curves exceeded the F^*_0 threshold roughly 16 hours prior to F^*_0, they did not exceed the F_0 threshold until 12 hours after F^*_0. One possible explanation for the delay between analyzed and forecast curves crossing the vorticity thresholds is the incorrect representation of the circulation in the NOGAPS model, with the correction occurring after the synthetic tropical cyclone observations are inserted into the model analysis.

Table 3.8. Timing error ($? t_2$) between the time when a forecast vorticity line crosses the F_0 vorticity threshold and when it crosses the F^*_0 threshold in Figure 3.6. Average timing error is 29.4 hours. A negative number indicates that the forecast time curve crossed the F_0 or F^*_0 threshold prior to F^*_0. A positive number indicates that the forecast time curve exceeded the threshold value after F^*_0. No F^*_0 data value is calculated for the +00 forecast time because, by definition, the threshold value is determined by the value of the analyzed curve (+00) at F^*_0.

Forecast Time	F_0 cross – F^*_0	F^*_0 cross – F^*_0	$? t_2$
+00	18	--	18
+12	24	-6	30
+24	18	-12	30
+36	18	-6	24
+48	12	-6	18
+60	12	6	6
+72	18	-42	60
+84	30	-42	72
+96	-12	-42	30
+120	-18	-12	6

(2) Subregion Assessments. To assess whether the NOGAPS model produced more accurate forecasts for specific regions within the western North Pacific, 850-mb relative vorticity was examined by subregion. The general trend of transitioning from over- to under-forecasts within 6 hours of F_0 was not readily apparent in each subregion. This may partially be due to the small sample size (a total 23 vortices in the three subregions).

The trend for the NOGAPS model transition from over- to under-forecasts of 850-mb relative vorticity apparent in Figure 3.5 is not evident in Figure 3.8, which represents only those vortices that developed within the South China Sea. This is likely due to the small sample size (five circulations) and limited number available for analysis. To plot the forecast curves in Figure 3.8, the minimum sample size was decreased from five cases per time interval to one case. A NOGAPS analysis of 850-mb relative vorticity was not available at –120 h, and model relative vorticity forecasts were not available prior to –60 h.

From 60 h prior to F_0 to 48 h after F_0, the analyzed relative vorticity curve in Figure 3.8 has a gradual increase as expected for slowly developing tropical cyclones. The notable decrease in vorticity after +60 h reflects the relatively short duration of SCS vortices compared to other subregions. The average vorticity value at F_0 for developing vortices in the SCS subregion is 4.8 x 10^{-5} s^{-1}, which is similar to the value (5.0 x 10^{-5} s^{-1}) for all developing vortices.

In general, 850-mb relative vorticity was under-forecast by NOGAPS at all times for vortices that developed within the SCS. The only forecast curves that exceeded the analyzed vorticity curve were +72 h and +96 h, and for forecasts made prior to F_0. Shorter-range forecasts ($\leq$ 60 h), while under-forecast at each temporal increment, were more accurate than the longer-range forecasts. The shorter-range forecasts more accurately depicted the slower increase and decrease in relative vorticity that is in the analyzed vorticity curve. No statistically significant errors (no dark shaded boxes as in Figure 3.5) occurred until 48 hours after F_0, and the errors that did occur were for relative vorticity less than analyzed.

Average analyzed and forecast 850-mb relative vorticity values for vortices that developed within the Philippine Sea subregion are shown in Figure 3.9. As in Figure 3.5, the general trend of the NOGAPS model forecasts is for increasing relative vorticity values with time, which indicates that development occurred relatively steadily, and the model forecasts of vorticity did not deviate substantially from the average analyzed values. While the forecast ? curves follow the same trend of increasing with time, there is no distinctive time at which forecast curves transition from over- to under-forecast as in Figure 3.5. The +24 h NOGAPS relative vorticity forecast curve (upper-left panel of
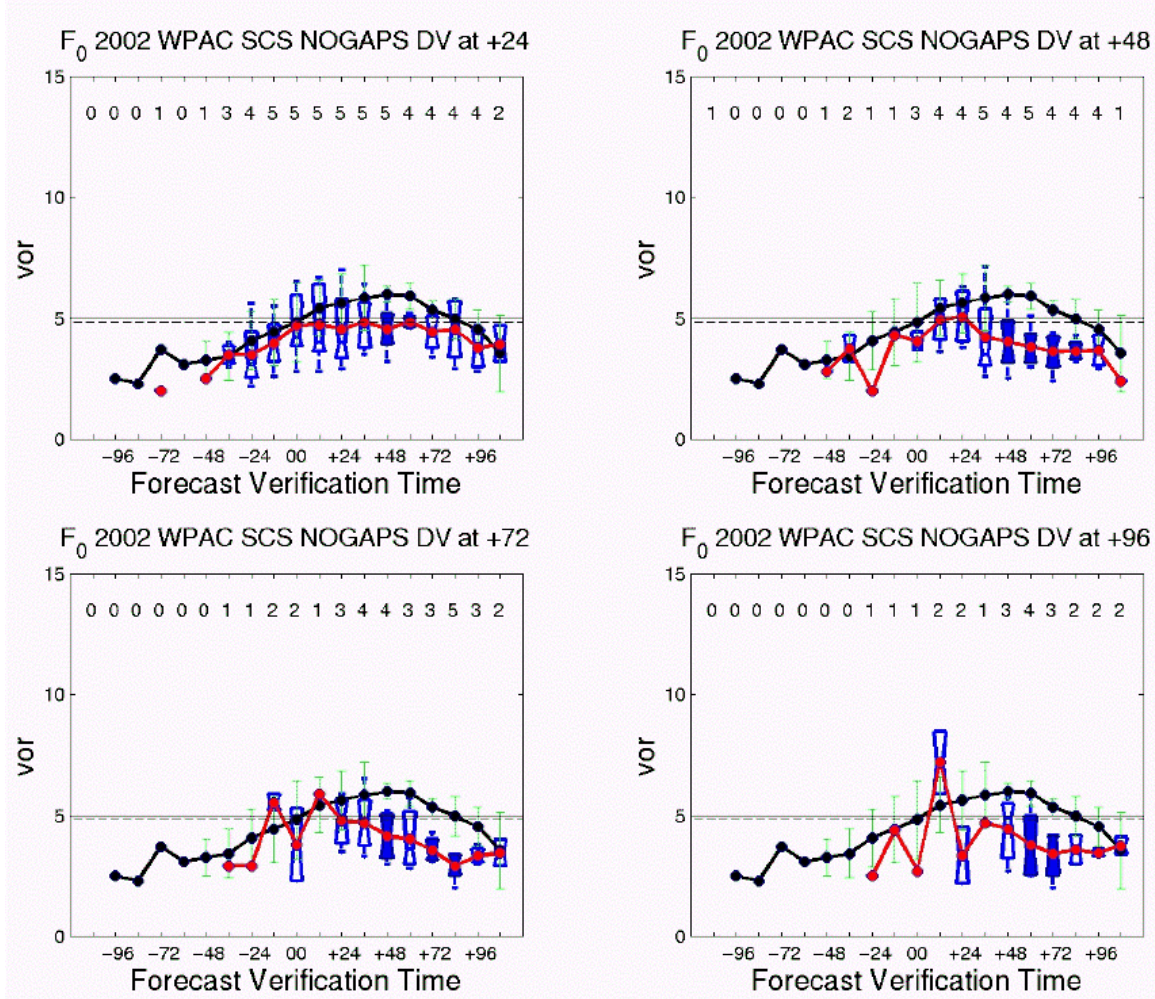
Figure 3.8. Average analyzed and forecast 850-mb relative vorticity as in Figure 3.5, except for vortices that developed within the SCS subregion. Heavy black line represents analyzed average 850-mb relative vorticity (at +00), and red line represents average forecast 850-mb relative vorticity for the indicated forecast time. Average analyzed vorticity relative to F_0 for developing vortices in the SCS (light dotted black line) was 4.8 x 10^{-5} s^{-1}. The light solid black line represents the $?_0$ threshold (5.0 x 10^{-5} s^{-1}) determined in Figure 3.5.

Figure 3.9) begins to increase 72 h prior to F_0 and exceeds the $?_0$ threshold determined for developing vortices in all subregions (5.0 x 10^{-5} s^{-1}) about 24 h prior to F_0. The +24 h forecast curve reaches a local maximum value at F_0 and then decreases in the 12 h immediately following F_0 before beginning to steadily increase again after +12 h. The increase prior to F_0 is associated with NOGAPS developing the vortex prior to the insertion of the synthetic tropical cyclone observation. The decrease after F_0 and the

36
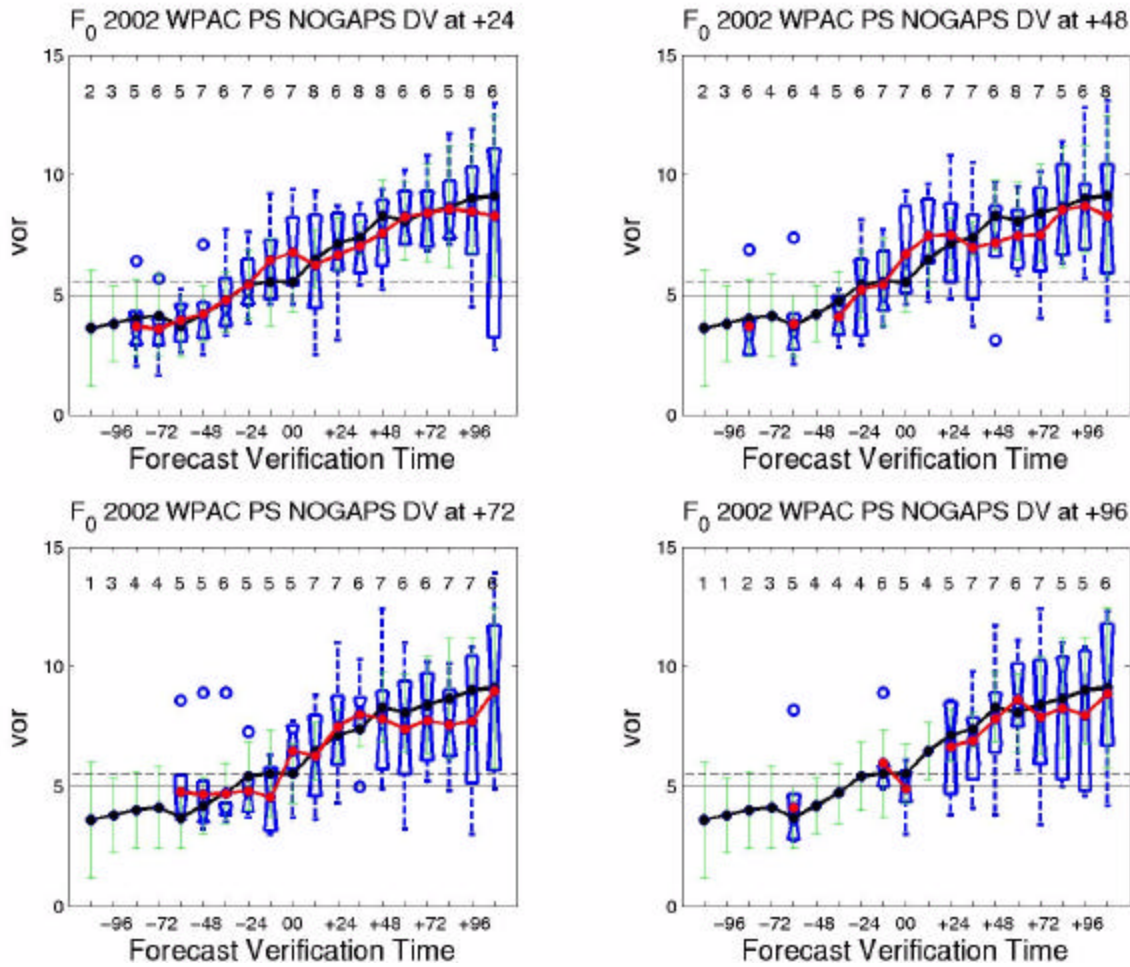
Figure 3.9. Average analyzed and forecast 850-mb relative vorticity as in Figure 3.5, except for vortices that developed within the PS subregion. Heavy black line represents analyzed average 850-mb relative vorticity (at +00), and red line represents average forecast 850-mb relative vorticity for the indicated forecast time. Average analyzed vorticity relative to F_0 for developing vortices in the PS (light dotted black line) was 5.5 x 10^{-5} s^{-1}. Light solid black line represents the $?_0$ threshold (5.0 x 10^{-5} s^{-1}) determined in Figure 3.5.

subsequent increase in vorticity following F_0 is attributed to the more accurate representation of the relative vorticity after the synthetic vortex was inserted.

The average vorticity for vortices developing within the PS region was 5.5 x 10^{-5} s^{-1}, which is slightly higher than the average for all developing vortices. This may be due to the higher background cyclonic vorticity associated with the monsoon trough.

The analyzed and forecast 850-mb relative vorticity curves for the EMT region (Figure 3.10) most closely resemble the relative vorticity curves for all vortices in Figure 3.5. That is, these storms have a general trend towards increasing relative vorticity

37

values with increasing time. As in Figure 3.5, the NOGAPS model tends to over-forecast relative vorticity in this subregion prior to F_0, and under-forecast it after F_0. The average analyzed 850-mb relative vorticity for vortices developing in the EMT subregion at F_0 is 4.7×10^{-5} s^{-1}, which is not significantly different from $?_0$ based on all storms. Almost all vorticity forecasts prior to F_0 are greater than the analyzed vorticity at each forecast time interval. The model transition to under-forecasts of vorticity occurs within 12 hours of F_0, as expected with the insertion of the synthetic tropical cyclone observations.
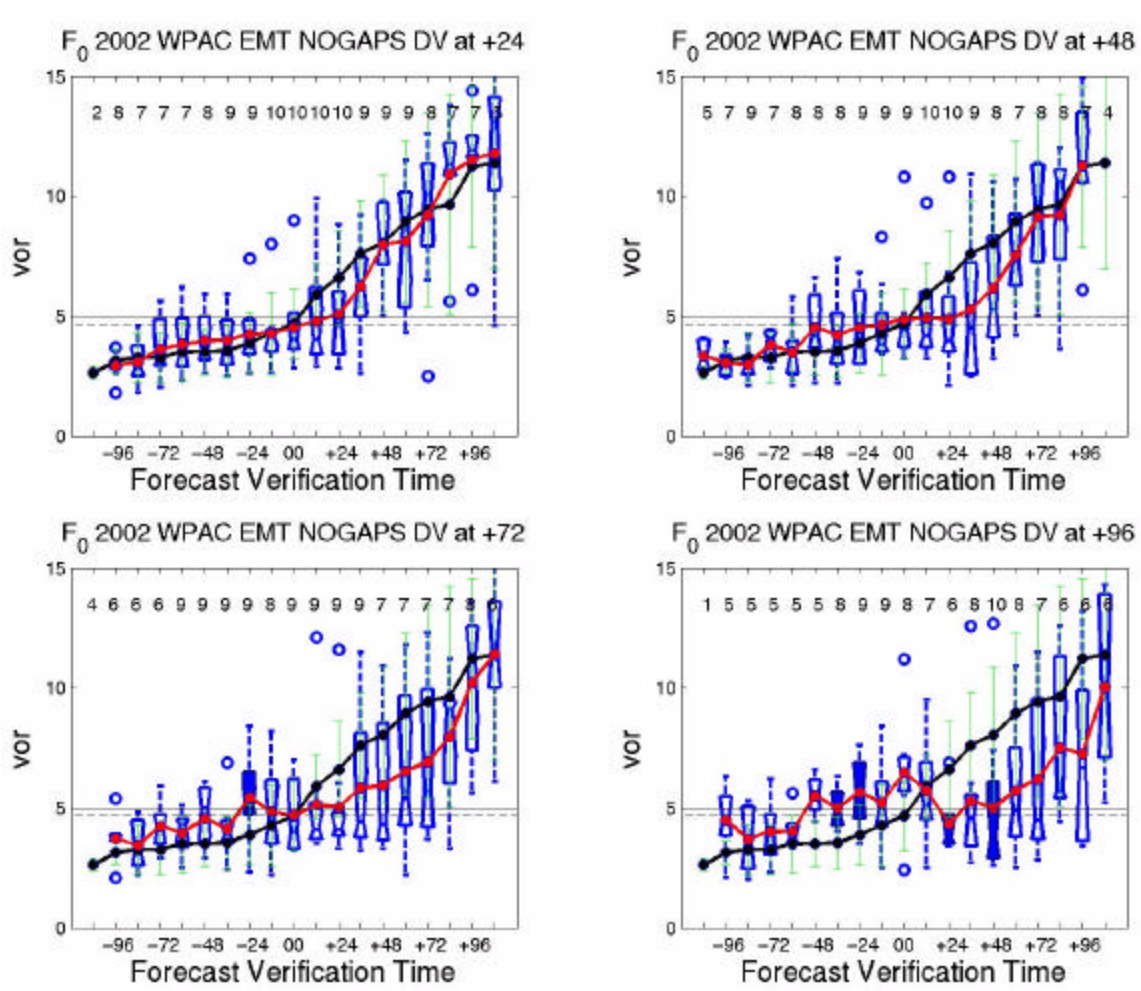
Figure 3.10. Average analyzed and forecast 850-mb relative vorticity as in Figure 3.5, except for vortices that developed within the EMT subregion. Heavy black line represents analyzed average 850-mb relative vorticity (at +00), and red line represents average forecast 850-mb relative vorticity for the indicated forecast time. Average analyzed vorticity relative to F_0 for developing vortices in the EMT (light dotted black line) was 4.7×10^{-5} s^{-1}. Light solid black line represents the $?_0$ threshold (5.0×10^{-5} s^{-1}) determined in Figure 3.5.

Interestingly, the NOGAPS model predicts maximum intensity too early in this basin for short-range forecasts. Maximum relative vorticity is forecast earlier in the +12 h forecasts than in the +36 h forecasts (not shown). The +48 h forecasts and +72 h forecasts (Figure 3.10) were more accurate on the timing and magnitude of maximum relative vorticity. This deficiency in the shorter-range forecasts may indicate a tendency of the NOGAPS model to intensify developing vortices in the EMT subregion too quickly.

(3) Assessment Relative to the TCFAs. To examine whether model guidance accuracy may be related to the accuracy of the placement of the TCFA forecast window relative to the actual formation time, relative vorticity was examined based on formation time relative to the TCFA-defined formation window for each JTWC-numbered circulation. By identifying formation time as the time of the first JTWC warning, the TCFA formation windows for developing circulations were verified. A positive verification occurred if the first JTWC warning was issued during the formation window defined in the TCFA for that storm.

Eleven of 27 (40.7%) TCFAs verified prior to the onset of the formation window. The average analyzed and forecast 850-mb vorticity curves for those 11 circulations that verified prior to the TCFA formation window are plotted in Figure 3.11. Prior to F_0, the analyzed and forecast curves for this subset of vortices are very similar to Figure 3.5, which contains curves for all developing vortices. However, the amount of under-forecasting following F_0 is much larger for this subset of vortices than in Figure 3.5 as shown by the amount of deviation between the analyzed and forecast ? curves. The change in slope of the analyzed (+00) vorticity curve in Figure 3.11 is more dramatic for this subset of developers, especially in the shorter-range forecasts. The combination of an early formation time relative to the TCFA formation window, the dramatic increase in slope and severe under-forecasting errors after F_0 suggest that these vortices may have undergone a period of rapid intensification.

The first warning was issued during the TCFA-defined formation window for 34.8% (8) of the 23 developing vortices. Analyzed and forecast 850-mb relative vorticity for these circulations are shown in Figure 3.12. Given this relatively small sample, the minimum number of cases has to be relaxed in this comparison (see samples sizes near
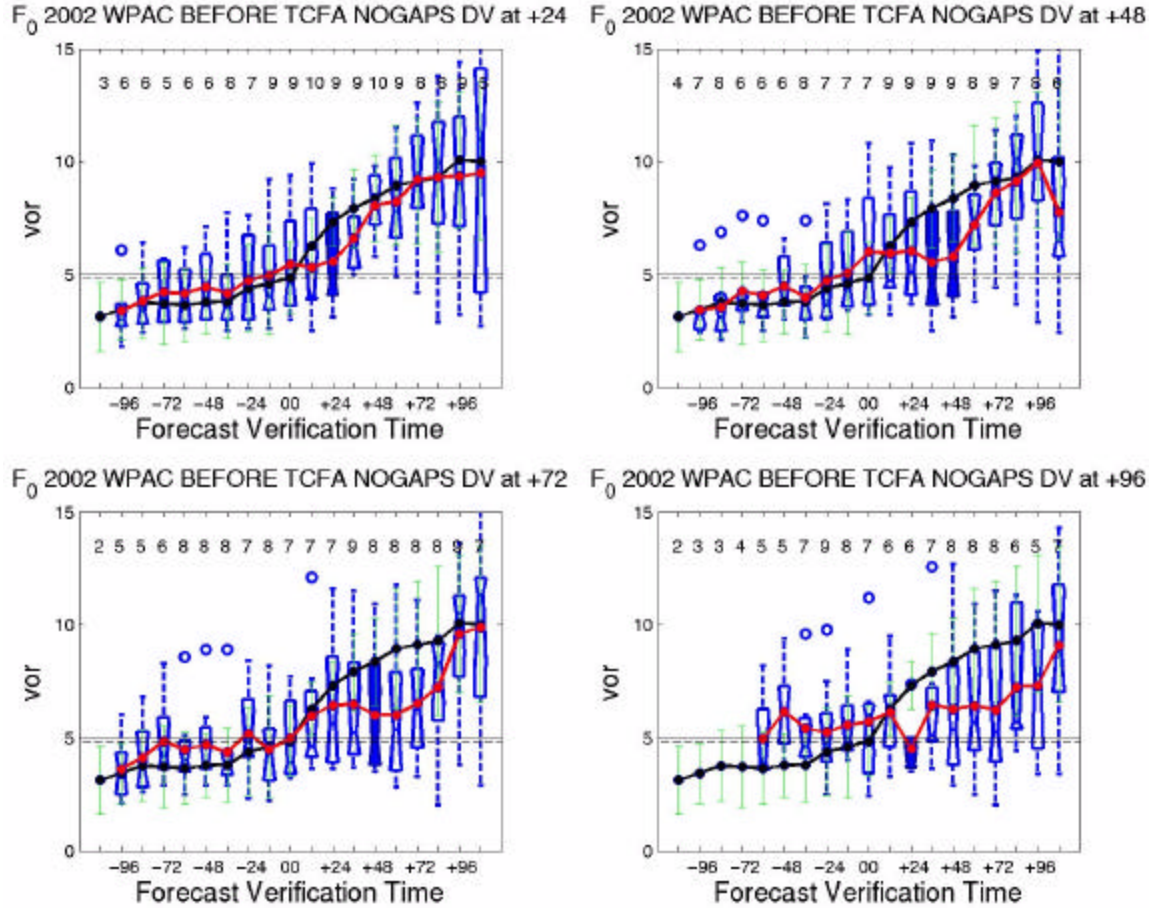
Figure 3.11. Average analyzed and forecast 850-mb relative vorticity displays as in Figure 3.5, except for 11 developing vortices that were warned on PRIOR to the TCFA-defined formation window. Heavy black line represents analyzed average 850-mb relative vorticity (at +00), and red line represents average forecast 850-mb relative vorticity for the indicated forecast time. Average analyzed vorticity relative to F_0 for vortices verifying prior to the TCFA formation window (light dotted black line) was 4.9 x 10^{-5} s^{-1}, and 5.0 x 10^{-5} s^{-1} for all vortices (light solid black line).

the tops of the panels), and thus the differences should be regarded as tentative. For this subset of developers, the forecast vorticity characteristics prior to F_0 are similar to the total set of all developing vortices in Figure 3.5. However, the transition from over- to under-forecasts begins as early as 12 hours prior to F_0, and continues until 36 hours after F_0 (not shown). The absence of a drastic slope change in the 24 hours surrounding F_0 indicates that rapid intensification did not occur for this subset, and suggests that the NOGAPS model may perform better during the formation and intensification process for this subset.
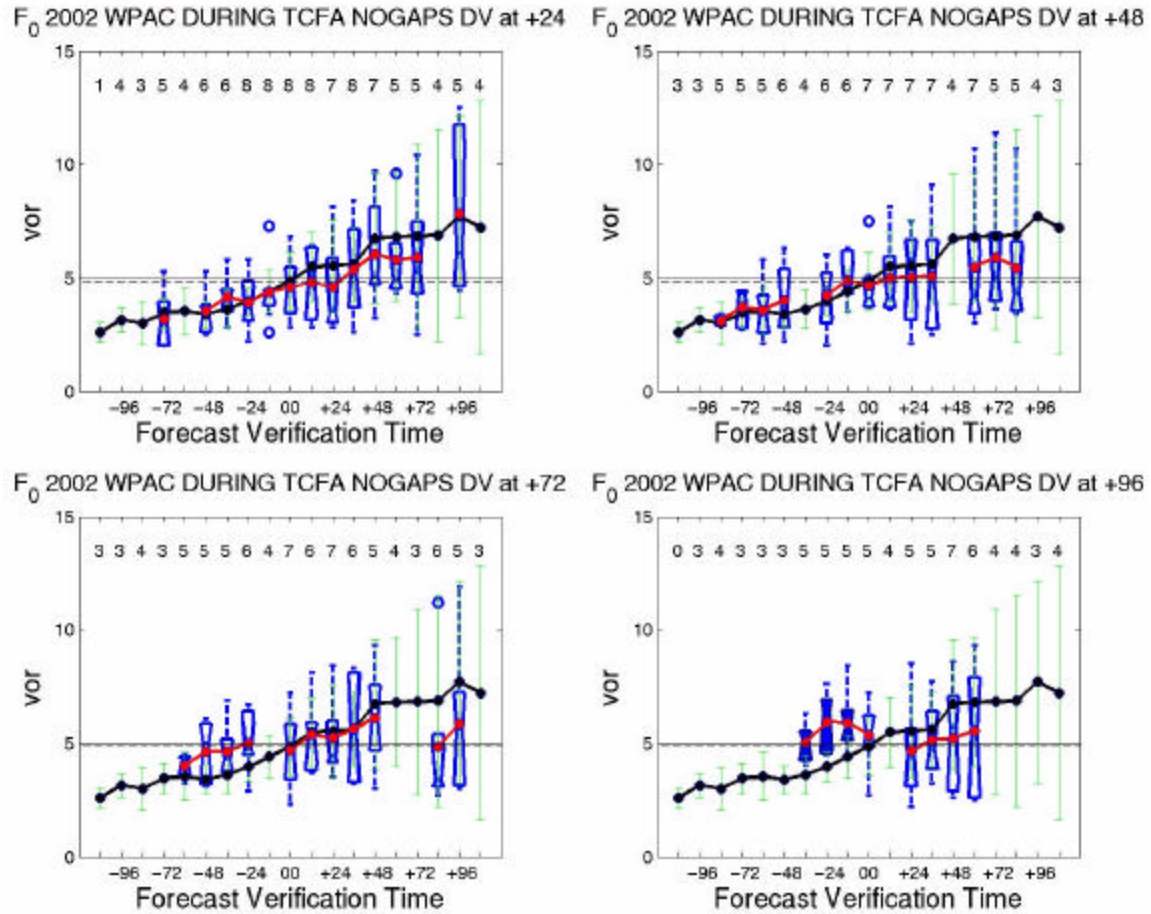
Figure 3.12. Average analyzed and forecast 850-mb relative vorticity displays as in Figure 3.5, except for developing vortices that were warned on DURING the TCFA-defined formation window. Heavy black line represents analyzed average 850-mb relative vorticity (at +00), and red line represents average forecast 850-mb relative vorticity for the indicated forecast time. Average analyzed vorticity relative to F_0 for vortices verifying during the TCFA formation window (light dotted black line) was 4.9 x 10^{-5} s^{-1} and 5.0 x 10^{-5} s^{-1} for all developing vortices (light solid black line).

Five of the 24 (20.8%) TCFAs verified after the specified TCFA formation window. All five of those TCFAs were reissued and subsequently four verified during the specified TCFA formation window and one verified before the specified formation window. These reissued TCFAs were included in the subset discussed above, while the original TCFAs that were changed are included in the subset of vortices that verified after the TCFA formation window. The average analyzed and forecast 850-mb relative vorticity for these five circulations are included in Figure 3.13. To show the forecast curves, the minimum number of cases displayed at each time interval was decreased to

41
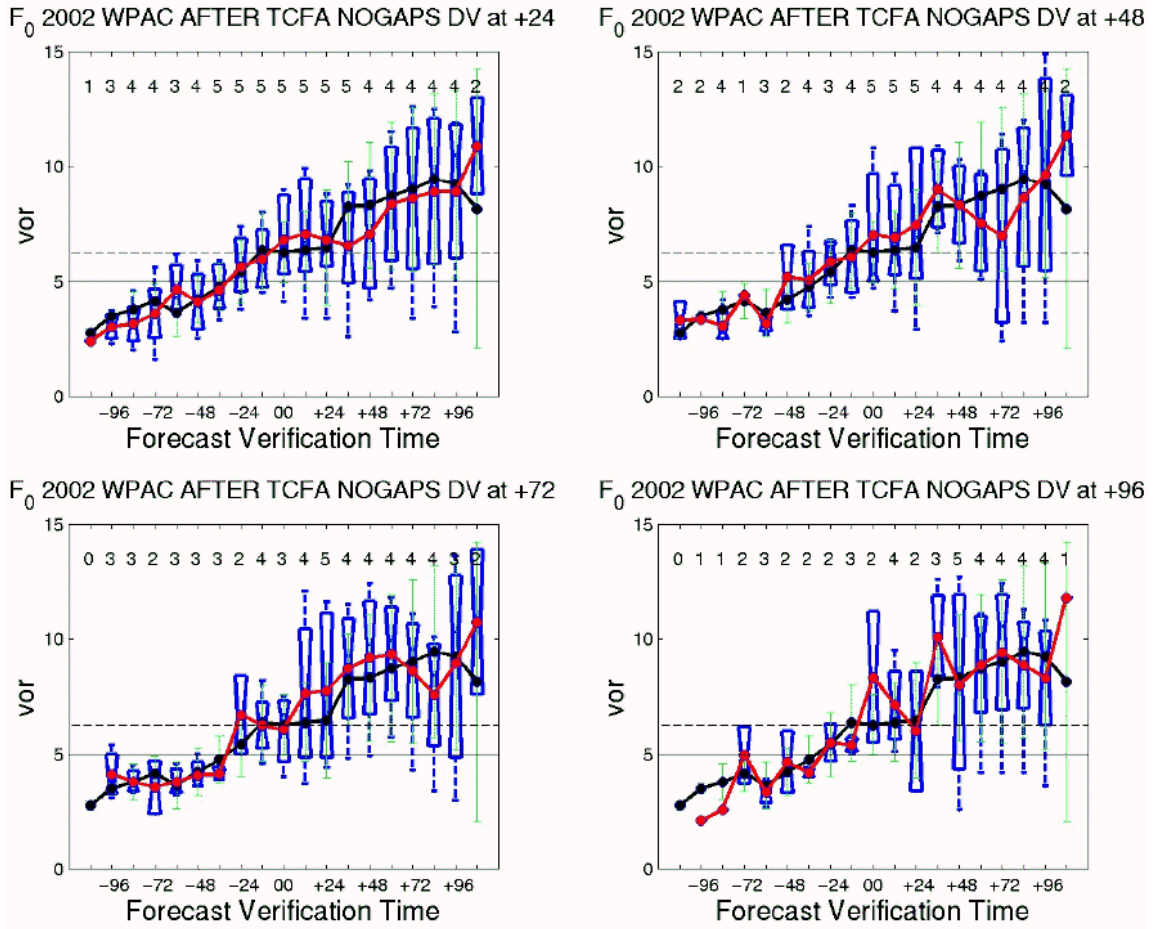
Figure 3.13. Average analyzed and forecast 850-mb relative vorticity displays as in Figure 3.5, except for developing vortices that were warned on AFTER the TCFA-defined formation window. Heavy black line represents analyzed average 850-mb relative vorticity (at +00), and red line represents average forecast 850-mb relative vorticity for the indicated forecast time. Average analyzed vorticity relative to F_0 for vortices verifying after to the TCFA formation window (light dotted black line) was 6.3 x 10^{-5} s^{-1} and 5.0 x 10^{-5} s^{-1} for all developing vortices (light solid black line).

one. The over- and under-forecast trends in 850-mb vorticity relative to the F_0 threshold evident in Figure 3.5 are not evident in Figure 3.13. The transition between over- and under-forecasts of relative vorticity instead occurs for short-range forecasts between 24 and 36 h after F_0. The lack of a change in the slope of the analysis curve at F_0, and the lack of the predominant under-forecasting that was evident with respect to early formations (Figure 3.11), and to a lesser degree with the on-time formations (Figure 3.12), suggest that these cases developed relatively slowly.

Also of interest is the relatively high average analyzed 850-mb relative vorticity value at F_0 for this subset of developers. The average analyzed vorticity for circulations verifying after the TCFA-specified formation window was 6.3 x 10^{-5} s^{-1}, which is noticeably higher than the average analyzed vorticity value at F_0 for the total set of developers. This number is likely erroneously high due to the small sample size of this subset. However, the higher value could also indicate that the circulation is more intense at the time of the first warning.

b. Deep Layer Wind Shear

While the deep layer wind shear (200-850 mb) variable provides insight about the relative magnitudes of the upper-level anticyclone and low-level cyclone associated with the developing tropical circulation, it primarily indicates the prevailing direction of the environmental flow surrounding the tropical circulation. A positive shear value indicates westerly shear, or an increase in westerly winds with height. A negative shear value indicates easterly shear, or in increase in easterly winds with height. While classic research on tropical cyclone formation by Gray (1968) indicates that minimum shear over the developing circulation is a necessary condition for formation, more recent research (i.e., McBride and Zehr 1981) points to the importance of a transition zone, with strong westerly shear to the north and strong easterly shear to the south of the developing tropical circulation. While the deep layer wind shear variable, as measured here, does not have a horizontal gradient of wind shear, it contains valuable information about the atmosphere in which the tropical circulation is developing. Kurihara and Tuleya (1981) found in a Global Fluid Dynamics Laboratory (GFDL) study that easterly shear is more favorable than westerly shear for tropical cyclone formation, which matches the westward translation speed of the wave with the deep-layer average easterly winds if there is easterly shear through the troposphere. Consequently, a negative (easterly) deep shear favors formation.

For this set of developing vortices (Figure 3.14), the analyzed deep layer wind shear transitions from positive (westerly) to negative (easterly) between 48 and 36 h prior to F_0. Interestingly, the shear remains just slightly negative (easterly) until F_0, when it begins to steadily decrease (become more negative) as the circulation intensifies. The average analyzed deep shear at F_0 was –1.8 m s^{-1}, which indicates easterly shear over the
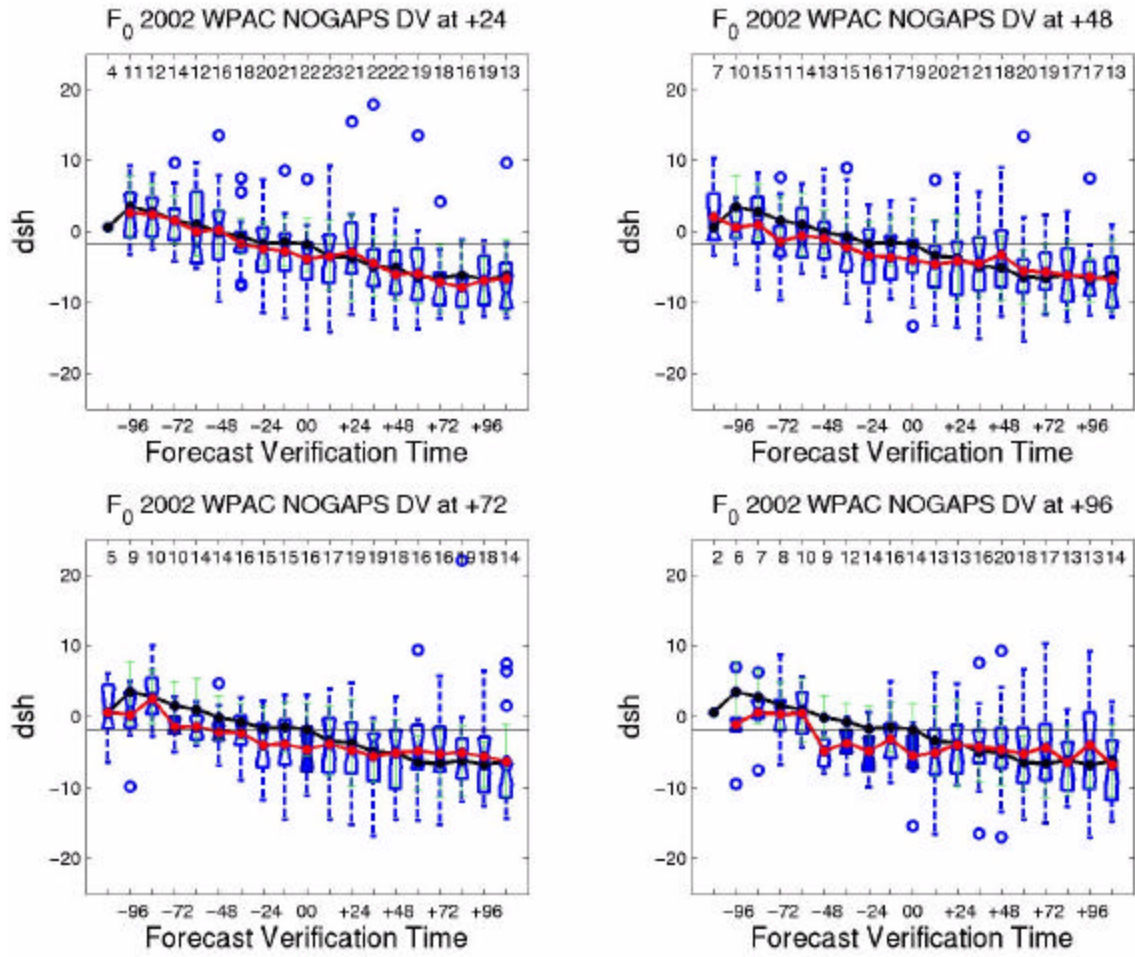
Figure 3.14. Analyzed and forecast deep wind shear (200-850 mb) for developing vortices relative to F_0, as in Figure 3.5. Heavy black line represents analyzed average deep wind shear (at +00), and red line represents average forecast deep wind shear for the indicated forecast time. Average analyzed deep wind shear at F_0 for developing vortices (light solid black line) was -1.8 m s^{-1}.

circulation center, which is favorable for the development of the tropical circulation. Since the deep shear variable can be either positive or negative (indicating directional change) the terms over-and under-forecast must be more specifically defined. An under-forecast of deep shear is then defined to not be a negative value, but a forecast value that is weaker or closer to zero than the analyzed value. Likewise, an over-forecast of deep shear is defined here as a forecast value that is stronger or greater than the analyzed value. As shown in Figure 3.14, the forecast deep layer shear curves transition from less than the analyzed shear to greater than the analyzed shear approximately 12 h prior to the insertion of the synthetic tropical cyclone observations.

44

The forecast deep wind shear prior to F_0 is too low due to excessive easterly wind shear associated with the NOGAPS model over-forecasts of 850-mb relative vorticity during the same period. At each forecast time, a slight increase in the deep shear variable occurs just prior to the insertion of the synthetic tropical cyclone observation. This increase in westerly shear is associated with the NOGAPS model over-forecasting the 850-mb relative vorticity, and thus strengthening easterly environmental flow. This coupling of vorticity and wind shear is expected in a hydrostatically and geostrophically balanced model.

Throughout the entire forecast period, the differences between the analyzed and forecast deep wind shear are small. This lack of significant variation is due to the already weak shear associated with the developing tropical circulation. Forecasts of vertical shear away from the center of the ellipse would likely show greater deviations from the analyzed values.

c. Sea-level Pressure

Sea-level pressure (SLP) varies only minimally in the tropics (McBride 1981). However, examining the SLP variable provides valuable information about the intensity of the developing circulation. As expected, the average analyzed and forecast sea-level pressure (SLP) decreases with increasing forecast time for these developing tropical cyclones (Figure 3.15). The mean analyzed SLP at F_0 (P_0) was lower (1006.9 mb) than the 1007.4 mb at F^*_0 (P^*_0) as expected from the deepening of the storm between these two times. Although the forecast SLP values were only slightly less than the analyzed SLP (Figure 3.15), this difference is important. Only small SLP drops occur during the early stages of tropical cyclone development when the warm core is relatively weak. The trend of NOGAPS SLP forecasts to be slightly lower than the average analyzed value is consistent with the model forecasts of 850-mb relative vorticity. This tendency is expected as the NOGAPS model fields should be in hydrostatic and geostrophic balance during the early stages of tropical cyclone development, and at these horizontal scales.

One significant trend in the NOGAPS model forecasts of SLP is the disproportionate number of forecasts that are too low when compared to the analyzed SLP values. All of the extreme values (indicated in Figure 3.15 by an open circle) err on the low side of both the analyzed and forecast curves. Additionally, most of the extreme
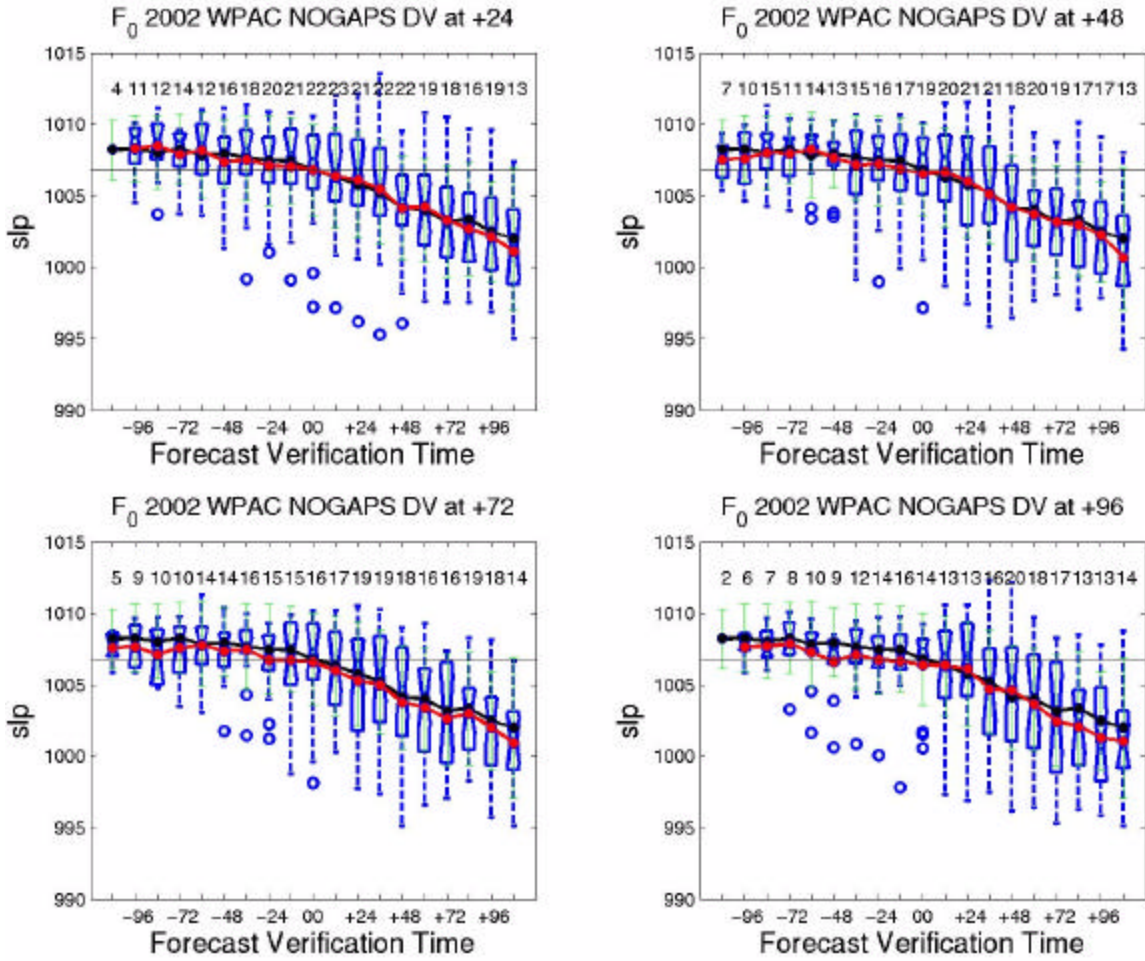
Figure 3.15. Average analyzed and forecast sea-level pressure (mb) for all vortices relative to F_0, as in Figure 3.5. Heavy black line represents analyzed average SLP (at +00), and red line represents average forecast SLP for the indicated forecast time. Average analyzed SLP at F_0 (light solid black line) was 1006.9 mb.

SLP values are forecast prior to F_0, with the exception of the +24 h forecasts. While the short-term (24 h) average forecast SLP is consistent with the analyzed SLP, the NOGAPS model tendency to err towards excessive and rapid development is evident in Figure 3.15.

d. *925-mb Wind Speed*

The 925-mb wind speed is another indicator of the intensity of the developing tropical circulation. This variable is closely linked to the 850-mb relative vorticity. As expected, a transition from over- to under-forecasts of 925-mb wind speed occurs in the first 12 hours after F_0 (Figure 3.16). The sudden increase in the slope of the forecast

46
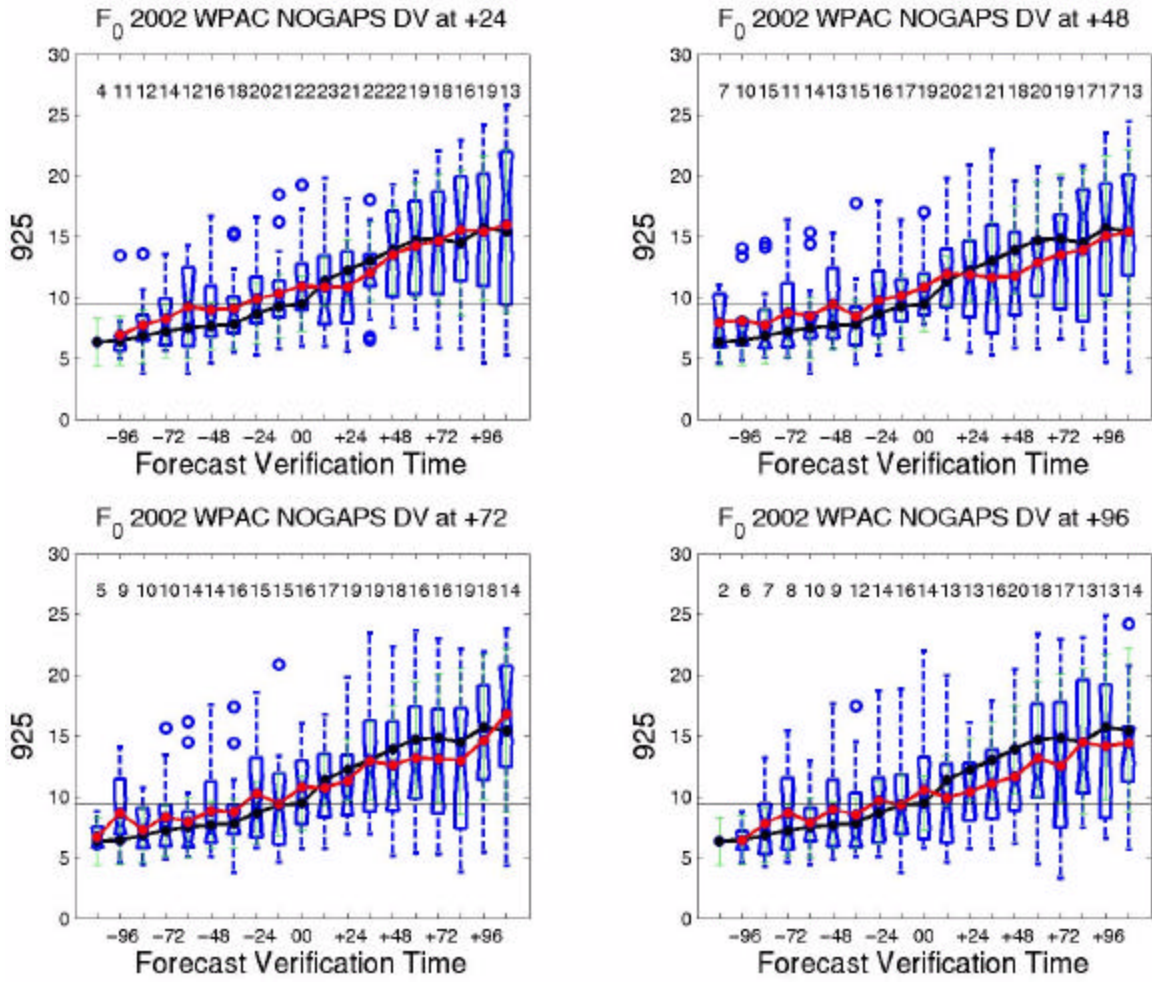
Figure 3.16. Average analyzed and forecast 925-mb wind speed (m s^{-1}) for all vortices relative to F_0, as in Figure 3.5. Heavy black line represents analyzed average 925-mb wind speed (at +00), and red line represents average forecast 925-mb wind speed for the indicated forecast time. Average analyzed 925-mb wind speed at F_0 (light solid black line) was 10.8 m s^{-1}.

wind speed curve in each panel of Figure 3.16 indicates the NOGAPS model reaction to the insertion of the synthetic tropical cyclone observations into the model analysis. In general, the deviation of the forecast wind speed from the analyzed wind speed increases with time, which indicates the continued intensification of the developing tropical circulation.

e. *Vapor Pressure*

The vapor pressure averaged over 500-700 mb (Pa) provides an indication of the amount of mid-level moisture available to the developing tropical cyclone. The slope of

the analyzed (at +00) vapor pressure (Figure 3.17) remains relatively flat throughout the development of the tropical circulation. This lack of change in the slope of the analyzed curve makes it a poor variable for use in the determination of a formation threshold.

At almost all forecast times in Figure 3.17 the NOGAPS model forecasts of vapor pressure are below the analyzed value. Another interesting factor is the set of extreme forecast values, which are indicated in Figure 3.17 by an open circle. These extreme values are almost all substantially below even the forecast vapor pressure (indicating a drier mid-troposphere than analyzed) and they tend to occur at extended forecast ranges.
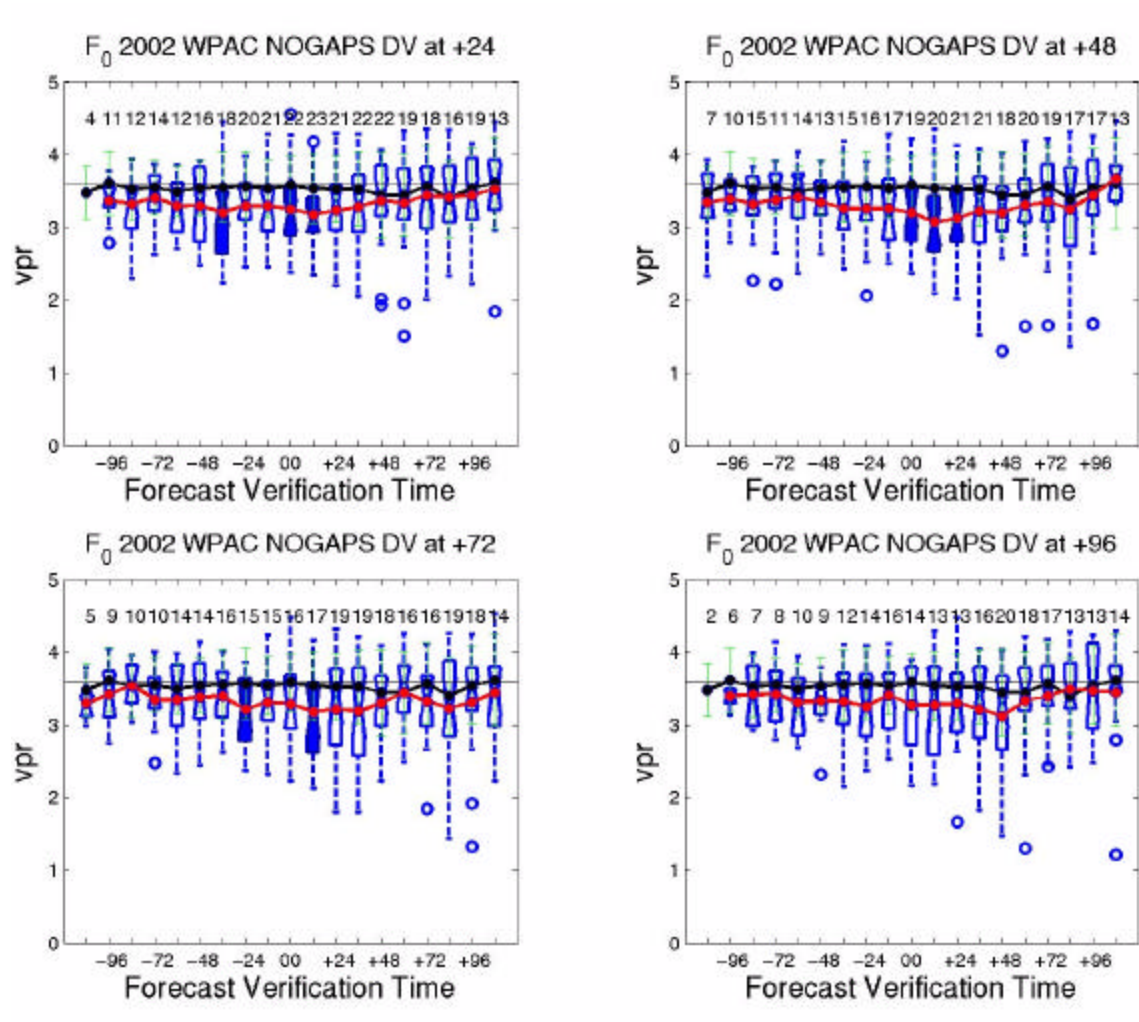
Figure 3.17. Analyzed and forecast vapor pressure (500-700 mb average) (Pa) for all vortices relative to F_0, as in Figure 3.5. Heavy black line represents analyzed average vapor pressure (at +00), and red line represents average forecast vapor pressure for the indicated forecast time. Average analyzed vapor pressure at F_0 (light solid black line) was 3.6 Pa.

Because of this tendency for the NOGAPS model to incorrectly forecast this variable, mid-level vapor pressure is not likely to be a good one for distinguishing developing from non-developing vortices.

Additionally, the consistent under-forecasting, evident in both the forecast curves and also the outliers of the forecast vapor pressure indicates that the NOGAPS model is not correctly assessing the interior vortex processes. This excessive dryness at the mid-levels is possibly a result of the convective parameterization. As noted in Elsberry (2003), a dry mid-troposphere inhibits formation by preventing the development of a warm core. However, within the NOGAPS model, this excessive dryness in the mid-troposphere may actually limit the number of tropical cyclone formations, both accurate and inaccurate, that the NOGAPS model develops. Formations then are a result of large-scale processes rather than the internal dynamics of the tropical vortex.

f. Other Variables

Seven variables (not shown) listed in Table 2.1 were examined to determine the presence of a forecast signal, but were not selected for further analysis. Of these variables, most showed little to no slope of the analyzed variable curve, and also had average forecast curves that were consistently lower than the analyzed curve, and a distinct trend toward excessively low forecast values. This flat slope, which is consistent with under-forecasting of developing vortices, and the lack of deviations from the analyzed values may provide value information regarding the atmosphere in which the tropical cyclone develops, or information regarding the developing circulation. Moreover, many of these variables were model-derived rather than directly analyzed variables and thus more likely contained model errors.

Vertical motion was consistently too large and positive after F_0. This error is likely due to the NOGAPS over-forecasts of precipitation. Total (convective plus grid-scale) precipitation in the storm-centered ellipse was consistently over-forecast for the developing vortices at all forecast times by NOGAPS. Excessive precipitation forecasting is attributed to the cumulus parameterization within the model.

Latent heat flux from the ocean was excluded from the selected variable list because it is a purely model-derived variable, and its accuracy is subject to the correct

representation of the wind speed and sea-surface temperature. It may also not be an important physical process at the early stages of formation.

Geopotential height thickness (200 - 1000 mb) had no strong signal for the developing vortices. The forecast values were consistently greater than analyzed for these developing vortices, which might be expected solely due to the increase in relative vorticity and falling 1000-mb heights associated with the intensification of the tropical circulation. Likewise, the shallow (1000 – 500 mb) warm anomaly variable showed no distinct signal for distinguishing these developing vortices. The lack of a lower tropospheric signal may be because the warm core first forms in the upper troposphere of developing storms.

The 700-mb wind speed forecasts did not show a significant difference from the analyzed curve prior to F_0, and the wind speed was consistently under-forecast after F_0. The under-forecasting of this variable did not become statistically significant until after +84 h. This variable, and the 500-mb wind speed variable, were excluded from analysis because, in addition to showing little prognostic value in the cases analyzed, they are indirectly contained in the deep layer (200 – 850 mb) wind shear variable.

Shallow layer (500 – 850 mb) wind shear was also excluded for lack of a prognostic signal for distinguishing developing vortices during 1 May – 31 October 2002. Whether this lack of a signal was indicative that low-level shear was not an important physical process in tropical cyclone formation, or a reflection that this variable is not well-predicted by the NOGAPS model, can not be determined from this sample.

## 2.	Non-developing Vortices

The threshold values for six forecast variables determined for the tropical vortices that developed into systems that were later numbered and warned on by JTWC will serve as a reference for the non-developing vortices. Three sets of non-developing vortices identified by the TCVTP algorithm will be compared to the thresholds determined for developing vortices. These datasets (see definitions in Chapter III.A) were: non-developing vortices that met the minimum duration criterion (ND1); non-developing vortices that did not meet the minimum duration criterion, but did meet the over-forecast criteria (ND2); and both model and TCFA false alarms.

Since no JTWC warnings exist for vortices that do not develop into tropical cyclones, the time (N_0) corresponding to the maximum analyzed 850-mb relative vorticity was used as the reference time for the non-developing vortices. This time was determined during post-storm analysis. The non-developing vortex dataset ND1 included 104 vortices that persisted for at least 24 consecutive hours. The ND1 dataset was further analyzed to identify model false alarms. The ND2 dataset that included non-developing vortices that did not meet the minimum duration criterion was analyzed to determine which vortices were model over-forecasts. Only 60 of 127 vortices in the ND2 dataset met all four model over-forecast criteria.

a. Non-developing Vortices (ND1)

The next data set considered consists of the non-developing vortices that met the minimum duration criteria of 24 hours (ND1). Of the 254 tracked circulations, 104 vortices met the minimum duration criterion (column 2 of Table 3.1). The average duration of ND1 vortices was 3.1 days.

(1) 850-mb relative vorticity.

(a) Entire Basin Assessment. In contrast to the analyzed 850-mb relative vorticity for the developing vortices (Figure 3.5), the analyzed 850-mb relative vorticity for ND1 vortices (Figure 3.18) has very little slope change throughout the lifetime of the potential tropical circulation. The average vorticity at N_0 represents a local maximum in the analyzed vorticity curve. The average analyzed relative vorticity at N_0 (3.3×10^{-5} s^{-1}) is less than the average analyzed relative vorticity at F_0 (5.0×10^{-5} s^{-1}) for developing vortices. The small standard deviations about the analyzed means indicate that overall these non-developers have significantly smaller 850-mb relative vorticity than the developing cyclones, which is favorable for distinguishing the non-developing vortices if the forecasts are accurate in amplitude and trend.

Prior to N_0 the analyzed vorticity increases only slowly. The relatively flat slope of the analyzed vorticity is attributed to the near steady states, or at most slow developments, of these tropical vortices or monsoon depressions. The slope of the analyzed vorticity in Figure 3.18 decreases in the 36 h following N_0, which indicates a broadening or weakening of the circulation. Although the analyzed vorticity value at N_0 appears to be again reached 96 h after N_0, the circulation size is fairly small by this time.
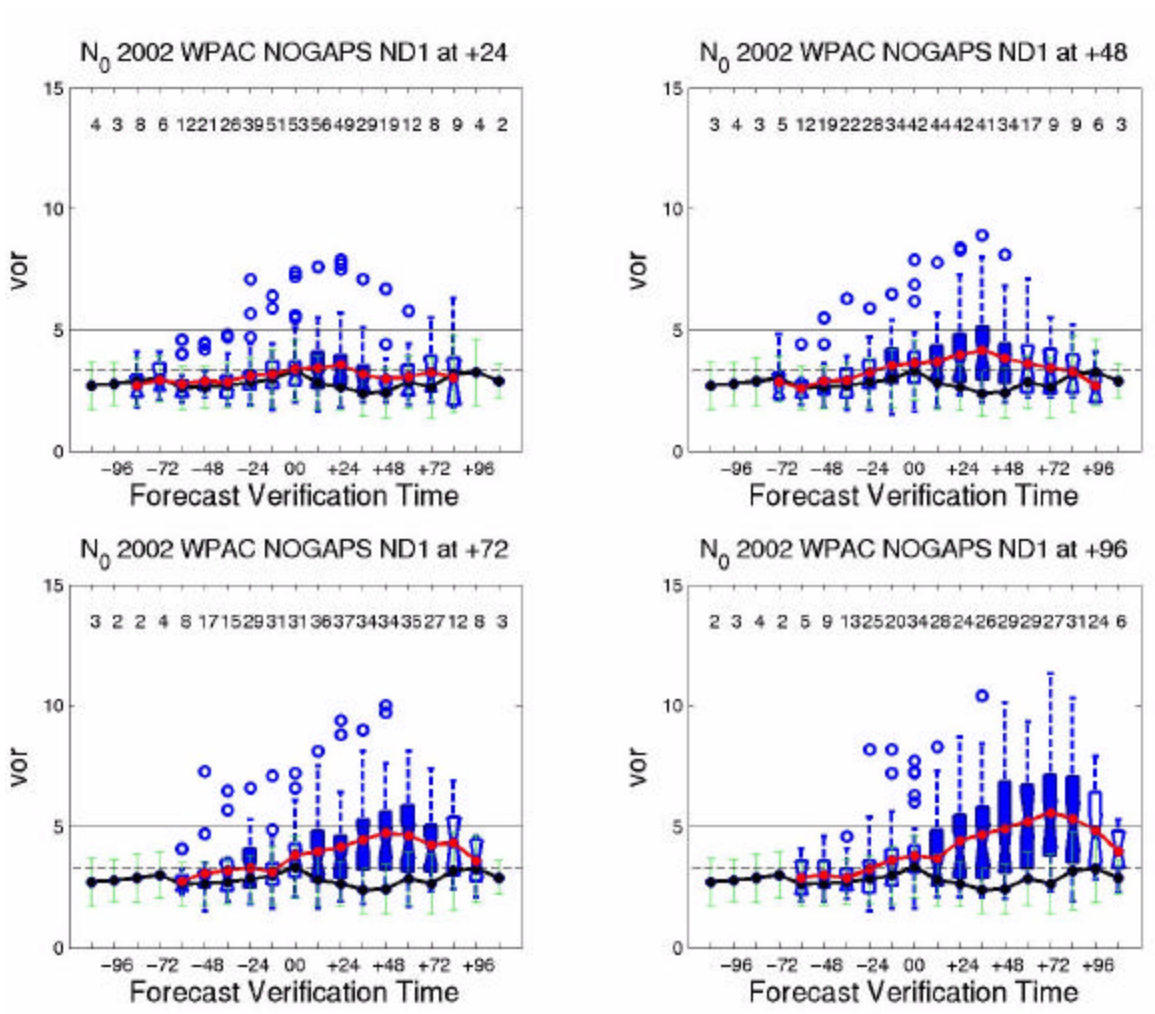
Figure 3.18. Average analyzed and forecast 850-mb relative vorticity as in Figure 3.5, except for non-developing vortices relative to N_0. Heavy black line represents analyzed average 850-mb relative vorticity for non-developing vortices (at +00), and red line represents average forecast 850-mb relative vorticity for the indicated forecast time. Average analyzed 850-mb relative vorticity at N_0 (light dashed black line) was 3.3 x 10^{-5} s^{-1}. The ζ_0 (light solid black line) of 5.0 x 10^{-5} s^{-1} is for the developing vortices in Figure 3.5 and provides a reference.

At forecast intervals of 72 h and less, the mean forecast 850-mb relative vorticity curves in Figure 3.18 do not exceed the ζ_0 value for developing storms at any forecast verification time. Therefore, in the mean the NOGAPS model correctly forecasts the non-development of these circulations. However, a few outliers at –24 h and +48 h (relative to N_0) do exceed the 5.0 x 10^{-5} s^{-1} ζ_0 value and thus could be mistaken for developing storms. In the 48-h forecasts in the upper-right panel of Figure 3.18, the

average 850-mb vorticity forecast values are significantly larger than the analyzed values from +12 h to +48 h (darkened boxes).

Although these average forecast values do not exceed the 5.0×10^{-5} s^{-1} ζ_0 value, the upper range and the outlier values do exceed the ζ_0 value, which again indicates erroneous 48-h formation forecasts are contained in this non-developing sample. This trend toward having a range of significantly larger forecast vortices than analyzed vortices continues for the 72-h and 96-h forecasts (lower-left and lower-right panels in Figure 3.18, respectively). Although the mean 72-h forecast vortices still do not exceed the 5.0×10^{-5} s^{-1} ζ_0 threshold, the box representing the upper 25% above the mean does exceed this threshold for the forecasts at the +36, +48, and +60 h verification times. For the 96-h forecast, even the mean exceeds the 5.0×10^{-5} s^{-1} ζ_0 threshold at the +60 h through +84 h verification times.

Interestingly, the time at which the maximum relative vorticity is forecast to occur increases with forecast range. In the upper-left panel of Figure 3.18, the maximum vorticity is forecast to occur 24 h after N_0. This coincidence of a 24-h forecast reaching maximum vorticity 24 h after the analyzed circulation reached a maximum value suggests the NOGAPS model has somehow continued the upward trend in analyzed values that occurred over the previous 24 h. In the 48-h forecasts (upper-right panel), the forecast maximum vorticity tends to occur 36 h after N_0. Similarly, the 72-h forecasts (lower-left panel) have maximum vorticity occurring at 48 h after N_0. The trend is continued for the 96-h forecasts (lower-right panel), where the maximum vorticity is forecast to occur 72 h after N_0. As noted above, the average magnitudes of the maximum vorticity forecasts also increase dramatically, along with the statistical significance of those average forecast errors.

The trends in Figure 3.18 confirm, similarly to Figure 3.5, that in 2002 the NOGAPS model tends to over-forecast relative vorticity. The growth of errors in the longer forecasts suggests a systematic error that may be attributed to an overly active convection scheme. If one assumes these non-developing storms do not contain the mesoscale convective systems (and vortices) that are assumed to exist in the developing systems, then the NOGAPS parameterizations of convection and friction may effectively simulate their effects in an excessive manner. An alternate explanation is that these

convective uncertainties are related to the unpredictability of the tropical atmosphere at extended time ranges.

To determine if inaccurate representation of the vortex was causing some of the forecast vorticity errors, vortex size was examined (Figure 3.19). During the 24 h before and after N_0, vortex size remains relatively consistent around the analyzed N_0 value of 54.6 grid cells, which is only slightly less than the average analyzed size at F_0 (60 grid cells). Otherwise, no distinct trend in vortex size was noted in Figure 3.19, although in the early stages of the vortex life cycle a small increase in vortex size may occur from 84 to 48 hours prior to N_0.
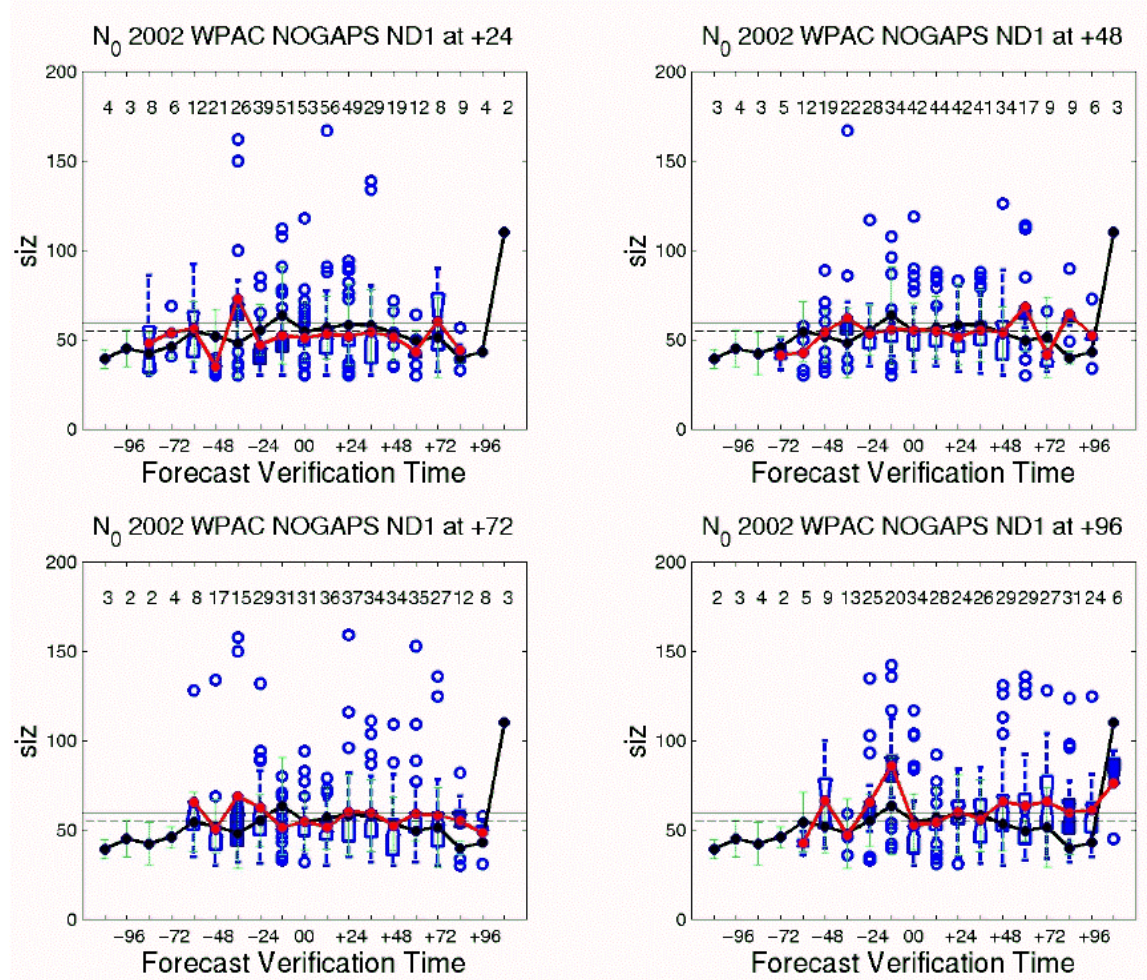
Figure 3.19. Average analyzed and forecast vortex size (grid cells) for all non-developing vortices relative to N_0 as in Figure 3.7. Heavy black line represents analyzed average vortex size for non-developing vortices (at +00), and red line represents average forecast vortex size for the indicated forecast time. Average analyzed vortex size at N_0 (light dashed black line) was 54.6 grid cells. Average size at F_0 was 60 grid cells.

That very little difference exists between the size of the developing vortices and non-developing vortices at the first JTWC warning and maximum vorticity time, respectively, implies that the size differences between the two circulations are small, at least early in life cycle of the circulation. At about 96 h prior to F_0, when the developing circulation (Figure 3.5) has the same analyzed relative vorticity as N_0 (3.3×10^{-5} s^{-1}), the corresponding average size of the developing circulations (Figure 3.7) is about 53 grid cells, which is comparable to the size of the non-developing vortices at N_0. The primary difference between these two data sets in the hours following this equivalence point is the steady increase in analyzed 850-mb relative vorticity for the developing circulations, and initial decrease in analyzed vorticity for the non-developing vortices. Since the sizes are about the same, the spin-up of the vorticity in the developing cyclones must be at interior points.

Forecasts of vortex size (Figure 3.19) were not preferentially over- or under-forecast, which indicates no strong trend in the NOGAPS model forecasts. Only a weak trend toward under-forecasting the vortex size was noted in the hours following N_0. Notice the trend for the outliers to be forecast to be too large by a factor of 2-3. An undersized vortex is expected with over-forecast relative vorticity in a hydrostatically and geostrophically balanced model.

        (b)   *Subregion Assessments.* To determine if the NOGAPS model preferentially developed vortices in one of the three western North Pacific Ocean subregions, the ND1 vortices were separated based on formation location. There were more non-developing vortices in the PS subregion (44%) than in the SCS (28%) or EMT (28%) subregions (column two of Table 3.1). Non-developing vortices in the SCS subregion persisted slightly longer (3.6 days) than vortices in either the EMT (2.9 days) or PS (2.7 days) subregions. The monsoon depressions in the SCS may drift slower due to opposing flows on either side of the monsoon trough leading to a small steering effect. In the PS, the westward motion may be larger and the circulations either develop or move out of the region. The longer duration of non-developing vortices in the SCS subregion is possibly associated with an earlier identification of the vortex in the NOGAPS model analyses, due to better observations or a more organized circulation in the NOGAPS

model analysis. It is possible that these vortices took longer to dissipate once the development ceased than in other subregions. Another possible explanation is that the non-developing vortices in the SCS experienced several growth and development pulses prior to dissipation, as might be inferred from the repeated increases and decreases in the slope of the analyzed vorticity in Figure 3.20.

The forecasts of relative vorticity the SCS subregion (Figure 3.20) do not reflect any pulses in intensity, but instead are consistently greater than analyzed, and also
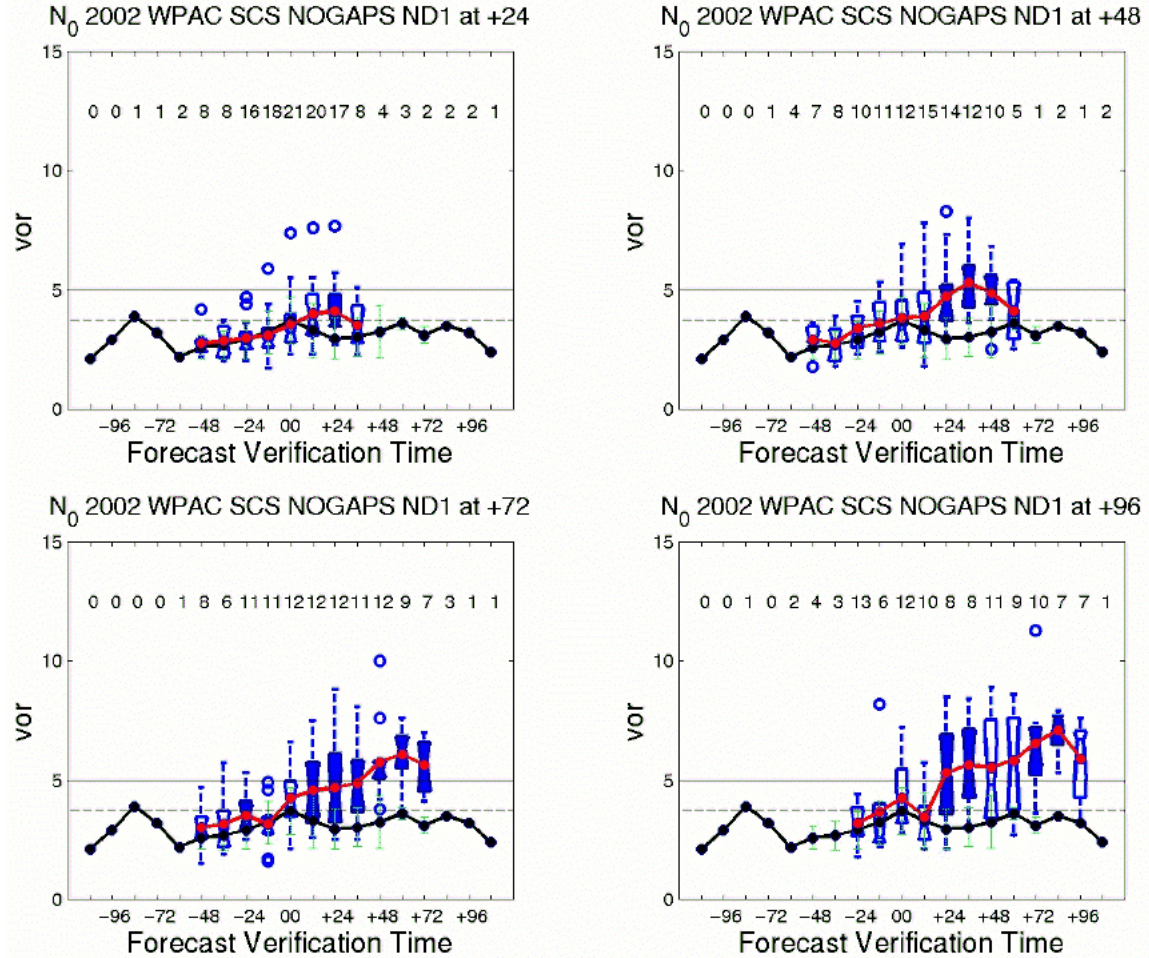
Figure 3.20. Average analyzed and forecast 850-mb relative vorticity (x 10^{-5} s^{-1}) as in Figure 3.18, except for non-developing vortices within the SCS subregion relative to N_0. Heavy black line represents analyzed average 850-mb relative vorticity for non-developing vortices (at +00), and red line represents average forecast 850-mb relative vorticity for the indicated forecast time. Average analyzed 850-mb relative vorticity for this subset of non-developing vortices at N_0 (light dashed black line) was 3.7 x 10^{-5} s^{-1}. $?_0$ (light solid black line) is 5.0 x 10^{-5} s^{-1}.

steadily increasing. As in the overall sample (Figure 3.18), the range of forecast values increases with increasing forecast range, as does the time of maximum forecast vorticity. However, the sample sizes quickly become small at extended forecast intervals.

The duration of the vortices in the PS (2.7 days) was slightly less than the average duration for all non-developing vortices (3.1 days). Less fluctuation about the analyzed vorticity in the early stages of development is observed in the PS (Figure 3.21) than in the SCS (Figure 3.20), with the profile of analyzed relative vorticity for the PS region subset more closely resembling the analyzed vorticity profile for all non-developers (Figure 3.18). The average analyzed vorticity for this subset of non-developers was 3.2×10^{-5} s^{-1}, which is just slightly less than the average analyzed vorticity for all non-developers $(3.3 \times 10^{-5} \ s^{-1})$.

As in the SCS subregion, little deviation between the analyzed and forecast values was noted in the short-range ($\leq$ 48 h) forecasts for the PS subregion in the hours leading up to N_0. This lack of significant error implies that the NOGAPS model accurately forecasts the early stages of development for these vortices. In the hours following N_0 the analyzed vorticity decreases while the forecast vorticity increases. This deviation is associated with the tendency of the NOGAPS model to continue development of a circulation that is actually beginning to dissipate. The amount of deviation between the analyzed and forecast relative vorticity increases with larger forecast range, as does the forecast time of maximum analyzed relative vorticity. However, the difference between forecast and analyzed vorticity after N_0 is not as large over the PS as it is over the SCS.

Interestingly, the analyzed 850-mb relative vorticity increases again 48 h after N_0 in Figure 3.21. At this secondary maximum, which exists only within the PS subregion, the 850-mb relative vorticity is roughly $4.0 \times 10^{-5} \ s^{-1}$, which is greater than the average analyzed vorticity at N_0 for both the subregion $(3.2 \times 10^{-5} \ s^{-1})$ and all the non-developing vortices $(3.3 \times 10^{-5} \ s^{-1})$. This secondary maximum could be associated with the reintensification of the non-developing vortex. However, since analyzed vorticity again decreases after this time, the vortex does not undergo further development, which implies this reintensification may be associated with a short-term increase in convection.
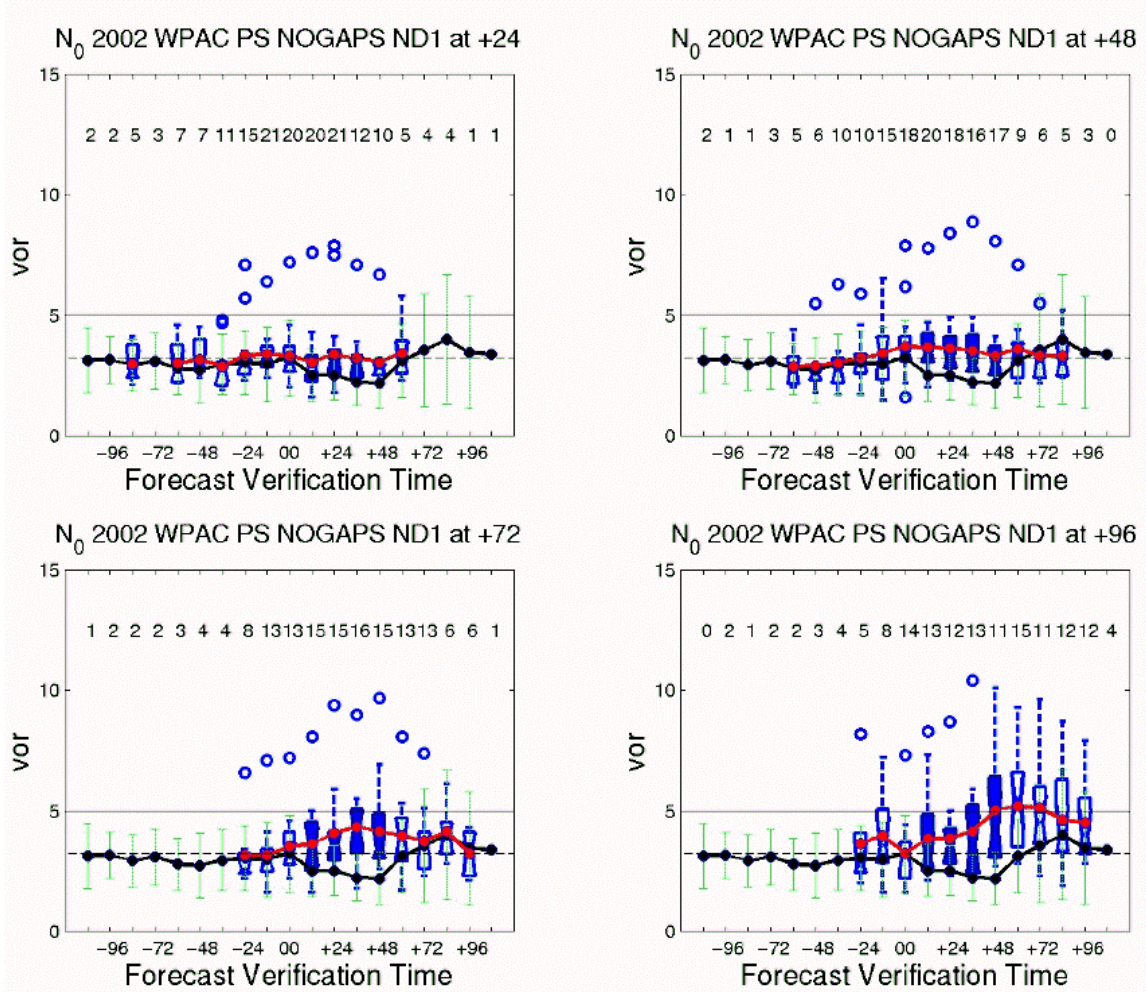
Figure 3.21. Average analyzed and forecast 850-mb relative vorticity (x 10^{-5} s^{-1}) for non-developing vortices relative to N_0 as in Figure 3.18, except within the PS subregion. Heavy black line represents analyzed average 850-mb relative vorticity for non-developing vortices (at +00), and red line represents average forecast 850-mb relative vorticity for the indicated forecast time. Average analyzed 850-mb relative vorticity for this subset of non-developing vortices at N_0 (light dashed black line) was 3.2 x 10^{-5} s^{-1}. ?0 (light solid black line) is 5.0 x 10^{-5} s^{-1}.

The average duration of non-developing vortices in the EMT subregion was 2.7 days, which is only slightly less that the duration for vortices developing in the PS subregion. The shorter duration of these non-developing EMT vortices, in direct contrast to the duration of the EMT developing vortices (5.0 days), may be associated with the shorter life cycle of vortices not associated with the main body of the monsoon trough.

The analyzed 850-mb relative vorticity for the non-developing vortices in the EMT subregion (Figure 3.22) closely resembles the analyzed vorticity for both the PS
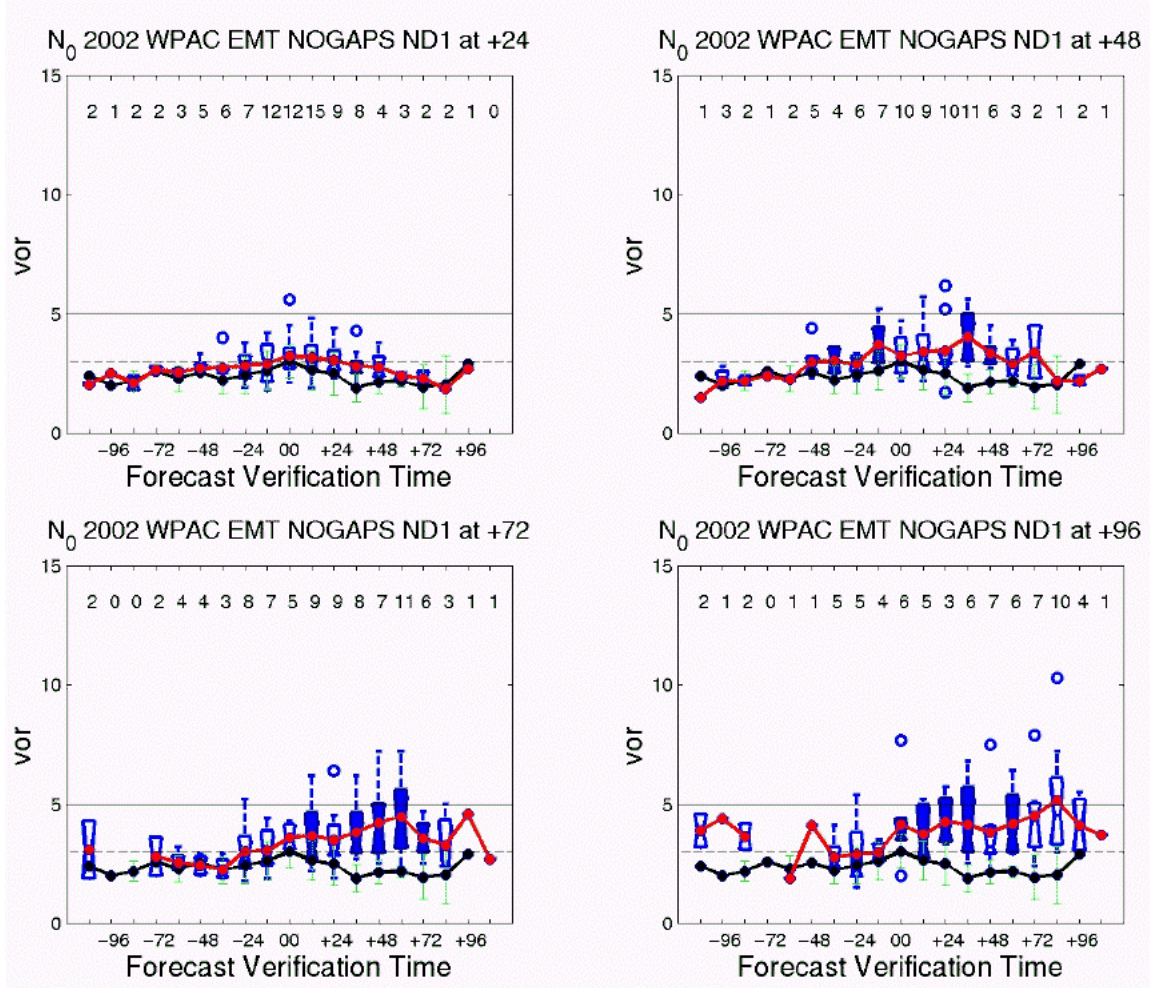
Figure 3.22. Average analyzed and forecast 850-mb relative vorticity (x 10^{-5} s^{-1}) for non-developing vortices relative to N_0 as in Figure 3.18, except for non-developing vortices within the EMT subregion. Heavy black line represents analyzed average 850-mb relative vorticity for non-developing vortices (at +00), and red line represents average forecast 850-mb relative vorticity for the indicated forecast time. Average analyzed 850-mb relative vorticity for this subset of non-developing vortices at N_0 (light dashed black line) was 3.0 x 10^{-5} s^{-1}. $?_0$ (light solid black line) is 5.0 x 10^{-5} s^{-1}.

subregion (Figure 3.21) and the entire basin (Figure 3.18). However, somewhat less drastic deviations from the average analyzed vorticity at N_0 are noted. As in the SCS subregion (Figure 3.20), the analyzed vorticity for the EMT non-developing vortices appears to fluctuate through several minor cycles of intensification and weakening, which may partially be a result of the sample size.

Although the vorticity forecasts consistently exceed the analyzed vorticity values, the 24-h forecasts contain the general increase and subsequent decrease in vorticity

relative to N_0, and have minimal deviations from the analyzed mean values. The fluctuations in forecast relative vorticity that are missing in the 48-, 72- and 96-h forecasts are likely associated with small sample size. Although the previous trend is for increasing forecast error with increased forecast range, the magnitudes are not as excessive in the EMT as in the overall sample (Figure 3.18).

Also of interest is the decrease in the number of extreme forecasts (open circles) in the EMT subregion, and the smaller standard deviation of the analyzed values (light green bars at each time interval in Figure 3.22. In addition to being associated with the smaller sample size, this is also due to a smaller spread in forecast vorticity values. While a smaller forecast spread does not directly indicate greater forecast accuracy, it does increase the probability of generating a more accurate forecast. This potentially increased analysis and forecast accuracy in the EMT may occur because the EMT vortices can be more easily distinguished from the background environment than those that occur in conjunction with the monsoon trough in the PS and SCS subregions.

(2) Deep Layer Wind Shear. As for the developing vortices, the terminology for over- and under-forecast must be outlined since the deep layer wind shear variable can be either positive or negative (indicating direction). Negative shear indicates increasing easterlies with height, and positive shear indicates the opposite, with increasing westerlies with height. The term over-forecast is applied to forecasts of decreasing westerly wind shear if they become less positive, or to decreasing easterly shear if the forecasts become less negative.

While the slope of the analyzed shear with time for the developing vortices in Figure 3.14 decreases steadily throughout the life cycle of the tropical circulation, this trend is not apparent for the non-developing vortices that met the minimum duration criterion (Figure 3.23). The analyzed deep wind shear value at N_0 for the ND1 data set was 4.1 m s^{-1}, compared to the -1.8 m s^{-1} analyzed at F_0 for developing vortices. Thus, the developing storms experienced easterly shear that is considered to be favorable for tropical cyclone formation. However, the non-developing vortices experienced an almost equal amount of westerly shear, which is considered to be less favorable. This easterly shear remained relatively constant in time relative to N_0 between -60 h and $+60$ h when a reasonable number of cases are available. Thus, this variable may be quite useful in
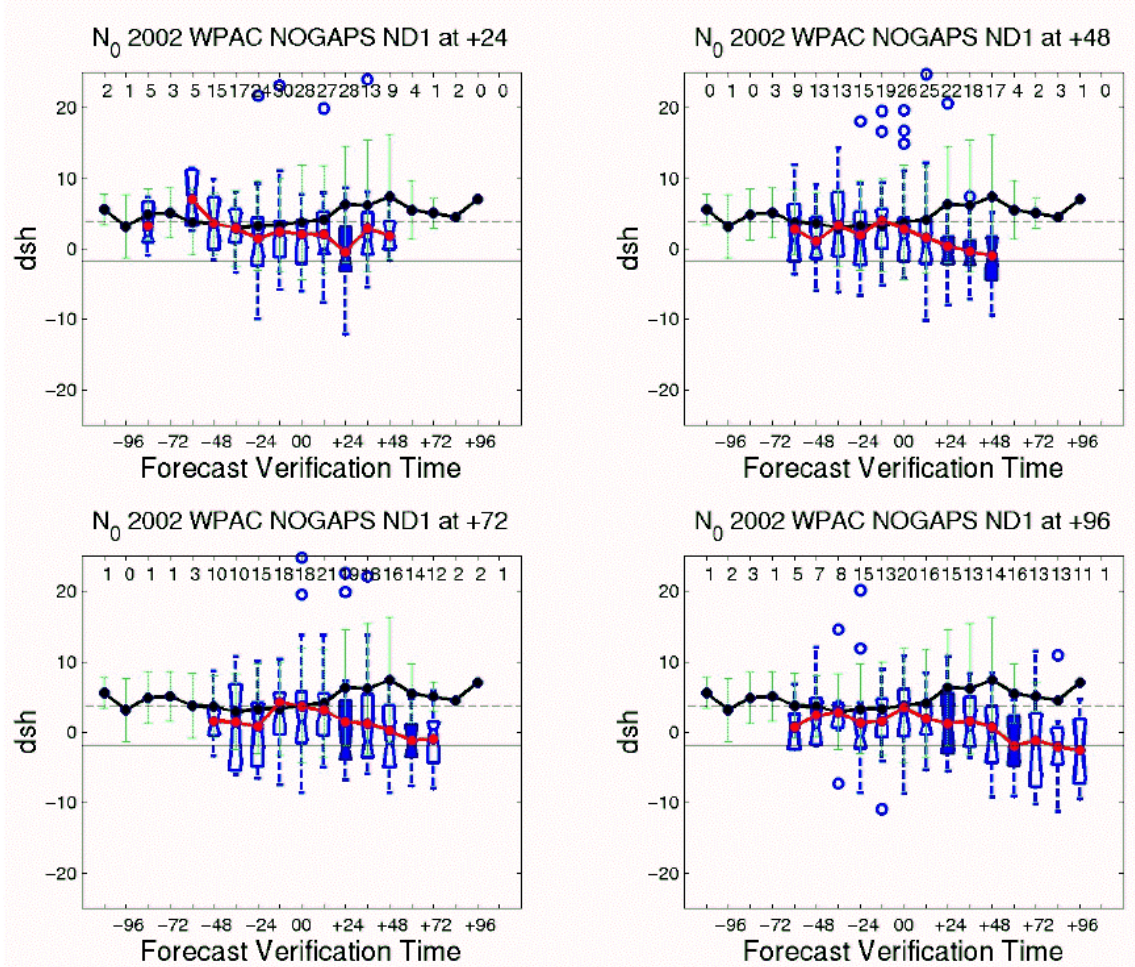
Figure 3.23. Average analyzed and forecast deep layer wind shear (200-850 mb) for non-developing vortices relative to N_0, as in Figure 3.18. Heavy black line represents analyzed average deep wind shear for non-developing vortices (at +00), and red line represents average forecast deep wind shear for the indicated forecast time. Average analyzed deep wind shear at N_0 (light dashed black line) was 4.1 m s^{-1}. V_0 (light solid black line) is –1.8 m s^{-1}.

distinguishing between developing and non-developing circulations if it can be accurately forecast.

Forecasts of deep shear for the ND1 data set are almost all less than the analyzed shear values at each of the four forecast intervals in Figure 3.23. Forecast deviations from the analyzed values increase with increasing forecast range. Whereas only one (+24 h) difference between mean forecast and mean analyzed value for the 24-h forecasts (upper-left panel of Figure 3.23) is statistically significant, five, six, and five values are significantly different for the 48-h, 72-h, and 96-h forecasts, respectively, commensurate

61

with the increases in forecast relative vorticity discussed above. The average deep shear forecasts are also preferentially lower than the analyzed deep shear, and do not transition from forecasts of westerly to easterly shear until approximately 24 h after N_0. Forecasts of easterly shear occur mainly in the extended range ($\geq$ 72-h) forecasts, and correspond to vorticity forecasts that exceed the $?_0$ threshold (Figure 3.18). Such a decreasing forecast vertical shear toward near-zero values is considered to be favorable for cyclonic development as the warm core will be less ventilated. Thus, this factor is a plausible physical explanation for the over-forecast of 850-mb relative vorticity (Figure 3.18) for this sample of non-developing vortices. What aspect of the NOGAPS model that might lead to this decreasing westerly shear over non-developers is not clear. One hypothesis might be that the cumulus momentum transfer is too larger and tends to minimize vertical wind shear.

Comparison of Figures 3.5 and 3.14 for the developing storms indicates that the transition from westerly to easterly analyzed shear occurs when analyzed 850-mb relative vorticity exceeds about 4 x 10^{-5} s^{-1}. This is also true for the non-developing vortices in Figure 3.18 and 3.23. When the forecast 850-mb vorticity in Figure 3.18 exceeds about 4 x 10^{-5} s^{-1} (+36 h for the 48-h forecasts), the forecast deep wind shear in Figure 3.23 transitions from westerly to easterly. This transition from westerly to the preferential easterly deep wind shear does not occur in the ND1 analyzed curve since the analyzed 850-mb relative vorticity for this data set does not exceed 4 x 10^{-5} s^{-1}. It is thus possible that this westerly shear prevented further development of the vortices in this data set, but the NOGAPS forecast of a decreasing vertical wind shear in time allowed some non-developing cases to intensify to 4 x 10^{-5} s^{-1}.

(3) Sea-level Pressure. The analyzed mean sea-level pressures for the ND1 data set (Figure 3.24) showed very little change relative to N_0 and throughout the life cycle of these non-developing vortices. At all times, the analyzed SLP for the ND1 data set was greater than the average analyzed SLP for developing vortices (Figure 3.15). The average analyzed SLP at N_0 was 1008.0 mb, which is 1.4 mb higher than the analyzed SLP for developing vortices (1006.6 mb). This difference, while small, is important in that it implies a less deep trough within which the vortex is trying to
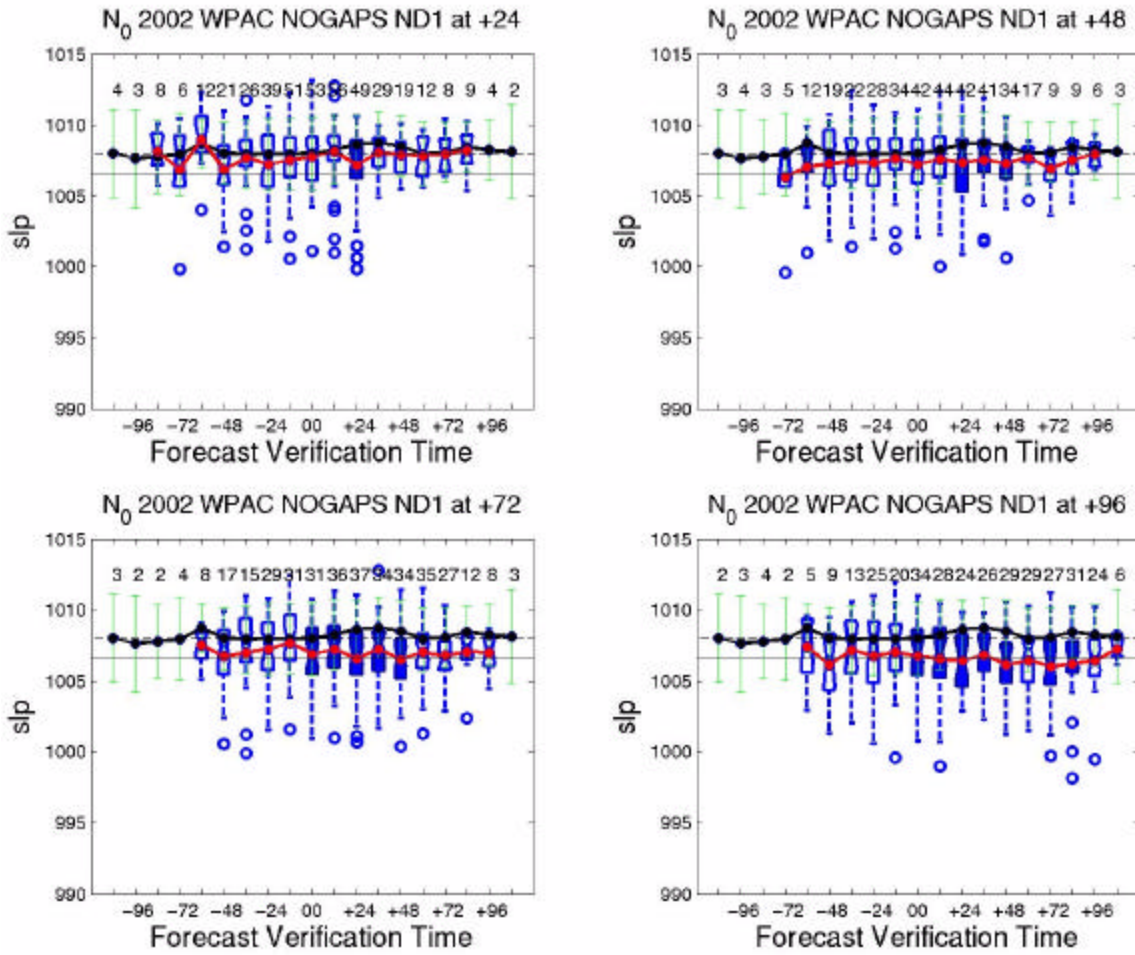
Figure 3.24. Average analyzed and forecast sea level pressure (SLP) (mb) for non-developing vortices relative to N_0, as in Figure 3.18. Heavy black line represents analyzed average SLP for non-developing vortices (at +00), and red line represents average forecast SLP for the indicated forecast time. Average analyzed SLP at N_0 (light dashed black line) is 1008.0 mb. P_0 (light solid black line) for developing circulations is 1006.6 mb.

develop. Slightly higher SLP implies a less-developed warm-core aloft. In this sense, the SLP may be more of a proxy as to the degree of development rather than a predictor.

The slight increase in the slope of the analyzed SLP line in the 24 h following N_0 is consistent with the weakening of the analyzed 850-mb relative vorticity (Figure 3.18) during the same time frame. While the slope of the analyzed SLP for developing circulations (Figure 3.15) decreased throughout the 120 h prior to and following F_0, no commensurate decrease is found for the analyzed SLP of the non-developing vortices. While part of the decrease after F_0 in analyzed SLP for the developing vortices was

associated with the insertion of the synthetic tropical cyclone observations, no similar insertion would occur for the non-developing vortices, which leads to the ND1 analyzed SLP profile more closely resembling the early stages of the developing vortices in Figure 3.15, i.e., prior to intensification of the developing circulation.

Forecasts of SLP for the non-developing vortices are typically for a lower SLP than the analyzed SLP (Figure 3.24). Deviations of the forecast SLPs from the analyzed SLPs increase with increasing forecast range from 24 h through 96 h. In particular, the forecast SLPs for the ND1 data set at 72 h (lower-left panel in Figure 3.24) and at 96 h (lower-right panel) are consistently at or below the SLP threshold (1006.6 mb) determined for the developing vortices. These decreases in forecast SLP can be associated with the over-forecast 850-mb relative vorticity at these longer forecast ranges in Figure 3.18.

Forecast error also increases with forecast range in Figure 3.24, which again suggests a systematic bias in the heating over these non-developing cases. Notice that the forecast extrema in Figure 3.24 are considerably lower than the analyzed SLP for non-developing vortices, and these outliers have SLPs well below those of the mean analyzed SLP for the developing cases than the analyzed SLP for the non-developing cases. These low extrema are expected given the NOGAPS model tendency to over-forecast vorticity and generally to over-intensify tropical circulations. The high SLP extrema were not expected. Although infrequent, these high SLP values represent NOGAPS forecasts that substantially weaken the circulation, or perhaps can be attributed to erroneous tracking of systems closer to the subtropical high.

(4) 925-mb Wind Speed. The analyzed 925-mb wind speed (Figure 3.25) has relatively small (~1-1.5 m s^{-1}) changes to N_0, although the slope does increase steadily from 60 h prior to N_0, decrease in the 36 h immediately following N_0, and then increases again after 36 h. The steady increase in wind speed prior to N_0 is attributed to the early developmental stages of the potential tropical cyclone. While the value of the wind speed at N_0 (7.0 m s^{-1}) is a local maximum, it is not the maximum analyzed value for the entire forecast period. However, the maximum value (about 8 m s^{-1}) occurs 120 h after N_0, but it is suspect since it is based on fewer than five cases. The decrease in wind speed in the hours immediately following N_0 is consistent with the decrease in 850-mb
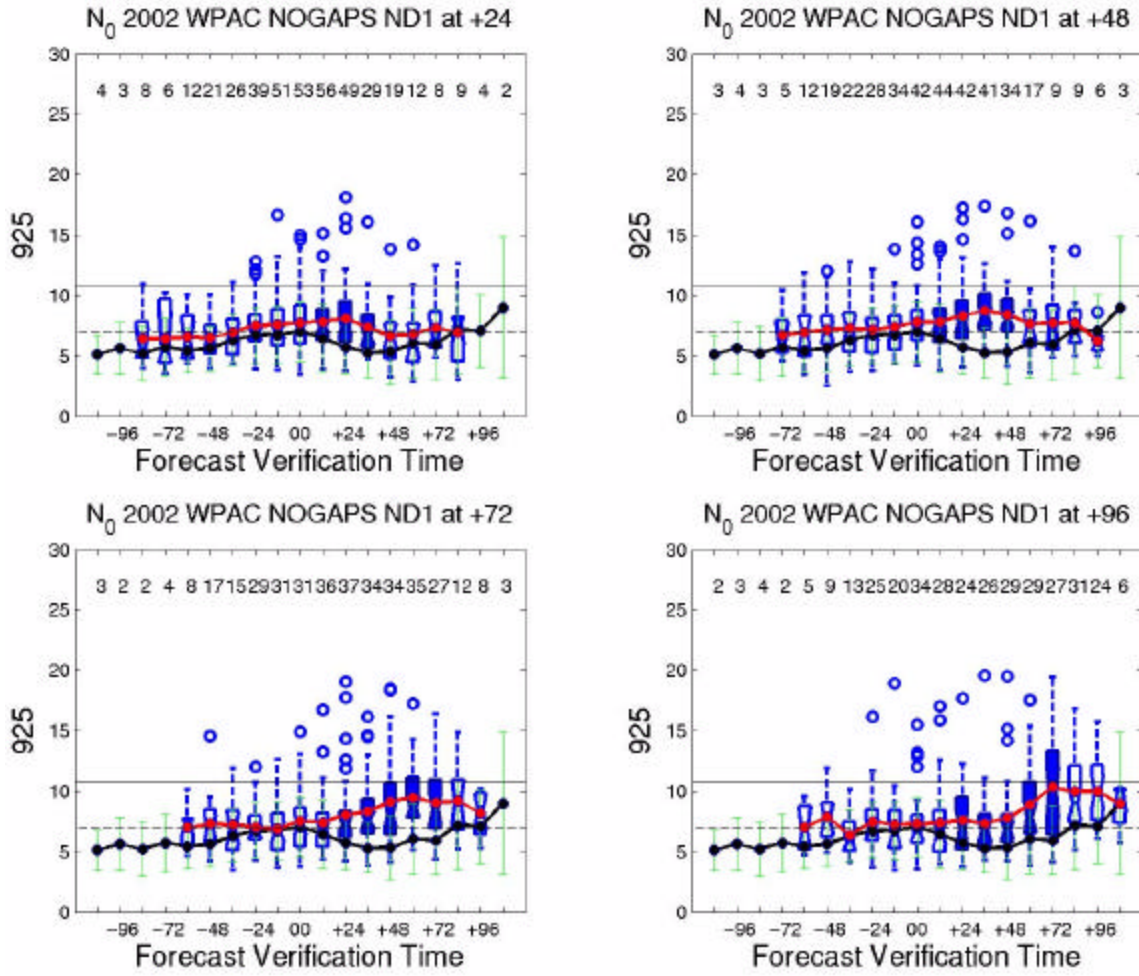
Figure 3.25. Average analyzed and forecast 925-mb wind speed (m s^{-1}) for non-developing vortices relative to N_0, as in Figure 3.18. Heavy black line represents analyzed average 925-mb wind speed for non-developing vortices (at +00), and red line represents average forecast 925-mb wind speed for the indicated forecast time. Average analyzed 925-mb wind speed at N_0 (light dashed black line) is 7.0 m s^{-1}. V_0 (light solid black line) is 10.8 m s^{-1}.

relative vorticity (Figure 3.18) that is attributed to a broadening and weakening of the tropical circulation. The increase in wind speed that begins 36 h after N_0 follows the slight increase in analyzed relative vorticity that occurs at the same time.

The difference of about 4 m s^{-1} between these 925-mb wind speeds for non-developing cases and developing cases potentially offers another distinguishing characteristic for formation. Since this wind speed has been averaged over the ellipse centered on the position, it is not surprising that the development sample has larger

values at later times than the non-developing cases. However, the standard deviations of the two samples are relatively small compared to the differences in the means.

Forecasts of 925-mb wind speed for the ND1 data set are consistently higher than the analyzed wind speed for the same vortices. However, forecasts of wind speed do not exceed the wind speed threshold determined for developing vortices (10.8 m s^{-1}). As was the case for the forecasts of non-developing vortices for other variables, the forecast spread and errors increase with increasing forecast range, and both the magnitude and occurrence time of the maximum forecast wind speed also increase. However, the forecast means for these non-developers do exceed the mean value for the developing cases (10.8 m s^{-1}) even for the 96-h forecasts.

The outlier values of wind speed are all greater than the analyzed wind speed at N_0, and also at F_0 for the developing storms, which is consistent with the over-forecasts of 850-mb relative vorticity. These extrema indicate a tendency of the NOGAPS model to over-forecast 925-mb wind speed, as expected in a hydrostatically and geostrophically balanced model that forecasts too large 850-mb relative vorticity and too low SLP.

(5) Vapor Pressure. Average 500-700 mb vapor pressure, which indicates the amount of mid-level moisture available to a developing tropical circulation, has more variation relative to the threshold value for non-developing vortices (Figure 3.26) than for the developing vortices (Figure 3.17). The average analyzed vapor pressure at N_0 (3.4 Pa) and F_0 (3.6 Pa) differ by only 0.3 Pa, which makes the vapor pressure a poor indicator of potential development.

The analyzed vapor pressure for non-developing vortices increases steadily from 96 hours prior to N_0 to a maximum value at N_0-12 h, and then steadily decreases until 36 h after N_0. This trend indicates intensification and then weakening of the non-developing warm-core vortex. The increase in vapor pressure 36 h after N_0 is attributed to a weak and unsuccessful reintensification of the warm core. That the analyzed vapor pressure never exceeds the threshold value for the developing circulations indicates that in addition to a drier mid-troposphere, the potential warm-core vortex is somewhat weaker.

The forecast curves for vapor pressure lie almost entirely below the analyzed vapor pressure curve, and for the most part, are also below the average analyzed vapor pressure at N_0. This small but consistent under-forecasting of vapor pressure by the
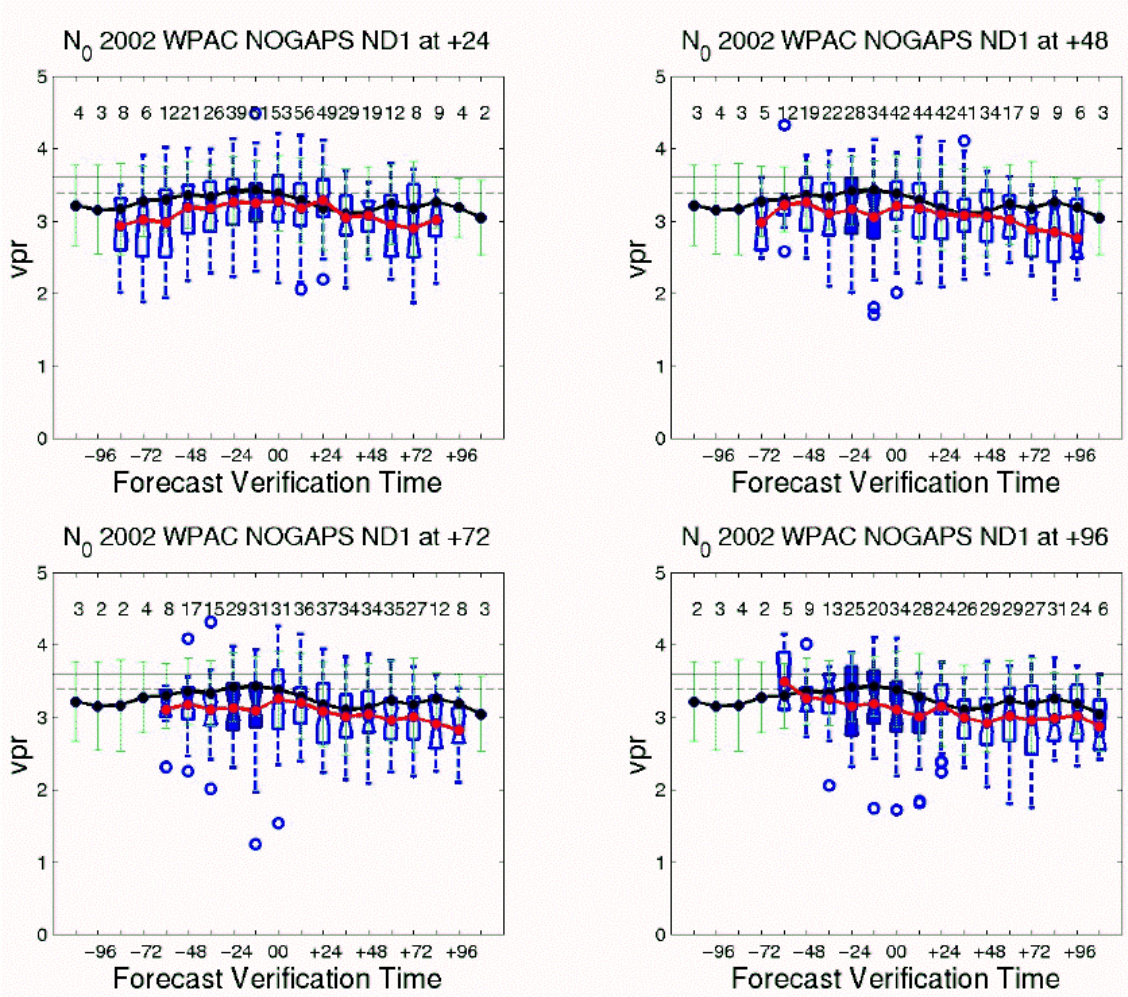
Figure 3.26. Average analyzed and forecast vapor pressure (500-700 mb average, Pa) for non-developing vortices relative to N_0, as in Figure 3.18. Heavy black line represents analyzed average vapor pressure for non-developing vortices (at +00), and red line represents average forecast vapor pressure for the indicated forecast time. Average analyzed vapor pressure at N_0 (light dashed black line) was 3.4 Pa. F_0 vapor pressure threshold (light solid black line) is 3.6 Pa.

NOGAPS model is likely a result of incorrect representation of the mid-level mesoscale warm core, and again shifts formation from a mesoscale event in the NOGAPS model forecasts to a large-scale event.

As with other forecast variables, forecast spread and error increase with increasing forecast range. The outlier values, while not all high or low compared to the average analyzed vapor pressure at any forecast interval, do have some exceedingly dry values. Such dry mid-tropospheric values would not be consistent with formation, as noted previously.

b. *Model Over-forecasts (NDOF)*

Model over-forecast vortices were identified as those for which the NOGAPS model forecast continued development of a circulation that did not meet the minimum duration criterion (existence in three consecutive model analyses). When determining whether or not an analyzed vortex was over-forecast, some simple rules were applied. If a vortex existed only once in an analysis panel (+00), then there had to be at least three corresponding forecast groups for it to be classified as an over-forecast. If the vortex existed for two consecutive analyses, then it had to have at least four consecutive forecast groups in common with the two analyses for it to be classified as an over-forecast. Vortices that existed in three or more analyses were not included in this category, but were instead included in the ND1 data set. Although the forecast circulation then existed at times when an analogous circulation (of at least $? = 1.5 \times 10^{-5}$ s^{-1}) could not be matched, this is not a false alarm – it is over-forecast in length of time and not necessarily in magnitude of some variable such as SLP. Of the 127 vortices rejected for not meeting the minimum duration criterion, 60 were classified as over-forecasts (column three of Table 3.1). Thus, this situation is a relatively common occurrence that needs to be examined.

An example of the analyzed and forecast tracks for an over-forecast circulation is shown in Figure 3.27. This circulation was initially rejected from the dataset since it did not exist in a NOGAPS analysis for at least three consecutive periods. However, it did meet the above criteria for an over-forecast circulation, since it existed for two analyses and at least four consecutive model forecasts. The PS subregion contained the most over-forecast circulations (28) compared to the SCS (18) and EMT (16) subregions.

(1) 850-mb Relative Vorticity. Since the minimum duration criterion was not met for the over-forecast non-developing vortices, a new reference time had to be determined. All the vortices that met the over-forecast non- developing vortex criteria existed in at least one NOGAPS model analysis. The new reference time (designated N_0*) from which forecast time intervals were calculated was defined to be the last time the vortex existed in a NOGAPS model analysis, rather than the time at which the maximum analyzed 850-mb vorticity occurred. Given the criteria for over-forecast non-developing vortices, the analyzed 850-mb relative vorticity values are available for at
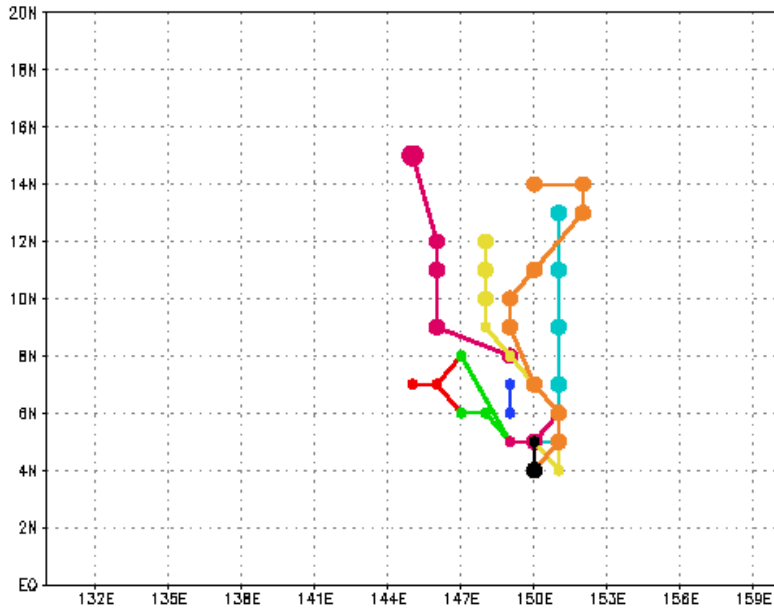
Figure 3.27. Example of forecast tracks for an over-forecast non-developing vortex. Circles indicate successive 12 h forecasts of the circulation center, with the size of the circle indicating the intensity. Black circles indicate analyzed values, and colored circles indicate separate forecast times.

most only two intervals (Figure 3.28). On average, the analyzed vorticity at N_0* (2.4 x 10^{-5} s^{-1}) is slightly less than the analyzed vorticity 12 h prior to N_0*, which implies a slight weakening of the analyzed vortex.

The forecasts of 850-mb relative vorticity are the defining feature of this subset of non-developing vortices because each of these over-forecast vortices was defined to exist in the forecasts for at least twice as long as it existed in the NOGAPS analysis. The forecast vorticities (Figure 3.28) are nearly all greater than the analyzed vorticities with very few exceptions. The longer-range forecasts ($\geq$ 72-h) tend to not only have longer durations, but also to forecast larger vorticity magnitudes than the shorter-range forecasts. Whereas the analyzed vorticity decreases from N_0*-12 h to N_0*, the vorticity is forecast to increase during and following that time. This tendency for the NOGAPS model to hold on to dissipating circulations is consistent with the general tendency to over-develop the tropical circulations in this sample. Although the mean forecast vorticities do not exceed the mean analyzed vorticity for developing vortices ($?_0$ = 5.0 x 10^{-5} s^{-1}), some of the outliers do cross this threshold and thus could be mistaken for developing vortices.
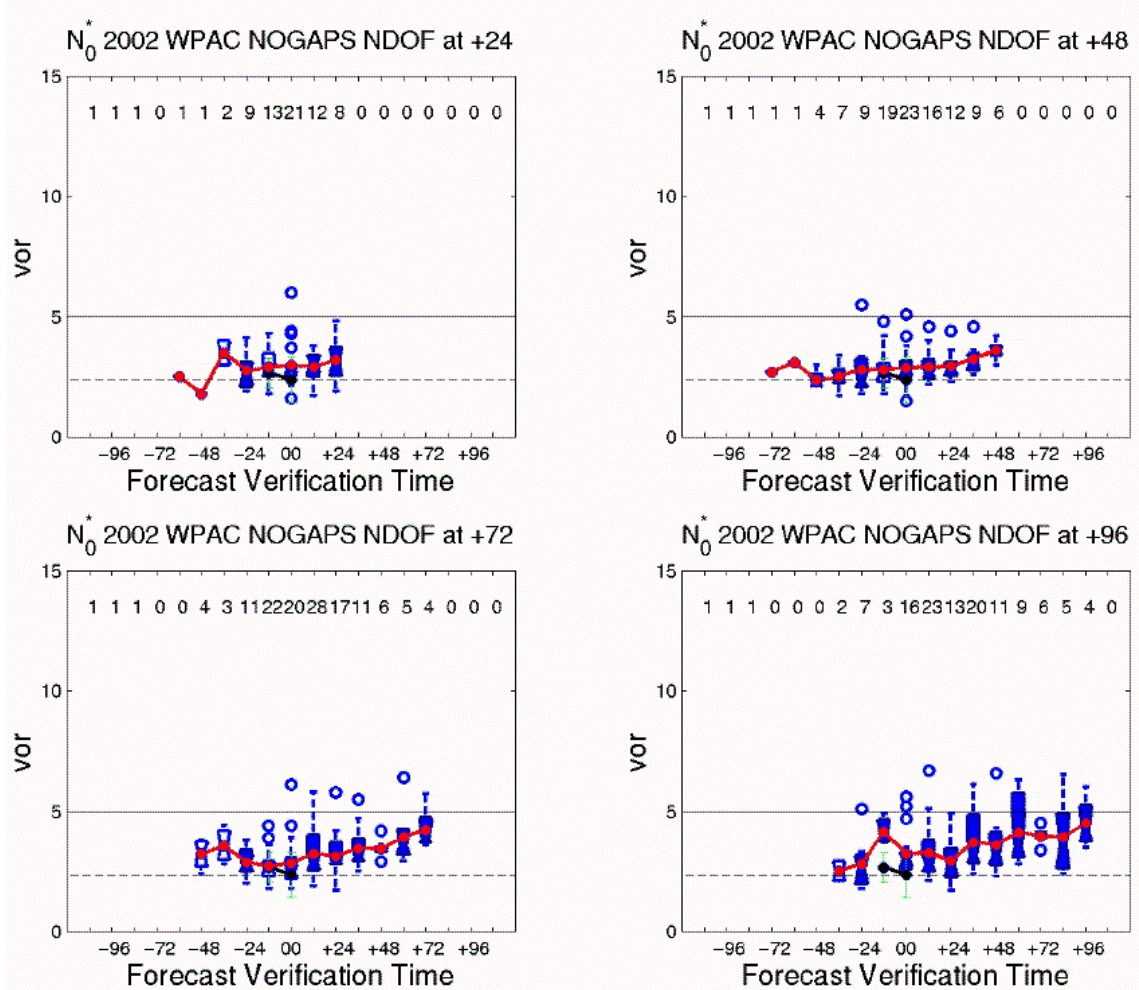
Figure 3.28.   Average analyzed and forecast 850-mb relative vorticity (x 10^{-5} s^{-1}) for over-forecast non-developing vortices as in Figure 3.18.   Heavy black line represents analyzed average 850-mb relative vorticity for over-forecast non-developing vortices (at +00), and red line represents average forecast 850-mb relative vorticity for the indicated forecast time.   Average analyzed 850-mb relative vorticity for this subset of non-developing vortices at N_0 (light dashed black line) was 2.4 x 10^{-5} s^{-1}. $?_0$ (light solid black line) is 5.0 x 10^{-5} s^{-1}.

(2) Deep Layer Wind Shear.   As was the case for the overall non-developer sample, the analyzed deep layer wind shear is westerly for these cases.   The magnitude of the analyzed deep wind shear for over-forecast non-developing vortices (Figure 3.29) does not change appreciably from N_0^*-12 h to N_0^*.   This lack of slope change is due to the short time elapsed between the two analysis intervals, which may be insufficient to reflect a change in wind shear as a response to the decrease in 850-mb relative vorticity at N_0^* in Figure 3.28.
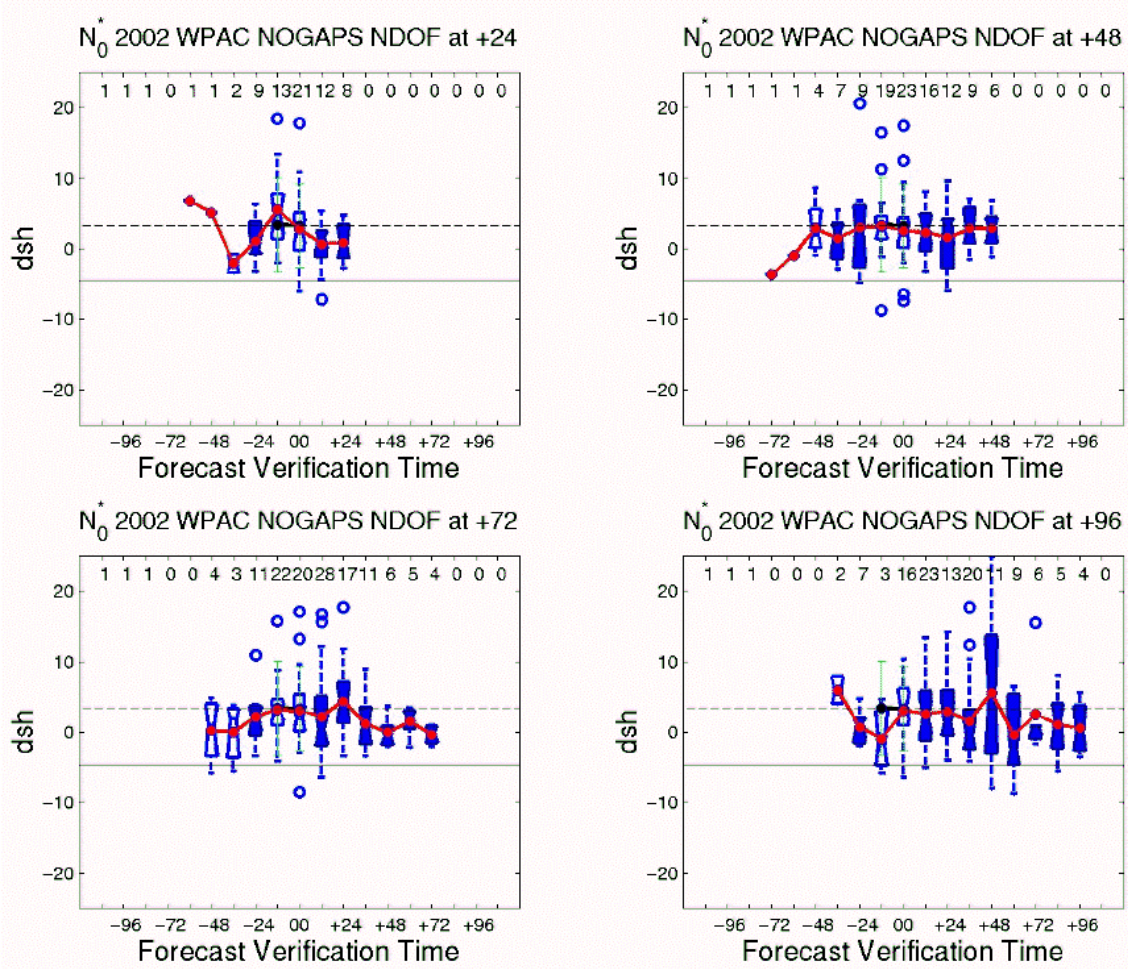
Figure 3.29. Average analyzed and forecast deep wind shear (200-850 mb) for non-developing over-forecast vortices relative to N_0. Heavy black line represents analyzed average deep wind shear for non-developing over-forecast vortices (at +00), and red line represents average forecast deep wind shear for the indicated forecast time. Average analyzed deep wind shear at N_0 (light dashed black line) was 3.2 m s^{-1}. V_0 (light solid black line) is –1.8 m s^{-1}.

The forecast deep layer wind shear at N_0* is very close to the analyzed value (3.2 m s^{-1}). There is no strong trend in the NOGAPS model for the forecasts to be substantially over- or under-forecast relative to N_0*. The forecasts generally indicate positive (westerly) shear, which was shown above to be common among the non-developing vortices. The trend identified above for a transition from westerly to easterly shear when the 850-mb relative vorticity is forecast to be greater than about 4.0 x 10^{-5} s^{-1} is not as apparent in Figure 3.29 as it is in Figures 3.23. Although more of the outlier

vertical shears are for large westerly shears, especially for the 72-h forecasts, some outliers with large easterly shear are forecast.

c. False Alarms

False alarms were separated into three categories: the non-developing vortices that met the minimum duration criterion, and were forecast to exceed the vorticity threshold determined for the developing circulations; the NOGAPS model false alarms, in which the model predicted development of a vortex that was never analyzed; and TCFA false alarms, in which the JTWC issued a TCFA for a circulation that, while it could be usually be matched with a circulation in the NOGAPS analysis, was never warned on.

(1) Non-Developing Vortices - Group 2 (NDG2). Group 2 represents the subset of non-developers that met the minimum duration criterion (ND1), but were relatively extreme in the sense that they were forecast to exceed the 850-mb relative vorticity value for developing vortices (5.0×10^{-5} s^{-1}). A total of 50 vortices met the criteria for inclusion in this data set (column four of Table 3.1). Whereas the cases contained in this data set are a subset of the ND1 data set, the analysis here is to determine if any single factor prevented these favorable-forecast vortices from developing into numbered tropical circulations. An example of a set of Group 2 tracks is shown in Figure 3.30. Intensity is indicated by the size of the circle at each position. The Group 2 circulations formed preferentially in the PS subregion (21), although the number of Group 2 circulations in the SCS was only slightly less (19).

(a) *850-mb Relative Vorticity.* More variability exists in the slope of the analyzed 850-mb relative vorticity for Group 2 (Figure 3.31) than in the overall ND1 data set. The slope of the line prior to the maximum analyzed vorticity at N_0 more closely resembles the slope of the analyzed vorticity for developing vortices in Figure 3.6 prior to F^*_0. However, the slope for the Group 2 vortices is slightly more shallow than the analyzed vorticity slope for the overall ND1 data set (Figure 3.18). The sudden decrease in analyzed vorticity at N_0 is attributed to a weakening of the vortex in the model associated with dissipation.

72
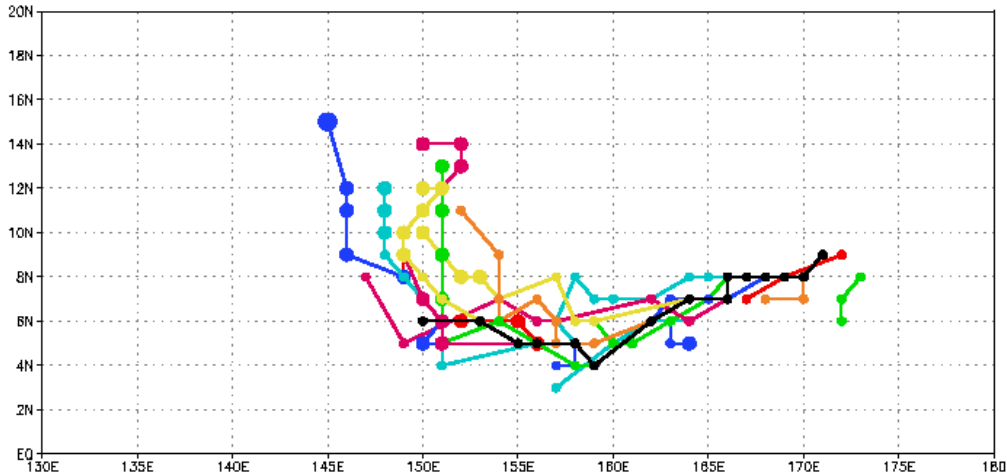
Figure 3.30. Example of forecast tracks for a Group 2 non-developing vortex. Circles indicate successive 12 h forecasts of the circulation center, with the size of the circle indicating the intensity. Black circles indicate analyzed values, and colored circles indicate separate forecast times.

The average analyzed vorticity at N_0 for this data set was 3.7×10^{-5} s^{-1}, which is between the threshold for developing vortices (5.0×10^{-5} s^{-1}) and non-developing vortices (3.3×10^{-5} s^{-1}), but slightly below the 4.0×10^{-5} s^{-1} threshold identified for transitioning of deep wind shear from westerly to easterly in the developing vortices.

Forecasts of 850-mb relative vorticity for these Group 2 cases (Figure 3.31) vary only slightly from the analyzed vorticity values in the 48 h leading up to N_0, especially for shorter-range forecasts (24- and 48-h). Following N_0, the NOGAPS model continued to forecast development of the vortex for a minimum of 24 h before decreasing the forecast vorticity. The most dramatic deviations between analyzed and forecast vorticities occur within 36 h of N_0. Although there are fewer forecast time intervals in Figure 3.30 in which the deviation between analyzed and forecast vorticities are statistically significant than in the forecast and analyzed vorticities of the overall ND1 data set (Figure 3.18), the errors appear more noticeable, possibly due to the small sample size.

     (b)   Deep Layer Wind Shear. Analysis of the deep wind shear curve for the Group 2 subset (Figure 3.32) indicates that the analyzed deep wind shear never transitioned from westerly to easterly, as is expected with analyzed vorticity that did not exceed 4.0×10^{-5} s^{-1} (refer to section C.2.a.2 of this chapter). Analysis data were not available at 72 h and 120 h after N_0. The average analyzed deep shear at N_0 was 2.8

73
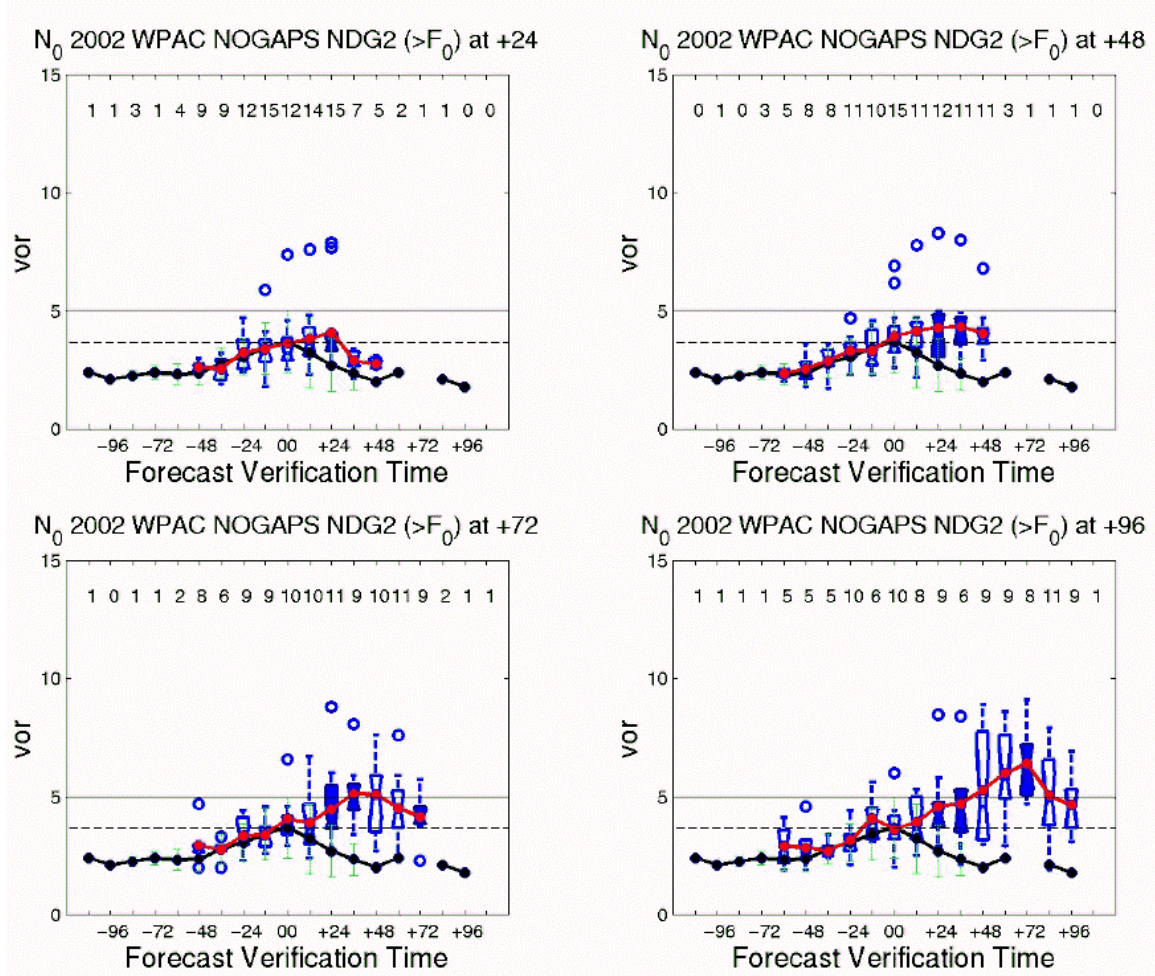
Figure 3.31. Average analyzed and forecast 850-mb relative vorticity as in Figure 3.18, except for the Group 2 subset of ND1 vortices. Heavy black line represents average analyzed 850-mb relative vorticity for the Group 2 subset of vortices, and heavy red line represents average forecast 850-mb relative vorticity for the time indicated. The light solid line represents average analyzed 850-mb relative vorticity at F0 for developing vortices (5.0 x 10-5 s-1), and the light dashed line represents average analyzed 850-mb relative vorticity at N0 (3.7 x 10-5 s-1).

m s^{-1}, which indicates a westerly wind shear, which has been shown to be unfavorable for tropical cyclone formation. Within 24 h of N_0, the analyzed wind shear not only remains positive but also increases in magnitude, which is not favorable for development of the potential tropical circulation. The early decrease in analyzed shear with time indicates a more favorable condition for the development and intensification of the tropical circulation. However, the lack of a pronounced decrease in the slope of the analyzed
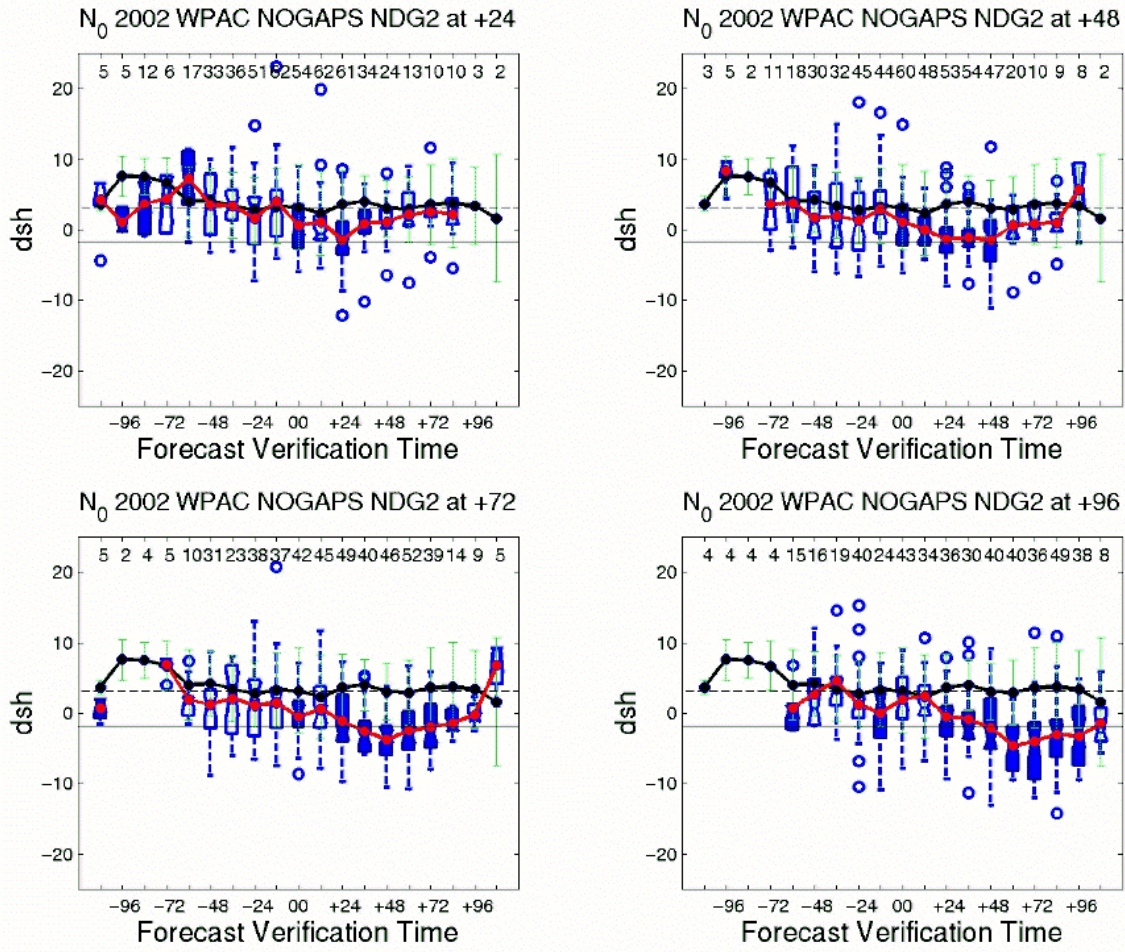
Figure 3.32. Average analyzed and forecast deep layer wind shear (200-850 mb) (m s^{-1}) for non-developing vortices that were forecast to exceed F_0, as in Figure 3.18. Heavy black line represents analyzed average deep layer wind shear for this subset of non-developing vortices (at +00), and red line represents average forecast deep layer wind shear for the indicated forecast time. Average analyzed deep layer wind shear 850 mb relative vorticity for this subset of non-developing vortices at N_0 (light dashed black line) was 2.8 m s^{-1}. V_0 (light solid black line) is –1.8 m s^{-1}.

deep shear as in Figure 3.15 would not lead one to expect the eventual development of a JTWC-numbered tropical circulation.

In general, the NOGAPS deep shear forecasts (Figure 3.32) become more negative with increasing time and forecast range. At each forecast time, the NOGAPS forecasts of deep shear become distinctly negative within 24 h of N_0, which indicates a transition of the shear from positive to negative, and thus more favorable conditions for development. As noted earlier, the transition from positive to negative shear tends to

occur when the 850-mb relative vorticity is forecast to exceed 4.0×10^{-5} s^{-1}. Since the analyzed vorticity 24 h after N_0 is distinctly below this threshold, this may be related to the fact that the deep wind shear remained westerly.

Interestingly, the outlier values in Figure 3.32 are almost all positive while the forecast range at each time interval is skewed toward negative shear. The range of more negative forecast values indicates that the NOGAPS model over-forecast the shear to be smaller than analyzed. However, the positive deep layer shear extrema that have no corresponding erroneously low vorticity forecasts must occur as a result of some other model forecast error.

(c) Other Variables. Trends for the other selected forecast variables for the Group 2 subset were very similar to those for the overall ND1 data set. The most noticeable difference was the same one evident in the comparison of 850-mb relative vorticity for Group 2 and ND1 – the Group 2 analyzed and forecast curves were more peaked than those for the overall ND1 set, and more closely resembled the curves for developing vortices, although both the analyzed and forecast values for the non-developers were smaller in magnitude than their counterparts for developing circulations.

The relatively small sample size may have contributed to the relatively large variation evident in the analyzed curves for Group 2. This variation, while not readily apparent in Figure 3.21, was distinctly more noticeable in the analyses and forecasts for some of the other variables, especially size, and vapor pressure (not shown).

(2) Model False Alarms. Model false alarms were identified from the forecast vortices stored in the Forecast Database (Figure 2.1a) that never corresponded to a verifying analysis. To qualify as a model false alarm, four criteria had to be met: the vortex had to exist for at least 24 hours (three consecutive model runs) in the forecast sequence; a potential match had to exist, meaning that the false alarm forecast circulation had to be matched to at least one other forecast; the match had to be within a 4° latitude radius circle of the vortex it was being matched to; and the match had to occur within ± 12 hours of when it was forecast to occur. Given these criteria, 15 vortices were identified as false alarms (column five of Table 3.1). The 850-mb relative vorticity for the model false alarms could not be compared to the developing circulation vorticity

threshold since no first JTWC warning time or time of maximum analyzed vorticity existed.

The NOGAPS predictions had more false alarm forecasts in the Philippine Sea (10) than in the South China Sea (4) and Eastern Monsoon Trough (1) combined (Figure 3.33). This regional distribution is consistent with the results of Cheung and Elsberry (2003). That more false alarms occurred subregions associated with the monsoon trough indicates that the NOGAPS model may have over-forecast the vorticity associated with smaller circulations within the monsoon trough. As discussed previously, over-forecast
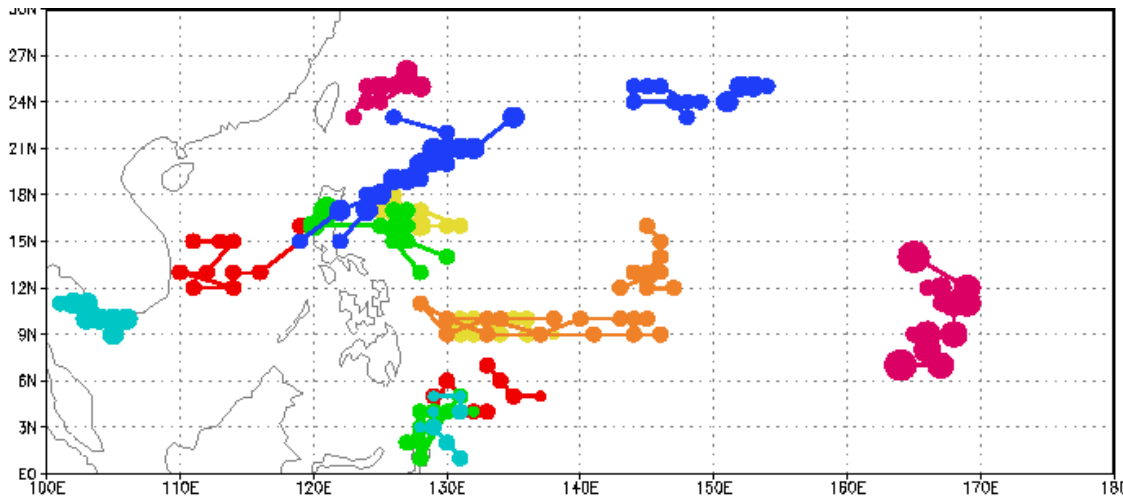
Figure 3.33. Locations of NOGAPS model false alarms in the western North Pacific during 1 May – 31 October 2002. Circles indicate successive 12-h analyses of each identified model false alarm. The size of each circle is related to the analyzed intensity of the circulation with a larger circle indicating a more intense circulation.

vorticity leads to forecasts of excessively easterly deep layer wind shear which is favorable for tropical cyclone formation. That more false alarms do not occur is possibly due to the excessive drying of the mid-troposphere, as noted above.

(3) TCFA False Alarms. During the study period, there were six TCFA false alarms. Since so few TCFA false alarms existed during 2002, the minimum sample size was relaxed for this dataset. Four of these six false alarms could be associated with non-developing vortices tracked in the NOGAPS analyses (Figure 3.34). Additionally, four of the six TCFA false alarms occurred in the Philippine Sea (PS), and three of those occurred between 136°E and 142°E. The first two false alarms
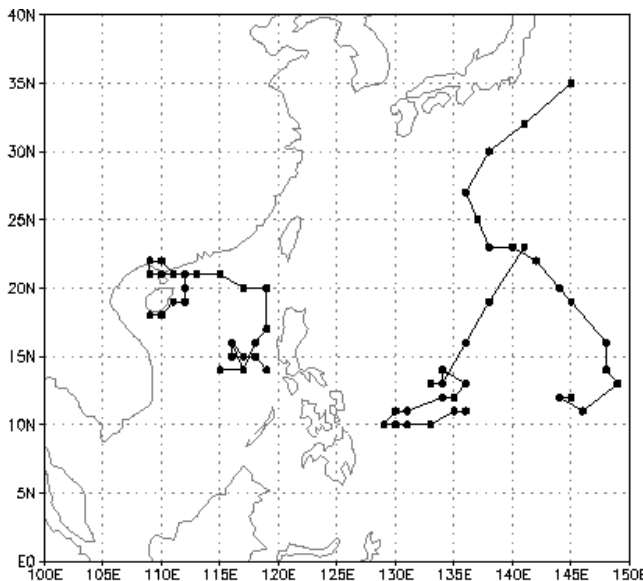
Figure 3.34. Locations of JTWC TCFA false alarms in the western North Pacific during 1 May – 31 October 2002. Circles indicate successive 12-h analyses of each identified model false alarm.

occurred within 6 hours of one another, and are likely for the same vortex. One false alarm in the PS subregion was for a vortex near 30°N, and thus might have been a subtropical development. The other two TCFA false alarms occurred in the South China Sea within three days of each other. It is possible that all six of these vortices represented weak circulations associated with the monsoon trough or monsoon depressions.

Although never warned on, the four of the vortices corresponding to TCFA false alarms did exist in at least one analysis panel. Therefore, N_0 could be determined. The mean analyzed vorticity (at N_0) for this subset of non-developing vortices (Figure 3.35) was 7.1×10^{-5} s^{-1}, which is about 2×10^{-5} s^{-1} higher than the vorticity threshold determined for the developing vortices (see Figure 3.5). The larger average analyzed vorticity for this subset of non-developers is unexpected for a series of vortices assumed to be associated with weak, disorganized monsoon depressions.

The slope of the analyzed vorticity for the four vortices included in Figure 3.35 dramatically increases from 36 h prior to N_0 and then decreases sharply in the 12 h following N_0. The slope of the analyzed vorticity for this subset of non-developers is steeper than the slope of the analyzed vorticity for the developing vortices in Figure 3.5,
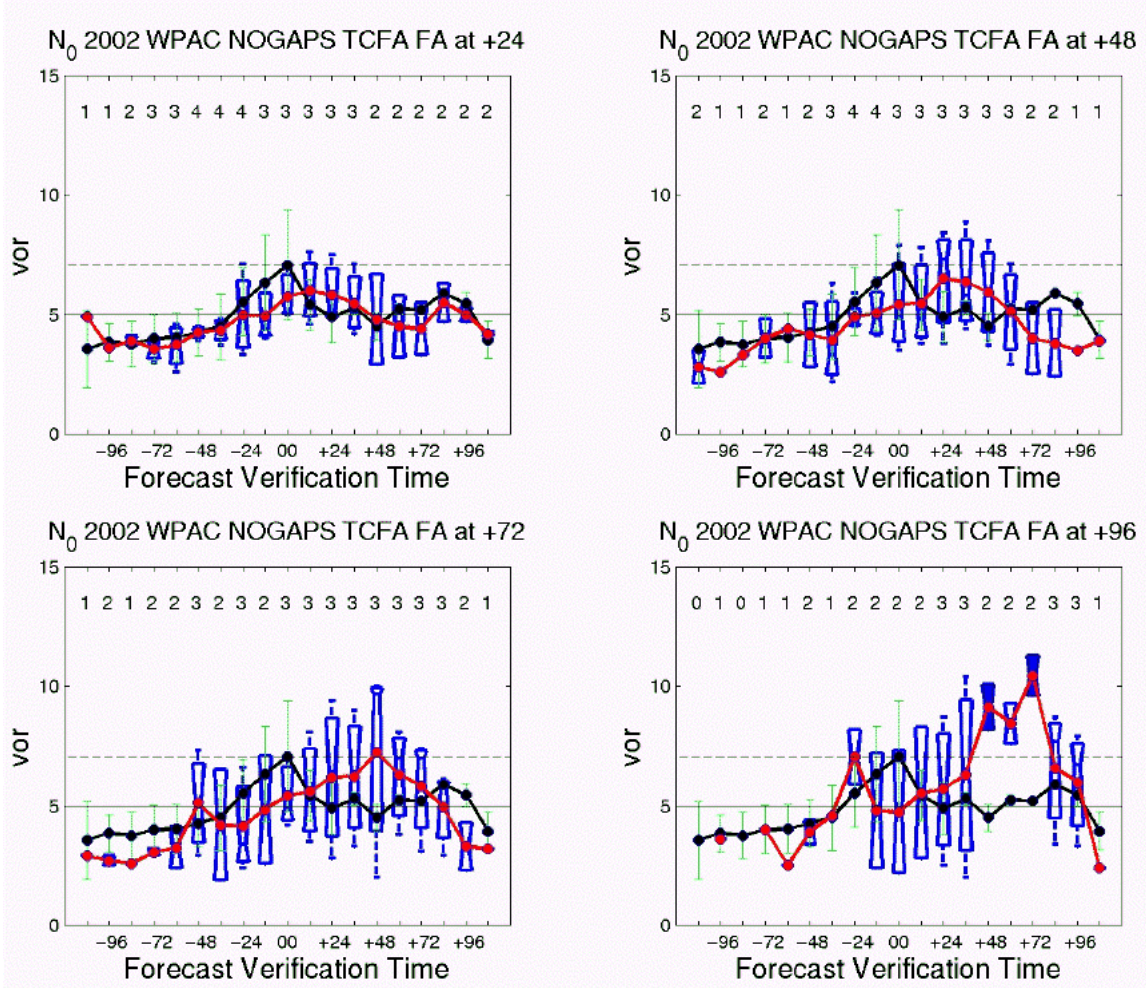
Figure 3.35. Average analyzed and forecast 850-mb relative vorticity (x 10^{-5} s^{-1}) as in Figure 3.5, except for the four TCFA false alarm vortices with corresponding NOGAPS analyses. Heavy black line represents analyzed average 850-mb relative vorticity (at +00) for this subset of non-developers, and red line represents average forecast 850-mb relative vorticity for this subset of non-developers for the indicated forecast time. Average analyzed vorticity relative at the time of maximum analyzed vorticity N_0 (light dotted black line) for these TCFA false alarm vortices was 7.1 x 10^{-5} s^{-1}, which is larger than the 5.0 x 10^{-5} s^{-1} for developing vortices at F_0 as in Figure 3.5.

but more closely resembles the slope of the analyzed vorticity prior to F_0 for the subset of developers that verified prior to the TCFA-specified formation window (Figure 3.11). This increase and sudden decrease is attributed to temporary spin-ups of vorticity that may be associated with overly active convection in the model. However, since four of these alerts corresponded to circulations that existed in the NOGAPS analysis, which likely were also tracked concurrently using satellite imagery, the NOGAPS analysis probably also reflects a relatively strong circulation in connection with the convection.

The variability of forecast range at each time interval for longer-range forecasts is evident in the 96-h forecasts of this data set (lower-right panel of Figure 3.35). While the 48- through 72-h forecasts predict vorticity substantially greater than the analyzed value, they are suspect since only two cases contributed to the mean calculated at each time interval. However, that the vorticity forecast at these three verification times is so much greater (and a statistically significant deviation at 48 h and 72 h) than the analyzed value indicates that at longer time ranges the NOGAPS model has again over-forecast the development, or more accurately the apparent dissipation of these circulations.

D.   CASE STUDY COMPARISON

To illustrate the effects of the forecast thresholds determined previously, two case studies were compared to the average analyzed profiles for 2002. One case study will examine a developing circulation (TS 24) that was consistently analyzed and forecast to be above the average analyzed values for all 2002 developing vortices, as well as the one model "miss" (TD 27) that occurred in 2002.

A second analysis line was added to the figures for the two case studies (Figures 3.36 and 3.37). This heavy blue line represents the average analyzed value of the selected forecast variable for the case study circulation. The light dashed line corresponds to the average value at F_0 for the selected variable. The heavy red line represents forecast values of the selected forecast variable for the case study circulation for the time indicated in the title of each forecast panel (24-, 48-, 72-, and 96-h in the upper-left, upper-right, lower-left, and lower-right, respectively). As in Figure 3.5, the heavy black line represents the average analyzed value (at +00) of the selected variable for all developing circulations in 2002, and the light green whiskers extending from this line indicate one standard deviation of variable values at each time interval. Box plots were not plotted for the forecast vorticity due to the small number of forecasts available at each time interval.

1.   Over-forecast Circulation (TS 24)

Tropical Storm 24 during September 2002 was a moderate circulation with maximum sustained surface winds of 55 kt in the South China Sea. The average analyzed 850-mb relative vorticity profile for TS 24 (Figure 3.36) was at almost all times

greater than the average analyzed vorticity for all developing circulations in 2002. The average analyzed vorticity at the time JTWC issued its first warning (F_0) for TS 24 was 8.2 x 10^{-5} s^{-1}, which is more than one standard deviation greater (over 3 x 10^{-5} s^{-1} higher) than the average analyzed vorticity at F_0 for all 2002 developing vortices. Had the averaged analyzed vorticity value of 5.0 x 10^{-5} s^{-1} been used as an indicator of formation, the time of the first JTWC-issued warning would have been about 60 h earlier. The weak increase in vorticity that occurs in the 24 h following F_0 for TS 24 represents that a small amount of adjustment occurred as a result of the synthetic tropical cyclone observations that were inserted within 12 h of F_0.

The deviation between the analyzed vorticity for all developing circulations and the analyzed vorticity for TS 24 increases with increasing time after F_0 for TS 24. In the early stages of the development of TS 24, the analyzed vorticity is very similar to the analyzed vorticity for all developing circulations in 2002. However, this similarity does not persist more than 24 h, and by 84 h prior to F_0, the analyzed vorticity for TS 24 increased almost to the vorticity threshold for all developing vortices. That the analyzed vorticity for TS 24 continues to increase after this point partially explains why the analyzed vorticity at F_0 is so much greater than the average analyzed vorticity at F_0 for all developing vortices.

The 24-h forecasts of 850-mb relative vorticity (upper-left panel of Figure 3.36) for TS 24 fluctuate between over- and under-forecasts throughout the 120 h before and after F_0. The vorticity is forecast relatively accurately from 120 to 84 h prior to F_0, and again from 36 h to about 12 h prior to F_0. Vorticity is over-forecast (forecast values exceed analyzed values) between those two periods of accurate forecasting, and again from roughly 12 h prior to F_0 until 24 h after F_0. The sudden decrease in forecast vorticity from 12 h after F_0 to 24 h after F_0 indicates a transition from forecasts made prior to the insertion of the synthetic tropical cyclone observations to those made after they were inserted. Following the insertion of the synthetic tropical cyclone observations, the forecasts of relative vorticity for TS 24 are consistently less than the analyzed vorticity. This tendency of NOGAPS to under-forecast circulation development after the synthetic tropical cyclone observations are inserted is consistent with the trend found for the overall sample of developing storms.
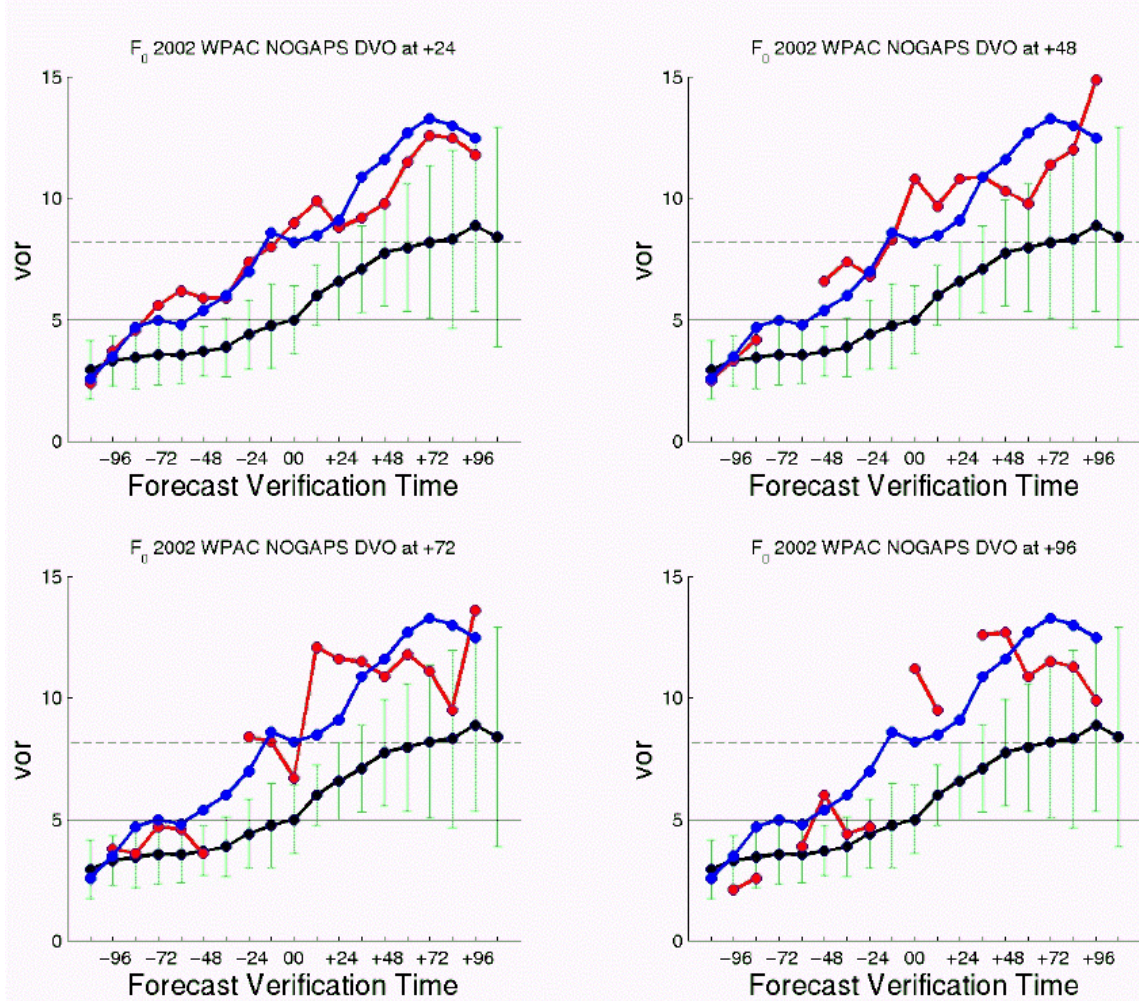
Figure 3.36. Average analyzed and forecast 850-mb relative vorticity (x 10^{-5} s^{-1}) as in Figure 3.5, except for TS 24 (2002). The heavy black line represents analyzed average 850-mb relative vorticity for all 2002 developing vortices (at +00), the heavy blue line represents average analyzed vorticity (at +00) for TS 24, and the heavy red line represents average forecast 850-mb relative vorticity for TS 24 for the indicated forecast time. Average analyzed 850-mb relative vorticity for TS 24 at F_0 (light dashed black line) was 8.2 x 10^{-5} s^{-1}. $?_0$ for developing storms in 2002 (light solid black line) is 5.0 x 10^{-5} s^{-1}.

A similar trend in the 12 h prior to F_0 is apparent in the 48-h forecasts for TS 24 (upper-right panel of Figure 3.36). The forecast vorticity at F_0 greatly exceeds the analyzed vorticity, and then is consistently over-forecast until 48 h after F_0. Once the synthetic tropical cyclone observations are inserted, at the forecast verification time corresponding to +48 h in the upper-right panel of Figure 3.36, the characteristics of the

82

vortex in the analysis are corrected, and the subsequent vorticity forecasts are less than the analyzed value.

The reliability of the forecast vorticity curves in the extended range forecasts (bottom panels of Figure 3.36) are questionable given the very small number of forecasts available at each of these forecast times and time intervals. Data are missing at many of the time intervals in the extended range forecasts, which indicates that forecasts verifying at these time intervals were not available, or possibly that the circulation was not forecast by NOGAPS at these times (data gaps).

Statistical significance at each forecast verification time could not be calculated for TS 24, since an insufficient number of cases were available at each time interval and forecast time. An ad hoc determination of statistical significant in Figure 3.36 is determined visually by noting whether or not the forecast value lies within the range of analyzed values for the mean curve at each forecast verification time. Most of the forecast values for TS 24 are greater than the analysis range, which suggests statistical significance using this rough estimate. However, most of the analyzed vorticity values for TS 24 also exceed the analysis range for all developing circulations, which indicates that TS 24 is likely one of those circulations that represents a forecast extreme for this year.

2.   Under-forecast Circulation (TD 27)

The TCVTP tracker failed to detect the developing circulation that became TD 27 prior to the first JTWC-warning time. This error represented the only major "miss" of the NOGAPS analyses during 1 May – 31 October 2002. TD 27 was a weak tropical depression with maximum sustained surface winds of only 30 kt (2002 ATCR) within the Philippine Sea.

Analyzed 850-mb vorticity values greater than 1.5×10^{-5} s^{-1} do not exist for TD 27 until after the first warning was issued by JTWC and the synthetic tropical cyclone observations were inserted into the NOGAPS analysis. Consequently, 24-, 48-, and 72-h forecasts are not available for TD 27 until after the synthetic observations were inserted, and no 120-h forecasts are available since the circulation was warned on for only 2.5 days by JTWC. To display the analyzed and forecast relative vorticity (Figure 3.37) for TD 27, the first warning time had to be shifted to 12 h after F_0, since the TCVTP process did

not identify the circulation in the NOGAPS analysis until that time. Thus, the vorticity value indicated at F_0 is actually the analyzed vorticity value at $F_0 + 12$ h. Similar displacement of the forecast curves is not necessary. The apparent phase shift in the start time of each forecast curve in Figure 3.37 is due to the lag time between F_0 and the forecast time, i.e., the 24-h vorticity forecasts (left panel of Figure 3.37) are not available until 24 h after F_0 since no forecasts were made for TD 27 until F_0. No forecasts were
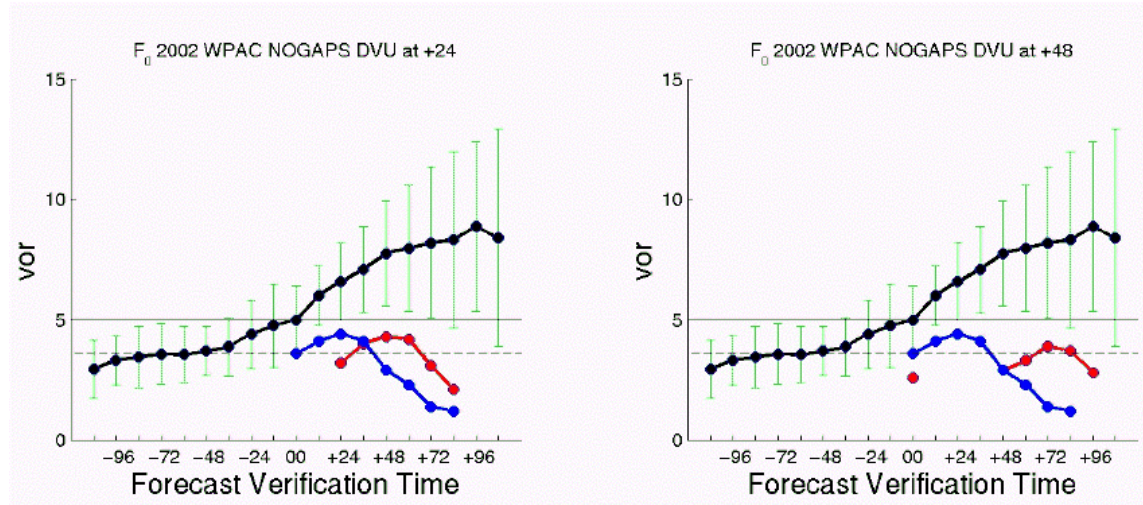
Figure 3.37. Average analyzed and forecast 850-mb relative vorticity (x 10^{-5} s^{-1}) as in Figure 3.5, except for TD 27 (2002). The heavy black line represents analyzed average 850-mb relative vorticity for all 2002 developing vortices (at +00), the heavy blue line represents average analyzed vorticity (at +00) for TD 27, and the heavy red line represents average forecast 850-mb relative vorticity for TD 27 for the indicated forecast time. Average analyzed 850-mb relative vorticity for TD 27 at F_0 (light dashed black line) was 3.6 ?$_0$ for developing storms in 2002 (light solid black line) is 5.0 x 10^{-5} s^{-1}.

available at 120 h, and so few forecasts were available at 72 h that neither of those forecast times are shown in Figure 3.37.

Examination of the analyzed 850-mb relative vorticity for TD 27 (Figure 3.37) indicates that after a weak development phase that lasted 24 h, the circulation began to weaken. At all times, the analyzed vorticity for this circulation was substantially less than the analyzed vorticity for all developing circulations, and never reached the vorticity threshold of 5.0 x 10^{-5} s^{-1} for developing circulations. If surpassing this threshold in the NOGAPS analyses were the only criterion for issuing a first warning, it would not be surprising for JTWC to have missed this warning. That is, evidence was lacking in the synoptic analyses, and JTWC had to rely on satellite imagery to issue its first warning.

After the brief phase of increasing vorticity, the analyzed vorticity for TD 27 decreased as the analyzed vorticity for all developing storms continued to increase, and never underwent a second pulse in development.

Most forecasts of relative vorticity that are available for TD 27 are all markedly in excess of the analyzed vorticity at the verifying time of the forecast, especially 36 h after F_0. The exception to this is the 24-h forecast (left panel of Figure 3.37), which does show a transition from under- to over-forecast vorticity values 24 h after the first JTWC warning time. This transition is in direct contrast to the shift in forecast values relative to the insertion of the synthetic tropical cyclone observations, but it does occur at the same time that any sort of forecast transition is expected. Additionally, the time of the forecast maximum vorticity increases with increasing forecast range, and with a small decrease in magnitude with increasing forecast range.

The apparent phase shift that occurs between the analyzed and forecast vorticity in Figure 3.37 is attributed to an inaccurate representation of the large-scale environment, and also that the vortex grew only to a small, weak tropical depression. The average analyzed vorticity at the first JTWC-warning time was 3.6×10^{-5} s^{-1}, almost 1.5×10^{-5} s^{-1} lower than analyzed for the full developer data set, and only 0.3×10^{-5} s^{-1} greater than the threshold for non-developing vortices. That the average analyzed vorticity value at F_0 was less than 4×10^{-5} s^{-1} indicates, from previous discussion, that shear should be westerly, which is not favorable for formation. For formation to occur, the shear must be less westerly, and perhaps very close to zero. It is possible that continued westerly shear existed and ventilated the developing vortex, and thus further development of TD 27 was prevented.

The failure of NOGAPS analysis to include the developing TD 27 circulation until it was artificially inserted into the analysis suggests that the formation environment of TD 27 may have been substantially disorganized, very weak, or misrepresented in the model analysis due to a lack of observations. The NOGAPS analysis only has a weak (1010 mb) low with a closed isobar, but has no closed 850-mb relative vorticity contour of at least 1.5×10^{-5} s^{-1}. Even after the insertion of synthetic observations, the circulation appears weakly in the NOGAPS forecasts. Perhaps access to other global and regional

numerical models would allow the TCVTP program to identify such weak, disorganized circulations.

E.   COMPARISON OF 2003 VORTICES TO 2002 VORTICES

Since 2003 was a year following a warm El Niño (EN) event, tropical cyclone activity in the western North Pacific was forecast to be below normal, and above-normal tropical cyclone activity was forecast in the South China Sea (Chan 2003). The anticipated cold phase of the El Niño-Southern Oscillation (ENSO), called a La Niña event, was much weaker than expected. Although the observed flow patterns and tropical cyclone formations in the SCS were consistent with a La Niña year (Chan 2003), below-normal formation numbers occurred in the SCS due to an anomalous anticyclonic circulation over the SCS from June – October 2003. This anomalous circulation is linked to interdecadal variations in the strength of the subtropical high (Chan 2003). Although numbered storms were fewer in 2003, the total number of tracked non-developing vortices in the NOGAPS model was similar to 2002 (see Tables 3.1 and 3.9).

1.   Developing Vortices

The western North Pacific Ocean basin was less active during 2003 than it had been during 2002, with 20 circulations numbered by JTWC from 1 May – 31 October 2003 compared to 24 in 2002. As in 2002, the NOGAPS failed to identify several circulations prior to insertion of the synthetic tropical cyclone observations. It is possible that the NOGAPS model was unable to distinguish these two weak circulations from the

Table 3.9. Circulations tracked in NOGAPS analyses from 1 May – 31 Oct 2003 numbered by the JTWC (column 1), non-developing circulations meeting the minimum duration criterion of at least 24 h (column 2), those non-developing circulations not meeting the minimum duration criterion (column 3), and the non-developing vortices that were forecast to occur, but were never analyzed in NOGAPS (column 4).

Formation Subregion	Numbered TCs	ND $\geq$ 24 h (ND1)	ND $<$ 24 h (NDOF)	Model False Alarms
South China Sea (105E-124E)	4	35	18	4
Philippine Sea (125E-159E)	14	64	28	18
East Monsoon Trough (160E-180E)	2	6	16	5
Total	**20**	**105**	**62**	**27**

background environment due to insufficient organization or relative vorticity. These circulations, TD 22 and TS 23, are thus excluded from Table 3.10 and also from the discussion below. Numbered storms again formed preferentially in the PS subregion (14 of 20), and percentages of developments in the SCS (4) and EMT (2) were consistent with 2002 (Table 3.10). It is worth noting that formation within a specific subregion, as noted in Table 3.10, is based on the first analysis time the TCVTP classified an ellipse for each circulation. Given this, it is likely that two of the developing circulations identified as developing in the PS subregion (near 126°E) may have first been warned on in the SCS subregion.

The average analyzed 850-mb relative vorticity for developing vortices in 2003 (Figure 3.38) was 4.8 x 10^{-5} s^{-1}, which is only slightly less than $?_0$ for 2002 (5.0 x 10^{-5} s^{-1}). The standard deviation at each time interval for the analyzed vorticity in 2003 was also notably larger, especially at the later time intervals, than during 2002. This greater variation is associated with greater variability of the developing circulations, but may also have been due to the NOGAPS transition in mid-October 2003 from the Multivariate Optimum Interpolation (MVOI) data assimilation scheme to the new Navy Data Assimilation System (NAVDAS).

Goerss et al. (2003) compared the performance of simultaneous runs of the NOGAPS using the NAVDAS scheme and the MVOI scheme during two periods in 2002, and during the beta-test during the spring of 2003. They found that tropical cyclone track forecasts to 72 h initiated from the two data assimilation schemes had only small differences. While performance was worse for 96- and 120-h track forecasts, these errors were based mainly on the variability of the individual developing circulations. Given this, it is unlikely that the variation between the 2002 and 2003 vorticity analyses

Table 3.10. Summary of tropical cyclone activity in the western North Pacific by subregion for 1 May – 31 October 2003. Intensities corresponding to each column are identified in Table 3.2.

Formation Subregion	TD	TS	TY	STY	**Total**
South China Sea (105E-124E)	2	2	0	0	4
Philippine Sea (125E-159E)	0	3	9	2	14
East Monsoon Trough (160E-180E)	0	0	2	0	2
Total	**2**	**5**	**11**	**2**	**20**

is due to the different data assimilation schemes. It is also noted that NAVDAS was only operationally used for the last three months of 2003 and during only one month of this study.

The slope of the analyzed 850-mb relative vorticity for developing circulations in 2003 (Figure 3.38) was steeper than the slope of the analyzed vorticity for the 2002 developing vortices (Figure 3.5), which possibly indicates that intensification during 2003 occurred in spurts rather than gradually. The increase in the slope of the analyzed vorticity in the first 12 h after F_0 in Figure 3.38 is substantially steeper than in 2002. This
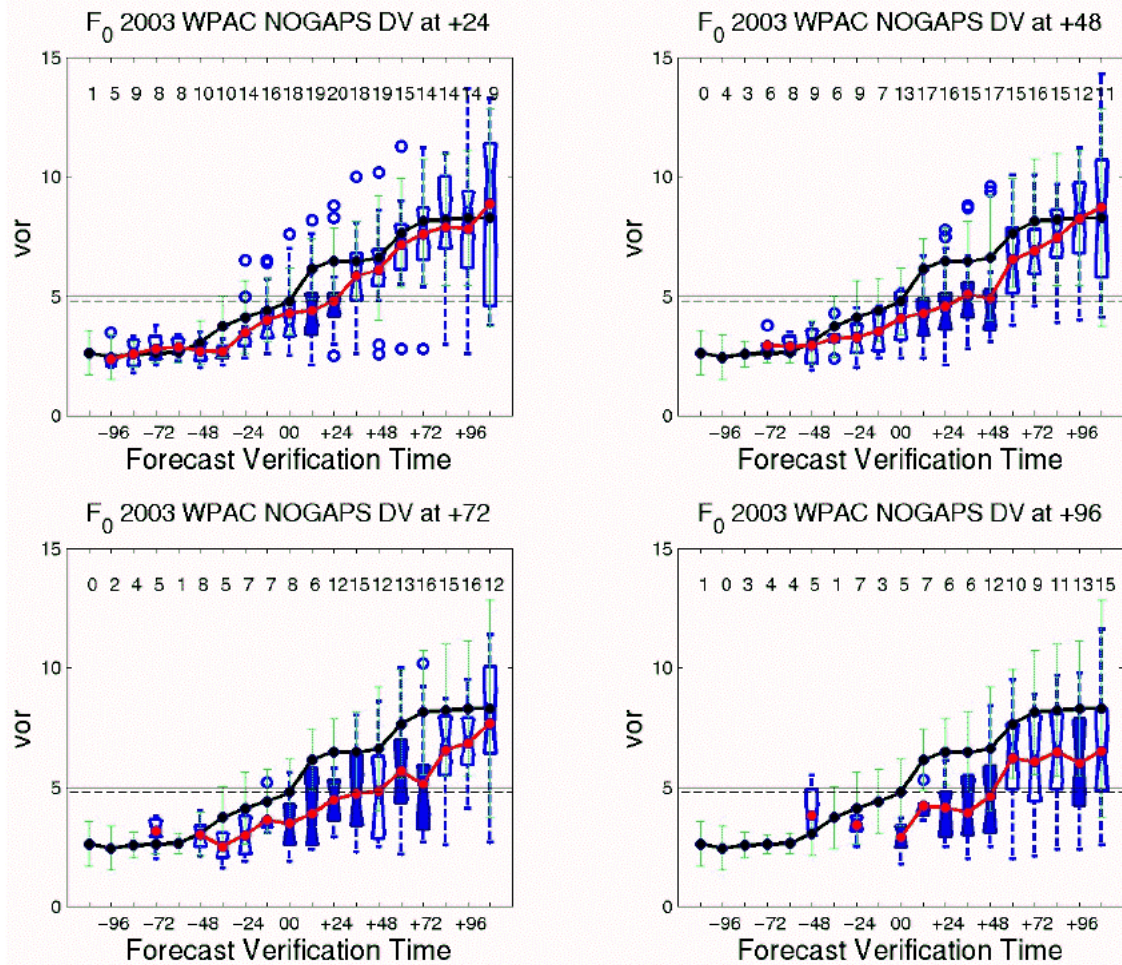
Figure 3.38. Average analyzed and forecast 850-mb relative vorticity (x 10^{-5} s^{-1}) as in Figure 3.5, except for developing vortices in 2003 relative to F_0. Heavy black line represents analyzed average 850-mb relative vorticity for developing vortices (at +00), and red line represents average forecast 850-mb relative vorticity for the indicated forecast time. Average analyzed 850-mb relative vorticity for 2003 developing vortices at F_0 (light dashed black line) was 4.8 x 10^{-5} s^{-1}. Light solid black line represents average analyzed vorticity at F_0 for 2002 developing vortices (5.0 x 10^{-5} s^{-1}).

dramatic slope increase corresponds to the insertion of the synthetic tropical cyclone observations, as discussed previously. That the analyzed vorticity is so distinctly different on either side of F_0 indicates that developing vortex was not being accurately represented in the model analyses prior to the insertion of the synthetic tropical cyclone observations.

The forecast curves of 850-mb relative vorticity for developing vortices in 2003 (Figure 3.38) were dramatically less than the analyzed vorticity at almost all forecast verification times at all forecast intervals. Notably, while the deviations between NOGAPS analyses and forecasts of relative vorticity at F_0 were not statistically significant for the circulations that developed in 2002, the differences were substantially larger for the 24- and 48-h forecasts (Figure 3.38) during 2003. In the 2002 data set, the forecasts of vorticity at F_0 were consistently at or greater than the analyzed vorticity, whereas in the 2003 data set, forecast vorticity was consistently less than the analyzed value at F_0.

The under-forecasting of relative vorticity at F_0 occurred partially due to the earlier transition from over- to under-forecast values of vorticity in the 2003 NOGAPS forecasts than in 2002. This transition occurred in the 2003 sample between 60 and 48 h prior to F_0 for the shorter-range forecasts, which is much earlier than during 2002 in which the transition from over- to under-forecasts did not occur until after F_0. This difference in the forecasts is not attributed to the data assimilation scheme, or the insertion of the synthetic tropical cyclone observations, but instead to the inability of the NOGAPS model to correctly represent the early formation environment of the developing vortices during 2003.

The insertion of the synthetic tropical cyclone observations in the NOGAPS analyses is less apparent in the 2003 forecasts (Figure 3.38) than in the 2002 forecasts (Figure 3.5). Although the data assimilation scheme was changed during October 2003, the process by which synthetic tropical cyclone observations were inserted into the model analysis did not change (B. Strahl, FNMOC, personal communication). Given this, the expected flattening of the forecast vorticity slope between F_0 and the forecast time in Figure 3.5 was not noted in Figure 3.38. Instead, the slope of forecast vorticities generally increased steadily between F_0 and the time corresponding to the forecast

interval (indicated in the title of each panel), and then increased dramatically after that. The forecast vorticity slope between F_0 and the forecast time appeared to increase with increasing forecast range (a shallower slope appears in the mean 24-h forecast than in the mean 72-h forecast). The apparent growth between F_0 and the forecast time is attributed to continued development of the circulation in the NOGAPS forecasts.

Additionally, the forecast spread increased with increasing forecast range, and tended more toward lower values than analyzed, rather than the expected over-forecasts. In many instances, the forecast maximum for a time interval identified at the top of the box plot was at or below the analyzed value. The forecast extrema during 2003 were also clustered around F_0, and included both over- and under-forecast values. The under-forecast extrema occurred only in the shorter-range forecasts ($\leq$ 48 h). Combining the extrema, forecast spread, and consistent under-forecasting evident in Figure 3.38, it is concluded that the NOGAPS model did not accurately characterize either the developing tropical circulations or the background environment.

The average analyzed deep layer wind shear for vortices developing in 2003 (Figure 3.39) has a slope similar to the average analyzed deep layer wind shear for the developing vortices in 2002, although the average analyzed deep shear at F_0 in 2003 was -1.6 m s^{-1}, which is slightly less easterly than the analyzed deep shear F_0 in 2002 (-1.8 m s^{-1}). As in the 2002 data set, the transition from westerly to easterly shear occurs when the analyzed vorticity exceeds 5.0×10^{-5} s^{-1}. In 2003, this transition occurs between roughly 24 and 12 h prior to F_0.

The weaker analyzed wind shear during 2003 is likely a result of the weak La Niña conditions that occurred in the western North Pacific during that year (Chan 2003). While the model analyses and forecasts reflect this, the range of the forecast deep shear at each forecast verification time is significantly smaller during 2003 (Figure 3.39) than they were in 2002 (Figure 3.14). While impacted by the smaller sample size in 2003, this decrease in forecast range at each forecast verification time is likely a result of modifications made to the NOGAPS Emanuel cumulus parameterization scheme during 2003 (Hogan et al. 2004). One of the key modifications made to the Emanuel cumulus parameterization scheme was to increase the amount of convective momentum transport, which then brings more easterly momentum downward and is countered by an increase in
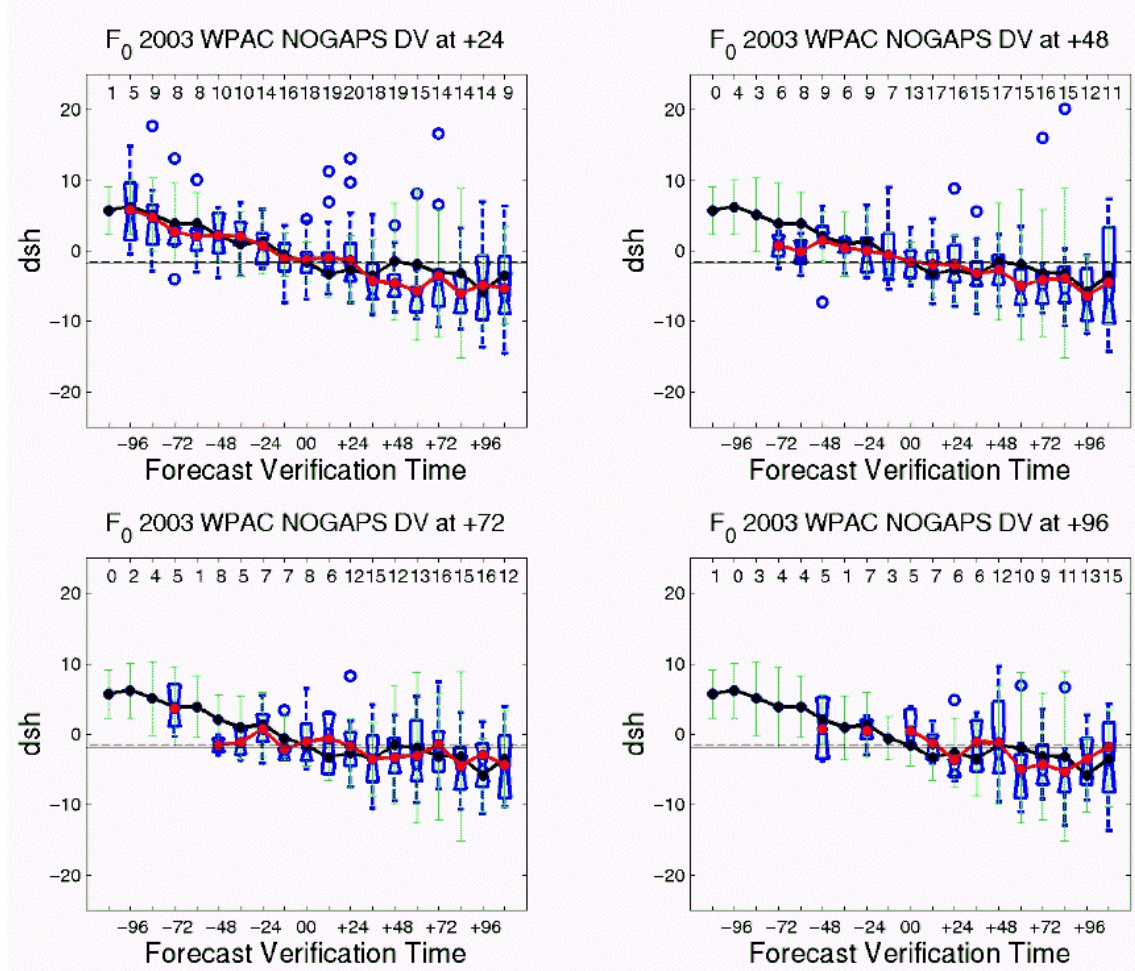
Figure 3.39. Average analyzed and forecast deep layer (200-850 mb) wind shear (m s^{-1}) as in Figure 3.5, except for developing vortices in 2003 relative to F_0. Heavy black line represents analyzed average deep layer wind shear for developing vortices (at +00), and red line represents average forecast deep layer wind shear for the indicated forecast time. Average analyzed deep layer wind shear for 2003 developing vortices at F_0 (light solid black line) was –1.6 m s^{-1}. Light solid black line represents average analyzed shear threshold for 2002 developing vortices (-1.8 m s^{-1}).

the vertical turbulent mixing by the parameterization of the planetary boundary layer (Hogan et al. 2004). The end result of this increase in convective momentum transport is a decrease in the magnitude of the low-level winds, which thus decreases the amount of easterly deep layer wind shear. Thus, not only are deep layer wind shear forecast ranges smaller at each verification time than in the 2002 NOGAPS forecasts, but they are also on average weaker or closer to zero.

NOGAPS forecasts of deep shear were remarkably close to the analyzed deep shear values, especially in the 24-h forecasts prior to F_0 (upper-left panel in Figure 3.39). The 24-h forecast closely resembles the analyzed deep shear for 2002 (Figure 3.14), and relatively accurately forecasts the transition from westerly to easterly deep layer shear by 12 h prior to F_0. Although the time of the occurrence of the maximum easterly shear is inaccurately forecast at 24 h, and correctly forecast at 48 h, the forecast maximum magnitude is within tolerable error limits.

The range of forecast values in Figure 3.39, which is larger farther away from F_0, is not statistically significant in the 2003 forecasts, whereas it is at a few time intervals prior to F_0 in 2002. This improvement in the forecast accuracy of 2003 is attributed to a smaller range of analyzed deep layer shear values in the developing circulations, especially within 24 h of F_0.

2. Non-developing Vortices

The average analyzed vorticity for non-developing vortices in 2003 (Figure 3.40) was similar to the analyzed vorticity for non-developing vortices in 2002 (Figure 3.18). The average analyzed vorticity at N_0 in 2003 for this data set was 3.0×10^{-5} s^{-1}, which is only slightly smaller than the average analyzed value at N_0 in 2002 (3.3×10^{-5} s^{-1}). This smaller average analyzed vorticity is attributed to the weaker circulations that formed in 2003 when compared to 2002.

In direct contrast to the developing vortices for 2003, forecasts for the non-developing vortices are almost entirely in excess of the analyzed relative vorticity. While these over-forecast errors in 2003 are consistent in deviation with the over-forecast in 2002, the smooth forecast increase and subsequent decrease relative to N_0 is not present in 2003. Considerably larger fluctuations exist in the longer-range forecasts (bottom panels of Figure 3.40) for 2003 than 2002, which may be partially due to the smaller sample size for 2003.

Consistent with the over-forecast vorticity at almost all forecast times, the extrema for this non-developing data set all exceed the analyzed vorticity, which indicates a tendency for the NOGAPS model to over-forecast tropical circulation development. This tendency among non-developing vortices is in direct contrast to the tendency towards under-forecasting for the developing vortices in 2003 (Figure 3.38). In
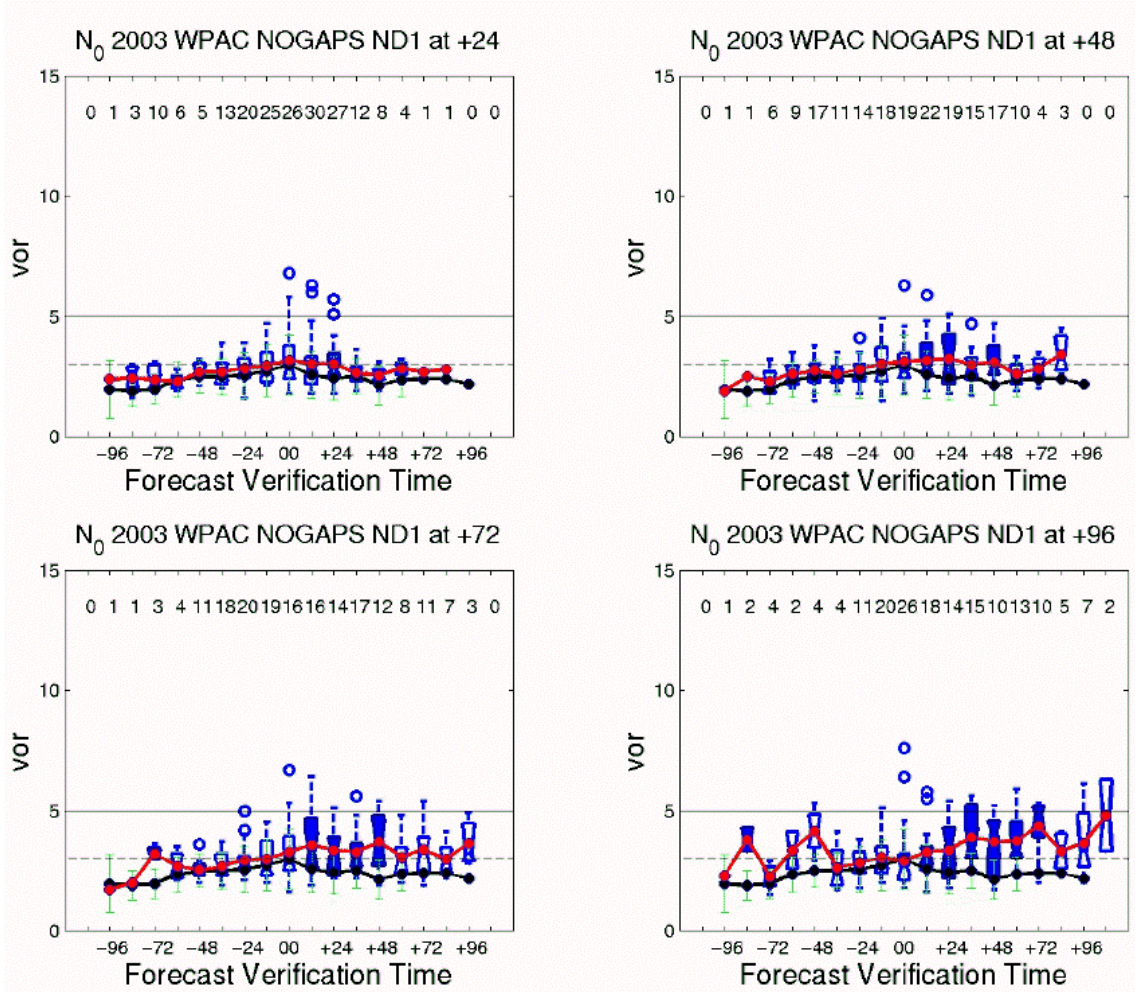
Figure 3.40. Average analyzed and forecast 850-mb relative vorticity (x 10^{-5} s^{-1}) as in Figure 3.18, except for non-developing vortices in 2003 relative to N_0. Heavy black line represents analyzed average 850-mb relative vorticity for non-developing vortices (at +00), and red line represents average forecast 850-mb relative vorticity for the indicated forecast time. Average analyzed 850-mb relative vorticity for 2003 non-developing vortices at N_0 (light solid black line) was 3.0 x 10^{-5} s^{-1}. Light solid black line represents $?_0$ threshold for 2002 developing vortices (5.0 x 10^{-5} s^{-1}).

the first 36 h of the life cycle of the developing vortices shown in Figure 3.38 (2.5 x 10^{-5} s^{-1}), the NOGAPS vorticity forecasts tend to exceed the analyzed value.

The 24-h forecasts of 850-mb relative vorticity (upper-left panel of Figure 3.40) most closely match the analyzed relative vorticity, with only minor deviations in the hours following F_0. This trend for accurate forecasting prior to F_0, and increasing forecast deviation from the analyzed value increases with increasing forecast range. In the 48-, 72-, and 96-h forecasts, this deviation becomes statistically significant 12 h after

93

F_0, as forecasts of 850-mb relative vorticity increase and the analyzed values steadily decrease. The 2002 trend for increasing forecast time of the vorticity maximum with increased forecast range is not present in the 2003 forecasts, which could indicate that NOGAPS better resolved the non-developing circulations in 2003 than it did in 2002.

The analyzed deep layer wind shear (Figure 3.41) for these non-developing cases fluctuates more in magnitude in 2003 than it did in 2002 (Figure 3.23), potentially because of the smaller number of cases in the 2003 data set. Notice that the vertical shear is even stronger westerly during 2003 than it was during 2002, which would be consistent
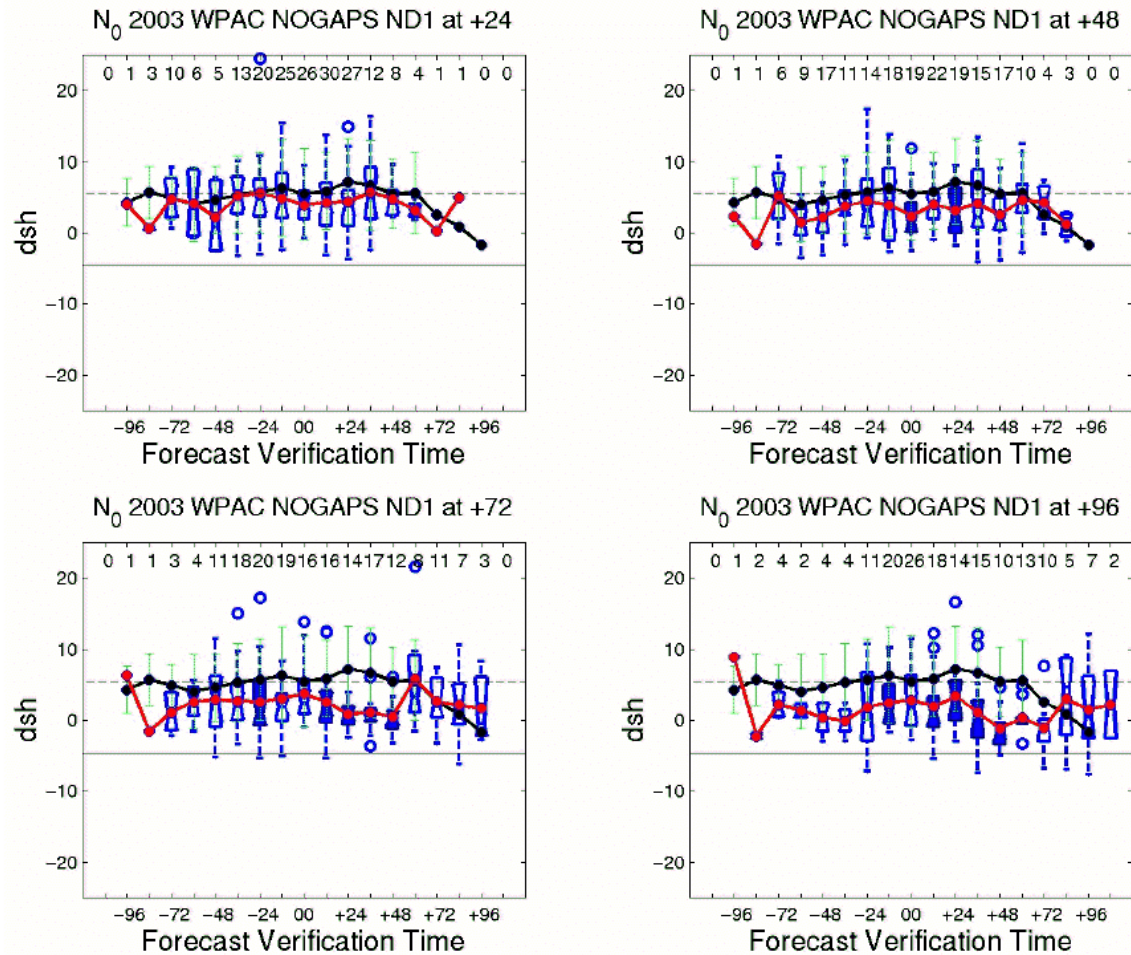
Figure 3.41. Average analyzed and forecast deep layer (200-850 mb) wind shear (m s^{-1}) as in Figure 3.18, except for non-developing vortices in 2003 relative to N_0. Heavy black line represents analyzed average deep layer wind shear for non-developing vortices (at +00), and red line represents average forecast deep layer wind shear for the indicated forecast time. Average analyzed deep layer wind shear for 2003 non-developing vortices at N_0 (light solid black line) was 5.5 m s^{-1}. Light solid black line represents average analyzed shear threshold for 2002 developing vortices (-1.8 m s^{-1}).

with less favorable formation conditions during 2003. This increase in westerly wind shear is likely due to the increased westerlies aloft associated with the weak La Niña event, or cold phase of the El Niño-Southern Oscillation, as noted above by Chan (2003).

The transition to easterly analyzed shear at +84 h is suspect due to the small number of cases at $\geq$ 72 h after N_0. The analyzed wind shear remains positive and westerly for this subset of non-developers, as in 2002, which is a primary indicator that these vortices will not likely undergo significant further development.

Forecast deep layer wind shear is at almost all times weaker (less positive and thus less westerly) than the analyzed shear, which is consistent with the NOGAPS tendency to over-forecast tropical circulations. No significant trend exists in forecast range compared to the forecast time, with too large shear errors nearly as common as too small shear errors at the longer forecast ranges. However, this may be due to the small sample size at extended forecast intervals.

3.   False Alarms

Surprisingly, the number of model false alarms (27) in 2003 increased significantly from 2002 (15). Formation of these model false alarms (Figure 3.42) occurred preferentially in the Philippine Sea, as in 2002. These erroneous forecasts are likely associated with spurious convective events within the monsoon trough.
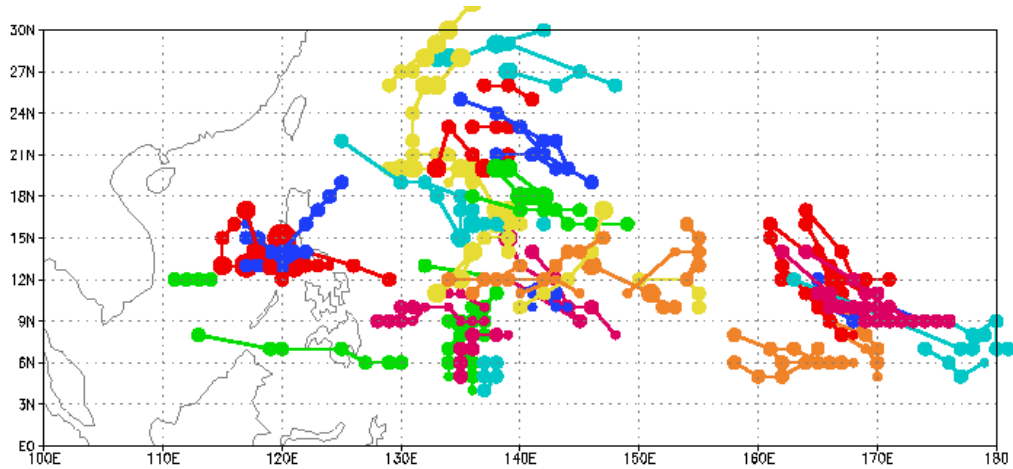
Figure 3.42. Locations of model false alarms in the western North Pacific during 1 May – 31 October 2003. Circles indicate successive 12-h analyses of each identified model false alarm. The size of each circle is related to the analyzed intensity of the circulation with a larger circle indicating a more intense circulation.

However, the number of Group 2-type false alarms decreased to fewer than five (from 50), which is attributed to modifications made to the Emanuel cumulus parameterization scheme late in 2002 that preferentially decreased the easterly deep layer wind shear by increasing the convective momentum transport. The 2003 model false alarms were not similarly decreased by this change to the cumulus parameterization since unlike the Group 2 non-developing vortices, they were never analyzed and also did not have excessive vorticity forecasts.

IV.   SUMMARY AND CONCLUSIONS

The performance of the NOGAPS model in predicting the formation of tropical circulations in the western North Pacific is assessed by tracking 254 circulations from 1 May – 31 October 2002. The Tropical Cyclone Vortex Tracking Program (TCVTP) developed by Professor Patrick Harr is used to identify circulations in the NOGAPS 850-mb relative vorticity analysis and forecast fields that have a value of at least 1.5×10^{-5} s^{-1}. An ellipse is fit to the outer closed vorticity contour to define the size of the circulation. Identified circulations are then matched when distance and movement criteria are met to define tracks in the analyses and forecasts.

Any circulations that formed north of 30°N were not tracked by the TCVTP. Additionally, circulations that formed east of 180°E were also excluded from the analysis data set. The remaining circulations were categorized according to whether they formed within the South China Sea (SCS), Philippine Sea (PS), east of the monsoon trough (EMT). A minimum duration of 24 h was imposed for the analyzed vortex in the analyses. Developing circulations were analyzed relative to their first JTWC-warning time, and relative to the first Best-Track time. Those same circulations were also analyzed based on whether they formed before, during, or after the TCFA-specified formation window. Additionally, non-developing vortices and both model and Tropical Cyclone Formation Alert (TCFA) false alarms were examined.

Tropical circulations within the Philippine Sea subregion accounted for 46.5% of the total tracked vortices, and 43.5% of the JTWC-numbered circulations during 2002. Of the 59 potential seedlings in the PS subregion, the ten vortices that developed to warning strength represented only a 16.9% formation rate. Formations at the east end of the monsoon trough accounted for only 22.8% of the total tracked vortices, but led to 34.8% of the numbered storms. The eight numbered storms that formed in the EMT subregion represented 27.6% of the 29 circulations that were identified within that subregion. Circulations that developed within the SCS accounted for 30.7% of the total tracked vortices, and 21.7% of the numbered storms. The formation rate was the smallest

97

in this subregion, with only 12.8% of the potential seedlings developing to at least Tropical Depression intensity.

A total of 27 TCFAs were issued for the 23 storms that developed during 1 May – 31 October 2002. TCFAs were not issued for two of the developing storms, and multiple TCFAs were issued for six developing storms. Two of these twice-issued TCFAs were not available for analysis. Formation occurred during the TCFA-specified formation window for 33% of the developing storms. Of the remaining 16 that failed to verify within the specified window, 61% verified prior to the TCFA-specified formation window. About 19% of the developing storms formed after the specified formation window. In general, when formation did not occur by the end of the formation window, a second TCFA was issued to correct the formation window and location, and formation typically did occur within the second specified formation window. Six false alarm TCFAs were issued for circulations that were never warned on by JTWC. Due to the small number of cases available when analyzing developing storms based on formation time relative to the TCFA formation window, significant systematic NOGAPS model trends cannot be identified. Before any conclusions can be drawn regarding the performance of NOGAPS in predicting formation relative to the TCFA-specified formation window, especially for those circulations that formed late, a study that includes more circulations meeting these criteria is necessary. Analysis based on formation region, rather than time, will be the focal point of further analysis.

A.   DEVELOPING VORTICES

Formation time for the circulations that were later numbered and warned on by JTWC was taken to be the time the first warning was issued. This time (designated F_0) was identified for each developing storm from the 2002 Annual Tropical Cyclone Report (ATCR) published by JTWC. A second formation time called the first Best-Track time, (designated F^*_0) was defined as the time the developing circulation was first apparent in the model analysis, which is determined by JTWC during post-analysis, and also published in the 2002 ATCR. The first Best-Track time always preceded the first warning time, normally by at least 12 hours.

The timing error (Δt_1) between when a forecast curve first crossed the analyzed 850-mb relative vorticity threshold (5.0×10^{-5} s^{-1}) and the first JTWC-warning time was calculated. On average the forecast curve crossed the vorticity threshold 16.7 h prior to F_0 for all forecasts, but only 6 h prior to F_0 for the short-term (≤ 48 h) forecasts. A timing error less than 6 h is not possible due to the resolution of the data. This relatively small (negative) timing error indicates that the NOGAPS model develops circulations slightly faster than they develop in the environment. Analysis of the analyzed and forecast vorticity curves in Figure 3.5 (upper panels) indicates that in the 36 h leading up to the first JTWC-warning time, the NOGAPS model forecasts of vorticity were only slightly greater than the analyzed vorticity at those forecast verification times. At the longer forecast ranges, the forecast vorticity exceeded the analyzed vorticity by less than 1×10^{-5} s^{-1}, which indicates an over-forecast, but not an excessive one. Given these relatively accurate forecasts, the NOGAPS model appears to be handling the physical parameterizations well in the formation environment.

Threshold values at these formation time definitions were determined for five selected forecast variables: 850-mb relative vorticity, deep layer (200-850 mb) wind shear, sea-level pressure, 925-mb wind speed, and vapor pressure. Additionally, the size of the circulation was analyzed to determine the accuracy of the NOGAPS representation of the circulation, but was not treated as a forecast variable. The threshold values corresponding to the average value of each variable at the first JTWC-warning time is given in the second column of Table 4.1. A second set of threshold values corresponded to the value of each variable at the first Best-Track time is given in the third column of Table 4.1.

Table 4.1. Summary of threshold values relative to F_0 and F^*_0. Values correspond to the average analyzed value of the variable at the reference time.

Forecast Variable	Analyzed Threshold Values	
	F_0	F^*_0
850-mb relative vorticity	5.0×10^{-5} s^{-1}	4.3×10^{-5} s^{-1}
Deep layer (200-850 mb) wind shear	-1.8 m s^{-1}	-3.8 m s^{-1}
Sea-level pressure	1006.9 mb	1006.6 mb
925-mb wind speed	10.8 m s^{-1}	9.5 m s^{-1}
Vapor pressure (500-700 mb average)	3.6 Pa	3.4 Pa

The strongest trends relative to the formation time were found in the 850-mb relative vorticity and the deep layer wind shear. When the analyzed average 850-mb relative vorticity value was approximately 4×10^{-5} s^{-1} the sign of the analyzed deep layer wind shear tended to change from westerly (positive) to easterly (negative). Classic research (Gray 1968) indicates that a minimum in vertical wind shear over the center of the potential tropical seedling is necessary for formation to occur, along with easterly shear to the north, and westerly shear to the south. Some research model studies (Tuleya and Kurihara 1981) indicate that zero shear above the developing circulation is less desirable than slightly negative (easterly) shear, which is consistent with this research. That is, the average shear over these developing tropical circulations was -1.8 m s^{-1}.

If it is assumed that the hours prior to F_0 represent the time during which the tropical cyclone seedling undergoes the formation process, then the analyses and forecasts of the selected variables during that time yield information about the formation environment. Focusing on the 850-mb relative vorticity and deep layer wind shear in the 24-36 h leading up to the first warning time, it is apparent that the over-forecasts of vorticity and deep layer shear are consistent with one another (increased vorticity forecasts correspond to more easterly shear). This consistency indicates that the NOGAPS model is accurately handling the physical parameterizations.

At the same time, NOGAPS forecasts of mid-level vapor pressure, which indicates the amount of moisture available to the developing circulation, were not only drier than analyzed, but also had a substantially smaller signal than was expected, since it varied less than 0.5 Pa over the lifetime of the analyzed storms. While the lack of variability of this variable during the early stages of development and intensification was surprising, the vapor pressure outliers were almost all significantly drier than the analyzed value. In a global model such as NOGAPS, erroneous vapor pressure forecasts are expected to be too moist, rather than too dry. This excessive drying of the mid-levels within the NOGAPS model is likely a function of the convective parameterization, and works against the formation processes. If, as in this case, the internal dynamics of the tropical seedling vortex inhibit formation, the formation process shifts from a mesoscale interaction to a large-scale process. Since the NOGAPS model is capable of accurately forecasting tropical cyclone formation with inhibited formation on the mesoscale, the

large-scale processes are more likely accurately represented by the model. However, improvements could be made in the modeling of formation if these mesoscale processes could be included.

Sea-level pressure and 925-mb wind speed had less-well developed indicators for developing circulations, and thus serve more as proxies for the intensity of the circulation, rather than providing an indication of the state of an atmospheric predictor that either enhances or inhibits formation. While these variables taken individually may not provide obvious indications of formation, they are significant to the formation forecast process in that they represent significant features within the large-scale atmosphere.

Several significant differences between the 2002 and 2003 data sets were noted. Fewer tropical cyclones were numbered by JTWC during 2003, during which a weak La Niña flow pattern dominated the western North Pacific. More variation existed in the analyzed vorticity curve for the 2003 developing circulations (Figure 3.37) than in 2002 (Figure 3.5), and the range of forecast values was smaller. The average analyzed vorticity at the first JTWC-warning time was similar (5.0×10^{-5} s^{-1} in 2002 versus 4.8×10^{-5} s^{-1} in 2003), although the change in vorticity in the first 12 h after the first warning time when the synthetic tropical cyclone observations were inserted into the NOGAPS model analysis was larger in 2003 than during 2002, which indicates that the model analysis may have been slightly below what actually occurred in the environment.

Similarly, the NOGAPS analyses of deep layer wind shear were very similar in 2002 and 2003, and the average analyzed value at the first JTWC warning time was slightly smaller in 2003 (-1.6 m s^{-1}) than 2002 (-1.8 m s^{-1}). The larger (more negative) value in 2002 indicates that the deep layer wind shear was more easterly in 2002. The weaker analyzed easterly wind shear in 2003 may be attributed to the weak La Niña flow pattern that dominated the western North Pacific during that year.

It is possible that some of the decrease in the forecast range of the variables in the 2003 data set is associated with changes made to the NOGAPS model during 2003. These changes include an increase in the amount of convective momentum transport in the Emanuel cumulus parameterization scheme, and an upgraded data assimilation system. The transition from a multivariate optimum interpolation (MVOI) data

assimilation scheme to the Navy Data Assimilation System (NAVDAS), which has the capability to ingest satellite observations in addition to traditional surface, radiosonde, and synthetic observations, occurred during October 2003. Changes made to the process by which synthetic tropical cyclone observations are assimilated into the NOGAPS model analysis should be transparent to the user (B. Strahl, FNMOC, personal conversation), but yield a more accurate model analysis. However, the changes to the convective momentum transport during 2003 may have yielded a decrease in the easterly deep layer wind shear, which decreased the number of false alarm circulations developed by the NOGAPS model.

B.   NON-DEVELOPING VORTICES

The non-developing vortices were separated into three main categories: those that met the minimum duration criterion of 24 h; those that did not meet the minimum duration criterion; and false alarms. The non-developing vortices that met the minimum duration criterion comprised the ND1 data set. The Group Two subset of non-developing vortices (NDG2) was extracted from the ND1 data set, and consisted of the non-developing vortices that met the minimum duration criterion, and also were forecast to exceed the 850-mb relative vorticity threshold (5.0×10^{-5} s^{-1}) established for developing vortices. The non-developing vortices that did not meet the minimum duration criterion were placed in the ND2 data set. Non-developing over-forecast vortices (NDOF) were identified from the ND2 data set as those that were forecast to exist for at least 24 hours longer than they actually existed in the NOGAPS model analyses. After the NDOF vortices were extracted, the remaining vortices in the ND2 data set were not analyzed further since the vortices contained therein corresponded to short-term convectively-driven circulations and one-time spurious circulations. The third main data set of model false alarms was identified as vortices that were forecast to develop for at least three consecutive model runs, but were never analyzed. These model false alarms were also compared to the TCFA false alarms.

Since no first warning time existed for each non-developing vortex, and no first Best-Track time had been established, the reference time for each non-developing vortex (N_0) that met the minimum duration criterion was defined to be the time of the maximum

analyzed 850-mb relative vorticity. This N_0 time could be calculated for each non-developing vortex in the ND1 and NDG2 data sets. Since the vortices in the ND2 and NDOF data sets corresponded to only one or two analyses, the reference time used for those data sets (N^*_0) corresponded to the last verifying analysis.

The threshold values for the non-developing vortices relative to N_0 and N^*_0 for each of the five selected variables (Table 4.2) may be compared to the threshold values determined for the developing circulations in Table 4.1. In general, the threshold values for the non-developing vortices were smaller, closer to zero, or less favorable for formation than the threshold values for the developing circulations.

Table 4.2. Summary of threshold values relative to N_0 and N^*_0. Values correspond to the average analyzed value of the variable at the reference time.

Forecast Variable	Analyzed Threshold Values (Reference Value)		
	ND1 (N_0)	NDG2 (N_0)	NDOF (N^*_0)
850-mb relative vorticity	3.3×10^{-5} s^{-1}	3.7×10^{-5} s^{-1}	2.4×10^{-5} s^{-1}
Deep layer (200-850 mb) wind shear	4.1 m s^{-1}	2.8 m s^{-1}	3.2 m s^{-1}
Sea-level pressure	1008.0 mb	1007.0 mb	1007.8 mb
925-mb wind speed	7.0 m s^{-1}	8.0 m s^{-1}	6.7 m s^{-1}
Vapor pressure (500-700 mb avg.)	3.4 Pa	3.6 Pa	3.4 Pa

The 850-mb relative vorticity threshold for the non-developing vortices (3.3×10^{-5} s^{-1}) was less than the vorticity for the developing circulations (5.0×10^{-5} s^{-1}), which indicates that less organization existed within the non-developing circulations at the time of maximum analyzed vorticity than in the developing circulations at the first JTWC-warning time. The analyzed vorticity for the developing circulations would have been equal to the analyzed value for these non-developing cases (at N_0) roughly 96 h prior to F_0. If it is assumed that this equivalence of vorticity values represents a similar developmental stage, this signifies the maximum intensity of the developing (non-developing) vortices do (do not) undergo further development.

The average analyzed shear at N_0 (3.3×10^{-5} s^{-1}) was also less than the minimum shear value (4×10^{-5} s^{-1}) at which deep layer wind shear transitioned from westerly to easterly. That the deep shear on average was less than this threshold value indicates that wind shear remained westerly throughout the lifecycle of the non-developing vortex, and never transitioned to the more formation-favorable easterly shear.

One potential explanation for the lack of further development of the non-developing vortices is considered to be the sign of the analyzed deep layer wind shear. Since the analyzed deep layer shear remains positive (westerly) throughout the lifetime of the non-developing vortices, the atmosphere in which these circulations exist is dominated by westerly shear, which is not favorable for tropical cyclone formation.

As was the case for the developing vortices, neither the sea-level pressure nor the vapor pressure variable had a strong signal for forecasting the development potential of these tropical storm seedlings. In contrast to the vapor pressure for the developing circulations, the vapor pressure for the non-developing cases did have more variation relative to the average analyzed value at N_0. While the occurrence time of the analyzed maximum vapor pressure did not correspond to the occurrence time of the analyzed maximum vorticity, the vapor pressure for the non-developing cases was consistently less than the threshold value (3.6 Pa) determined for the developing circulations, which indicates both a weaker potential warm core and that the formation environment may be less favorable for further development of the tropical storm seedling.

Additionally, the outliers of vapor pressure for the non-developing circulations were predominantly less than the analyzed vapor pressure for this data set, which indicates forecasts for a drier mid-troposphere than was analyzed. Forecasts for excessive dryness in the mid-levels are counter-intuitive, since it is expected, in general, that the global models will forecast excessive moisture as a result of convective parameterization of meso- and smaller-scale processes. As noted for the developing circulations, this excessive dryness indicates that the internal dynamics of the tropical vortex are working against formation. While accurate formation forecasts are possible with this counter-balance, it is also assumed that this helps to prevent more false alarms and over-forecasts than those already observed.

The analyzed sea-level pressure for the non-developing vortices was at all times higher than the average analyzed sea-level pressure for the developing vortices. While the sea-level pressure in the early stages of development for both the developing and non-developing circulations was similar, the sea-level pressure for the developing vortices began to distinctly decrease about 48 h prior to F_0, and the sea-level pressure for the non-developing vortices never showed a corresponding decrease. Rather, the sea-level

pressure for the non-developing vortices remained consistently within about 1 mb of the average analyzed value at N_0.   Since the non-developing vortices never experienced a substantial decrease in sea-level pressure, the magnitude of the warm core of the non-developing vortices was presumably smaller than for the developing circulations.

Although the 925-mb wind speed variable did not provide a strong formation signal, it nonetheless is a proxy for the intensity of the low-level circulation.   This analyzed wind speed fluctuates throughout the lifetime to indicate pulses of development and decay that occurred.   The average analyzed wind speed for non-developing vortices was at all times less than the threshold value determined for the developing circulations (10.8 m s^{-1}).   Even at 120 h prior to F_0, the 925-mb wind speed of the developing circulations was greater than any of the reliable analyzed wind speed values for the non-developing vortices.   Thus, the non-developing vortex never achieved the same intensity as the developing circulations, and the low-level circulation never achieved the magnitude capable of further development from air-sea fluxes.

1.   False Alarms

False alarms in the NOGAPS model are a result of the model tendency to over-forecast the development of tropical circulations.   Two types of false alarms were identified: model false alarms, which included non-developing vortices that were forecast to occur for at least three consecutive forecasts, but were never analyzed; and the so-called Group 2 false alarms that included analyzed non-developing vortices that were forecast to exceed the relative vorticity threshold determined for developing circulations.

The forecasts for the model false alarms in which a vortex was never analyzed, approximately resemble the early-stage forecasts of developing circulations, with the forecast 850-mb relative vorticity forecast to exceed the analyzed values. Examination of the selected forecast variables would likely reveal excessive 850-mb relative vorticity, and more easterly deep layer wind shear. It may be that the forecasts for the model false alarms are similar to those for the non-developing circulations that were forecast to exceed the 850-mb relative vorticity threshold (NDG2) determined for developing vortices $(5.0 \text{ x } 10^{-5} \text{ s}^{-1})$. A more easterly wind shear is also expected in conjunction with this vorticity over-forecast. This tendency cannot be confirmed here as analyses for the selected forecast variables are not available since these vortices never existed in an

analysis panel. However, incorrect forecasts of these two variables yields excessive development of what might otherwise be a short-lived convective event.

The 15 model false alarms that occurred during 1 May – 31 October 2002 represent about 13% of the total number of tracked circulations. Thus, more than one model false alarm was detected for every two developing circulations (24), which indicates a problem for the forecaster in interpreting NOGAPS formation forecasts. During 2003, the number of model false alarms jumped to 27 (column four of Table 3.10).

The Group 2 false alarms in which a non-developing vortex was forecast to exceed the 850-mb relative vorticity threshold determined for developing circulations (5.0×10^{-5} s^{-1}) represent the second type of false alarms in the NOGAPS model. These false alarms pose a serious challenge for operational forecasters because each vortex must be examined since it exists in the NOGAPS analysis. Examination of the 850-mb relative vorticity and deep layer wind shear profiles indicate that the early stages of development of these vortices are very similar to similar stages in the lifecycle of the developing circulations. Short-range vorticity forecasts prior to the time of the maximum analyzed vorticity are very similar to the analyzed vorticity values, which indicates that the NOGAPS model is accurately handling both the physical parameterizations of the vortex and the large-scale environmental flow. The mechanism that leads to the sudden decrease in the analyzed 850-mb relative vorticity is unclear.

Though the number of NOGAPS model false alarms in 2003 was greater than in 2002, there was a significant decrease in the number of Group 2-type false alarms. Since fewer than five Group 2 false alarms were forecast in 2003, these were not analyzed due to small sample size. The decrease in the number of Group 2 false alarms may be attributed to the increase in convective momentum transport of the Emanuel cumulus parameterization scheme (Hogan et al. 2004). The ultimate result of increasing the amount of convective momentum transport was to decrease the easterly deep layer wind shear that was forecast by the NOGAPS model, which, in turn, significantly decreased the number of false alarm forecasts that were generated by NOGAPS during 2003.

Despite the significant decrease in the number of Group 2 false alarms during 2003, the number of model false alarms (27) actually increased from 2002 (15). This

increase is attributed to year-to-year environmental variability in the western North Pacific basin. A detailed explanation of this increase required a more extensive investigation of the analysis and forecast fields associated with these vortices. The tentative explanation is that the overall environmental conditions were less favorable for tropical cyclone formation during 2003. However, the NOGAPS model continued to over-forecast the spin-up of vortices for at least three consecutive forecasts that simply did not verify in this less-favorable environment during 2003. Thus, the number of model false alarms can be larger even though the over-forecast vorticity tendency of NOGAPS with the generally weaker initial vortices during 2003 did not lead to forecasts exceeding 5.0×10^{-5} s^{-1}, which is the definition of Group 2 false alarms (markedly decreased during 2003).

2. Model Over-forecasts

Model false alarms were distinguished from over-forecast non-developing vortices in that the model false alarms never existed in a NOGAPS analysis, whereas the over-forecast non-developing vortices existed in one or two NOGAPS analyses. The existence of over-forecast non-developing vortices is another indicator of the NOGAPS tendency to over-develop tropical circulations. The reasons for this over-development are likely linked to the NOGAPS model parameterization schemes that define and develop the internal vortex of the system. That a circulation can be identified in the NOGAPS model analyses indicates that a potential tropical cyclone seedling is present in the environment. However, the actual and forecast development profiles of these vortices differ.

In general, these over-forecast non-developing vortices existed in two consecutive analyses, and had a relatively low analyzed 850-mb relative vorticity (2.4×10^{-5} s^{-1}) compared to the vorticity thresholds determined for the non-developing (3.3×10^{-5} s^{-1}) and developing circulations (5.0×10^{-5} s^{-1}). Solely based on the average analyzed vorticity at the reference time (the last analysis time, N_0 and F_0, respectively), the analyzed vorticity for this subset of non-developers is lower than the minimum (4×10^{-5} s^{-1}) identified previously that is necessary in order for deep layer wind shear to transition from the inhibitive westerly to the more favorable easterly.

However, the forecast 850-mb relative vorticity always exceeded the analyzed vorticity, and was generally forecast to continue to increase in time. The erroneous vorticity forecasts produced by the NOGAPS model for these non-developing vortices had an associated erroneous easterly deep layer wind shear. Furthermore, the sea-level pressure forecasts indicated a more favorable environment for formation than was analyzed. Why these vortices were so significantly over-forecast is unclear. Since these vortices formed preferentially in association with the monsoon trough (in the South China Sea and Philippine Sea), it may indicate that they may have been short-lived convective events, or weak circulations associated with the monsoon trough or depression. Inaccurate representation of either the seedling disturbance or the formation environment may have yielded incorrect forecasts of development by the NOGAPS model.

Since the number of over-forecast non-developing vortices decreased dramatically during 2003, the modifications made to enhance the convective momentum transport of the Emanuel cumulus parameterization scheme during late 2002 were effective. Increasing the amount of convective momentum transport resulted in a decrease in the amount of easterly wind shear, and evidently made the forecast environment less favorable for formation. Weaker easterly shear decreased the number of spurious convective events, and thus the number of non-developing vortices that were forecast to develop to tropical depression strength or greater.

V. RECOMMENDATIONS FOR FURTHER STUDY

The use of the TCVTP in assessing model performance in the prediction of tropical cyclone formation should be continued in other studies. Specifically, subsequent studies in the following list would be beneficial to tropical cyclone formation prediction assessment while also documenting the real-time potential of the TCVTP:

- Further analysis of the selected variables based on a multiple year sample of circulations in the western North Pacific.
  - Identify predictors for objective assessment of potential tropical cyclone formation.
  - Stratification of the larger data set by examining circulations that formed in the South China Sea, Philippine Sea, and east of the monsoon trough, and in addition to separating the Philippine Sea into the monsoon trough and a new subregion north of the monsoon trough.
  - Further analysis of the larger sample by examining circulation formation time relative to the TCFA formation window.
- Further study that applies the TCVTP in the western North Pacific to other global numerical models for comparison to NOGAPS.
  - Comparative studies of formation thresholds for circulations forming in different tropical cyclone basins.
  - Application and use of the TCVTP in real-time operations.
- Further analysis of model false alarm vortices and non-developing over-forecast vortices, including assessment of the large-scale environment and vortex characteristics throughout the forecast lifetime of the circulation.
- Further study using the first Best-Track time as the formation time, as well as the first time the TCVTP captured the circulation in the analysis.

THIS PAGE INTENTIONALLY LEFT BLANK

APPENDIX A: TCFA CRITERIA CHECKLIST – WESTERN NORTH PACIFIC & NORTH INDIAN OCEANS

The JTWC uses the following checklist to determine whether or not a Tropical Cyclone Formation Alert (TCFA) should be issued for a suspect circulation center. Items denoted with an asterisk are progressive in nature. For example, if any wind speed within 5 degrees of the circulation center, as determined by satellite imagery and/or hand analysis, is 35 knots, then a total of 6 points will be contributed by items E, F, and G. A TCFA is issued when the sum of points is 30 or greater.

Point Value   Item:

                    I.   SFC/ Gradient Level

2 _____   A. A circulation is evident in the wind field
4 _____   B. A circulation has been evident for 24 hours
4 _____   C. Environmental MSLP – CNTR SLP = 4MB (EST)
3 _____   D.* Westerly SFC/Gradient level winds of at least 10 kt
                         south of the circulation center

                    II.   Disturbance, and within 05 degrees of center

1 _____   E.* Any wind associated with center is at least 20 kt
2 _____   F.* Any wind associated with center is at least 25 kt
3 _____   G.* Any wind associated with center is at least 30 kt
1 _____   H.* 24 hour pressure decrease at nearby station = 2 MB
3 _____   I.* 24 hour pressure decrease at nearby station = 3 MB
1 _____   J.* EST. MSLP of TD is $\leq$ 1008 MB
2 _____   K.* EST. MSLP of TD is $\leq$ 1006 MB
3 _____   L.* EST. MSLP of TD is $\leq$ 1004 MB

                    III.   500 mb

1 _____   A. There is evidence of at least a trough
2 _____   B. There is evidence of a closed circulation

                    IV.   200 mb

1 _____   A. TUTT to the northwest of the TD
3 _____   B. Evidence of an anticyclone over the center of the TD
1 _____   C. 200 mb wind in the center $\leq$ 25 kt

V. SST

1 _____   A. SST $\geq 28\,°C$

VI. Satellite Data:

1 _____   A.* The TD has persisted for at least 24 hours
2 _____   B.* The TD has persisted for at least 48 hours
3 _____   C.* The TD has persisted for at least 72 hours
2 _____   D.* Dvorak classification of at least T0.0
4 _____   E.* Dvorak classification of at least T1.0
              F.* Dvorak classification of at least T2.0 (warning
                     should already be issued)

VII. Miscellaneous:

3 _____   A. Double vortex interaction (cross-equatorial) exists
5 _____   B. Tropical disturbance is within 72 hours of a DoD
                     resource
2 _____   C. Synoptic circulation and satellite fix are consistent in
                     location (within 02 degrees)
1 _____   D. 20 kt synoptic wind reports within 3 degrees of the
                     satellite fix (does not apply to winter gales)

_____
   61   Total Points Possible

APPENDIX B: GENERATION OF BOX PLOTS

Box plots for each selected variable indicate the range of specified forecast variable values at each forecast time relative to the F_0, F^*_0, or N_0, which are the first JTWC warning time for numbered storms, the first Best-Track analysis time for numbered storms, and the time corresponding to the maximum analyzed 850-mb relative vorticity for non-developing vortices, respectively. Each figure consists of four panels, which represent the forecast intervals of 24-h, 48-h, 72-h, and 96-h (see Figure B.1). Although the features within each figure are similar, the reference time used to calculate the values varies depending on the data set analyzed. The title on each panel indicates the reference time (e.g., F_0), the year and basin in which the vortex occurred (e.g., 2002 WPAC), the numerical forecast model (e.g., NOGAPS), the data set to which the vortex belonged (e.g., Developing DV or Non-developing ND1), and the forecast time (e.g., +24). The abbreviations used to identify the data set used are: DV, ND1, NDG2, ND2, NDOF, where DV represents those vortices that developed into storms that were later numbered by JTWC, ND1 represents the non-developing vortices that met the minimum duration criterion, NDG2 represents the non-developing vortices that met the minimum duration criterion and were forecast to exceed the η_0 threshold, and ND2 represents the non-developing vortices that did not meet the minimum duration criterion. NDOF represents the non-developing vortices that did not meet the minimum duration criterion, but did meet the over-forecast criteria.

Separate charts for each formation region (SCS, PS, and EMT) were also created for the 850-mb vorticity variable for the DV, and ND1 data set. The thin horizontal lines drawn across each regional chart indicate the mean forecast variable value for that region. For example, the mean vorticity value at F_0 for all developing vortices is 5.0×10^{-5} s^{-1}, while the value for those vortices developing in the SCS is 4.8×10^{-5} s^{-1}, 5.5×10^{-5} s^{-1} in the PS region, and 4.7×10^{-5} s^{-1} in the EMT region.

A.   ANALYSIS DATA

The heavy black line in each panel represents the average analyzed value (at +00) of the indicated variable, and thus represents a threshold value for either developers or for non-developers as appropriate. The thin green whiskers that extend from the average
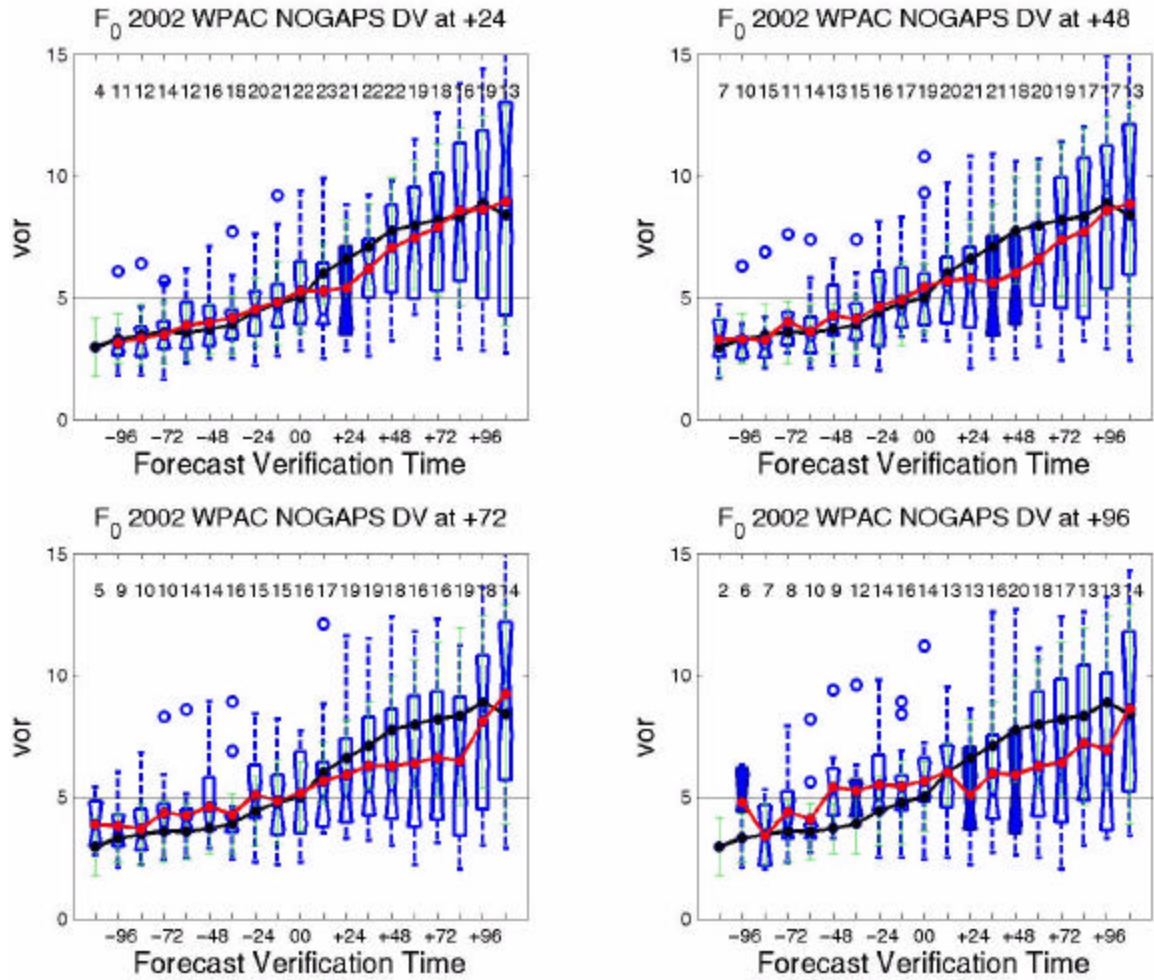
Figure B.1. Average analyzed and forecast 850-mb relative vorticity for developing vortices relative to the first JTWC warning time (F$_0$). Heavy black line represents analyzed average 850-mb relative vorticity (at +00), and red line represents average forecast 850-mb relative vorticity for the indicated forecast time. Average 850-mb relative vorticity at F$_0$ (light solid black line) was 5.0 x 10^{-5} s^{-1}, which is then a reference for the vorticity magnitudes before (to the left) and after (to the right) the first warning time. The sample sizes available for comparison of the forecast values at each forecast verification time are listed near the top of each panel for 24-h (upper-left), 48-h (upper-right), 72-h (lower-left), and 96-h (lower-right) forecasts of these developing storms.

analyzed value represent the standard deviation (i.e., Table B.1) of the selected variable at each time interval. The thin black horizontal line extending from –120 h to +120 h cross each plot is the mean value of the selected variable for the developing vortices at the +00 analysis time.

B. FORECAST DATA

Separate box plots were created for each forecast verification time relative to F_0, F^*_0, and N_0 from +00 to +120 h if the forecast can be verified. For example, the 24-h forecast in the upper-left panel of Figure B.1 represents all of the 24-h 850 mb relative vorticity forecasts for a sample of developing vortices that verified at various times relative to F_0. Similarly, the upper-right panel in Figure B.1 represents all 48-h 850-mb relative vorticity forecasts that verified at various times relative to F_0. The heavy red line in each panel represents the average forecast value at the time indicated at the end of the title for each panel (i.e., +24, +48, +72, or +96). The total number of forecasts included in each column for each forecast time relative to F_0, F^*_0, or N_0 are indicated at the top of the column. The range of forecast values for each variable that can be verified at that time relative to F_0 is indicated at each time interval by the blue box plots. The top, middle, and bottom horizontal lines that make up each box represent the upper quartile, median, and lower quartile. The dashed whiskers extending from the box indicate the values that are not within the lower and upper quartiles, and the outliers are indicated by an open circle. The dashed horizontal line in the lower portion of the plot is the mean

Table B.1. Summary of standard deviations of 850-mb relative vorticity (x 10^{-5} s^{-1}) for each forecast time for +96 hour forecasts of developing vortices.

Forecast Time	Std Dev	Forecast Time	Std Dev
-120	0.71	+00	2.21
-96	1.54	+12	2.00
-84	1.34	+24	2.08
-72	1.81	+36	2.63
-60	1.65	+48	3.00
-48	1.84	+60	2.93
-36	1.58	+72	3.33
-24	1.92	+84	3.25
-12	1.59	+96	3.42
--	--	+120	3.69

value of the selected variable at the F^*_0 or N_0 times, or the region-specific average value, as indicated. Data from non-developing vortices were not included in the plots of F_0 and F^*_0, which refer only to the developing vortices.

THIS PAGE INTENTIONALLY LEFT BLANK

LIST OF REFERENCES

Chan, J. C. L., 2003: Verification of forecasts of tropical cyclone activity over the western North Pacific in 2003. City University of Hong Kong, Department of Physics and Materials Science, Laboratory for Atmospheric Research. 11 March 2004. [Available online at http://aposf02.cityu.edu.hk/~mcg/tc_forecast/2003_Verification.htm.]

Cheung, K. K. W., and R. L. Elsberry, 2003: Tropical cyclone formations over the western North Pacific in the Navy Operational Global Atmospheric Prediction System forecasts. *Wea. Forecasting*, **17**, 800–820.

Davis, C. A., and L. F. Bosart, 2001: Numerical simulations of the genesis of Hurricane Diana (1984). Part I: Control simulation. *Mon. Wea. Rev.*, **129**, 1859-1881.

_____, and _____, 2003: Baroclinically induced tropical cyclogenesis. *Mon. Wea. Rev.,* **131**, 2730-2747.

Dorics, T. G., III, 2002: An assessment of NOGAPS performance in the prediction of tropical Atlantic circulation formation. M.S. thesis, Naval Postgraduate School, 72 pp.

Elsberry, R. L., 2003: "MR3252 Tropical meteorology course notes, Chapter 2: Tropical cyclone formation." Naval Postgraduate School. Monterey, CA.

Enagonio, J., and M. T. Montgomery, 2001: Tropical cyclogenesis via convectively forecast Rossby waves in a shallow water primitive equation model. *J. Atmos. Sci.*, **58**, 685-706.

Goerss, J. S., T. Hogan, K. Sashegyi, T. Holt, M. Rennick, T. Beeck, and P. Steinle, 2003: Validation test report for the NAVDAS/NOGAPS data assimilation system. Naval Research Laboratory Monterey, Monterey, CA. 11 March 2004. [Available online at https://www.fnmoc.navy.mil/PUBLIC/ADMIN/ NAVDAS_ValidationTestReport.doc.]

_____, and R.A. Jeffries, 1994: Assimilation of synthetic tropical cyclone observations into the Navy Operational Global Atmospheric Prediction System. *Wea. Forecasting*, **9**, 557–576.

Harr, P. A., R. L. Elsberry, and J. C. L. Chan, 1996: Transformation of a large monsoon depression to a tropical storm during TCM-93. *Mon. Wea. Rev.*, **124**, 2625-2643.

Hennon, C. C., and J. S. Hobgood, 2003: Forecasting tropical cyclogenesis over the Atlantic basin using large-scale data. *Mon. Wea. Rev.*, **131**, 2927-2940.

Hogan, T. F., and W. M. McClune, 2002: A description of the impact of the increase in NOGAPS resolution to T239 with 30 levels. Naval Research Laboratory, Monterey, CA. 16 Mar 2004. [Available online at: https://www.fnmoc.navy.mil/PUBLIC/.]

Hogan, T. F., M. F. Peng, J. A. Ridout, Y.-J. Kim, J. Teixeira, and R. L. Pauley, 2004: The Navy Operational Global Atmospheric Prediction System: Current status and testing of convective momentum transport in the Emanuel cumulus parameterization scheme. *Extended abstract,* 84th Annual Conference, Seattle, WA, Amer. Meteor. Soc., 1-8. [Available online at: http://www.ams.confex.com/ams/pdfpapers/68798.pdf.]

Holland, G. J., 1995: Scale Interaction and the western North Pacific monsoon. *Meteor. Atmos. Phys.*, **56**, 57-79.

Kurihara, Y., and R. E. Tuleya, 1981: A numerical simulation study on the genesis of a tropical storm. *Mon. Wea. Rev.*, **109**, 1629–1653.

McBride, J. L., 1981: Observational analysis of tropical cyclone formation. Part I: Basic description of data sets. *J. Atmos. Sci.*, **38**, 1117–1131.

_____, and R. Zehr, 1981: Observational analysis of tropical cyclone formation. Part II: Comparison of non-developing versus developing systems. *J. Atmos. Sci.*, **38**, 1132–1151.

Molinari, J., D. Vollaro, S. Skubis, and M. Dickinson, 2000: Origins and mechanisms of eastern Pacific tropical cyclogenesis: A case study. *Mon. Wea. Rev.*, **128**, 125–139.

Nielsen-Gammon, J., Hurricanes. 1996-1998. Texas A&M University, Meteorology Department. 1 Sep 2003. [Available online at http://www.met.tamu.edu/ATMO151/tut/hurricane/hurrmain.html.]

Ritchie, E. A., 1995: Mesoscale aspects of tropical cyclone formation. Ph.D. dissertation, Centre for Dynamical Meteorology and Oceanography, 167 pp.

Simpson, J., E. Ritchie, G. J. Holland, J. Halverson, and S. Stewart, 1997: Mesoscale interactions in tropical cyclone genesis. *Mon. Wea. Rev.*, **125**, 2643–2661.

Sobel, A. H., and C. S. Bretherton, 1999: Development of synoptic-scale disturbances over the summertime tropical Northwest Pacific. *J. Atmos. Sci.* **56**, 3106–3127.

USCINCPAC, 2002: Tropical cyclone operations manual, U. S. Commander-in-Chief Pacific Instruction 3140.1X. [Available online at http://www.dtic.mil.]

INITIAL DISTRIBUTION LIST

1.   Defense Technical Information Center
      Ft. Belvoir, VA

2.   Dudley Knox Library
      Naval Postgraduate School
      Monterey, CA

3.   Air Force Weather Technical Library
      Asheville, NC

4.   Air Force Institute of Technology
      Wright-Patterson Air Force Base, OH

5.   Professor Carlyle Wash
      Naval Postgraduate School
      Monterey, CA

6.   Professor Russell Elsberry
      Naval Postgraduate School
      Monterey, CA

7.   Professor Patrick Harr
      Naval Postgraduate School
      Monterey, CA

8.   Director, Joint Typhoon Warning Center
      Naval Pacific Meteorology and Oceanography Center
      Pearl Harbor, HI

9.   Captain Caroline Bower
      Joint Typhoon Warning Center
      Pearl Harbor, HI